TOWARDS A BETTER UNDERSTANDING OF CONTAMINANT FATE IN PLASTIC PLUMBING SYSTEMS AND THEIR REMEDIATION

by

Xiangning Huang

A Dissertation

Submitted to the Faculty of Purdue University

In Partial Fulfillment of the Requirements for the degree of

Doctor of Philosophy

Lyles School of Civil Engineering

West Lafayette, Indiana

December 2018

THE PURDUE UNIVERSITY GRADUATE SCHOOL
STATEMENT OF COMMITTEE APPROVAL

Dr. Andrew J. Whelton, Chair

Lyles School of Civil Engineering, Purdue University

Division of Environmental and Ecological Engineering, Purdue University

Dr. Chad T. Jafvert

Lyles School of Civil Engineering, Purdue University

Division of Environmental and Ecological Engineering, Purdue University

Dr. Amisha Shah

Lyles School of Civil Engineering, Purdue University

Division of Environmental and Ecological Engineering, Purdue University

Dr. John A. Howarter

School of Materials Engineering, Purdue University

Division of Environmental and Ecological Engineering, Purdue University

Approved by:

Dr. Dulcy Abraham

Head of the Department Graduate Program

Dedicate to

My Dearest Parents Xiuqin and Chao

and

My Loving Husband Shou

ACKNOWLEDGMENTS

I am very grateful and blessed with my graduate student life at Purdue. The journey for me was not always straight forward. I constantly doubted about myself and I could have failed not once but twice. But luckily I met some amazing people who always believed in me and gave me courage and strength to continue my journey.

First, I would like to thank my major advisor Dr. Andrew J. Whelton, who took me during one of my hardest times and healed me as a better and happier person. He was always there for me and convinced me that I could do better and I was capable. After half a year I joined the group, magic happened, I started enjoying my work and the lab environment. And I started thinking more and want to learn more. Then everything just turned right to me. Even today, I still think joining Professor Whelton's group was one of the best choice I have ever made. He is the great mentor, excellent advisor and always be supportive and enthusiastic with students' achievements, big or small. Thanks are extend to my committee members Dr. Chad T. Jafvert, Dr. Amisha Shah and Dr. John Howarter. They not only guided me to solve some technical questions, but also helped me to define my research topics and shared insights on how to prepare my presentations. Without their help, the dissertation would not have been completely.

I would also like to thank my parents Xiuqin and Chao, who supported me throughout my graduate study, financially and mentally. Because of them, I always feel secure and I know they will be always there for me for ups and downs. Lastly, I thank my husband Shou for his unconditionally support and love. Our story started from the first day of college and since then we have grown so much, but luckily we always hold each other's hand and never give up. Shou is very productive in his research area, and he is helping me constantly to troubleshoot my experimental questions. He is the one that can comfort me when I am stressed out and also brings me so much joy and laugh.

Lastly, I want to thank Purdue University for supporting diversity, respect and equality. As an international student, we do easily miss our home country, but Purdue provides a friendly and supportive environment that make me feel more comfortable and welcomed. I think I would miss Purdue a lot and I send my best wishes to Purdue.

TABLE OF CONTENTS

LIST OF TABLES

LIST OF FIGURES

ABSTRACT

Author: Huang, Xiangning. PhD
Institution: Purdue University
Degree Received: December 2018
Title: Towards A Better Understanding of Contaminant Fate in Plastic Plumbing Systems and Their Remediation
Committee Chair: Andrew J. Whelton

This dissertation focused on better understanding the fundamental processes that control organic and inorganic contaminant interaction with plastic plumbing pipes. Plastic pipes are increasingly being installed for drinking water plumbing, but their role in affecting drinking water quality has received little study. It is well-known that plastic pipes can sorb and release organic contaminants and be difficult to decontaminate. Several problems were identified in the literature and through discussions with industry: (1) Past guidance issued to communities affected by petroleum contaminated water does not seem to specifically consider plastic plumbing pipe remediation, (2) investigators have also identified heavy metals can accumulate on pipe inner walls, (3) Others have proposed certain heavy metals can catalyze plastic water pipe degradation, (4) No nondestructive cleaning methods were found for removing metal scales from plastic pipes. These topics were a basis for studies conducted because lack of information inhibits greater protection of public health, safety, and welfare.

This dissertation involved the application of knowledge and techniques from the environmental engineering and science, polymer engineering, and material science disciplines. Chapter 1 focused on the response of copper and plastic pipes (i.e., chlorinated polyvinylchloride (cPVC), high-density polyethylene (HDPE), crosslinked polyethylene (PEX)) exposed to petroleum contaminated drinking water. Bench-scale results revealed that pipe rinsing followed by a single 3 day water stagnation period removed target monoaromatic hydrocarbons (MAH) from copper pipes, but much longer ($\geq$15 days) time was required for decontaminating cPVC, HDPC, and PEX pipes. Benzene, trimethylbenzene and polynuclear aromatic hydrocarbons, some of which are not typically considered in drinking water contamination investigations, were found desorbed into clean drinking water from pipes. Future plumbing decontamination guidance should consider the conditions necessary for plastic pipe remediation. Chapter 2 describes the influence of drinking

water conditions on heavy metal contaminant – low density polyethylene (LDPE) pellet surface interactions. Mixed metal drinking water solutions were applied and contained Cu, Fe, Mn, Pb and Zn at 30 µg/L. LDPE was selected as the model polymer because of its prior use for piping in Europe, use in bench-scale studies by others, and similarity to products used for the manufacture of more complex materials in the USA (HDPE, PEX). As expected, metal loadings were about 5 times greater for aged LDPE pellets suspended in solution compared to new LDPE pellets. This difference was attributed to the aged plastic surfaces having oxygen containing functional groups, increased surface area, and enhanced hydrophilicity. Metal loading was lower at pH >9.5 and in the presence of dissolved organic contaminants. The presence of free chlorine and corrosion inhibitor also decreased metal adsorption onto LDPE pellets. These factors likely enabled metal precipitation thereby not allowing metal species to adsorb to LDPE pellets suspended in water. XPS results showed deposited metals (i.e., Cu, Pb, Zn) primarily consisted of hydroxides and oxides. To further understand heavy metal – plastic pipe interactions, Chapter 3 involved the use of metal and plastic pipe rigs and exhumed PEX plumbing pipes. Exhumed cold and hot water PEX pipes contained a noticeable amount of heavy metals (i.e., most abundant metals were 2049 mg/m^2 Fe, 400 mg/m^2 Ca, 438 mg/m^2 Zn and 150 mg/m^2 P). Metal release and deposition onto PEX pipe was examined using bench-scale pipe rigs that contained new PEX pipe, brass valves, and copper pipe. Two water matrices (pH 4 and 7.5) and two temperatures (23^{o}C and 55^{o}C) were explored. The pH 4 water often accelerated metal leaching from brass valves, and a greater amount of heavy metals deposited on PEX pipes at high water pH and temperature (pH 4 and 55^{o}C) conditions. Oxygen containing functional groups were detected on PEX pipes connected to a brass valve or a brass valve combined copper pipe, but were not found on PEX pipe only (controls) samples, indicating that certain configurations may facilitate plastic pipe degradation. The last chapter describes the ability of a new lignin derived ligand to remove metal deposits from exhumed PEX plumbing pipes. When the ligand concentration was ≥ 5mM, more than 95% of sorbed metals (i.e., Cu, Fe, Mn, Pb and Zn) were removed. The ligand favored certain metals over others (Cu > Zn > Fe > Mn > Pb) and heavy metal removal mechanisms were proposed. This dissertation provides insights into the role of plastic pipes on drinking water quality. As plastic pipes continue to be installed, it is in the interest of public health, welfare, and safety to understand their role in positively and negatively affecting drinking water safety.

AUTHOR'S PREFACE & ATTRIBUTION

Four manuscripts are enclosed as four separate studies (chapters) in this dissertation. The topics covered in this dissertation relate to drinking water safety, water chemistry and polymer science. For each study, the literature was reviewed, knowledge gaps and objectives were identified. Experiments were designed and conducted based on the knowledge-gaps identified and results were presented and thoroughly discussed.

Financial support for the efforts described in each chapter are as follows: Chapter 1 was funded by the Water Research Foundation and American Water Works Association's Water Industry Technical Action Fund (WITAF). Chapters 2 and 3 were funded by the United States Environmental Protection Agency (USEPA) (grant number: R836890). Chapter 4 was funded by the United States National Science Foundation (grant number: CBET-1228615) and Purdue Research Foundation Innovation Research Fund.

Attribution

A concise description of coauthors' contributions is listed as below. Xiangning Huang. and Dr. Andrew J. Whelton (Associate Professor in Lyles School of Civil Engineering and Division of Environmental and Ecological Engineering, Purdue University) contributed to all chapters.

Chapter 1

Ms. Stephane Andry (Division of Environmental and Ecological Engineering, Purdue University) contributed to conduct the literature search work.

Mr. Jessica Yaputri (Division of Environmental and Ecological Engineering, Purdue University) assisted experiment preparation and cleaning work.

Mr. Devin Kelly (Division of Environmental and Ecological Engineering, Purdue University) helped the experimental preparation and water samples collection.

Dr. David A. Ladner (Department of Environmental Engineering and Earth Sciences, Clemson University) made the contribution to solve technical problems and provided paper feedbacks.

Chapter 2

Mr. Dmitry Zemlyanov (Birck Nanotechnology Center, Purdue University) assisted with XPS and SEM measurements.

Ms. Lixby A. Diaz (School of Materials Engineering, Purdue University) made the contribution to BET test.

Dr. Maryam Salehi (Lyles School of Civil Engineering, Purdue University) helped with FTIR test.

Dr. Lia Stanciu (School of Materials Engineering, Purdue University) helped to solve technical problems during the BET test.

Chapter 3

Dr. Kelsey J. Pieper (Department of Civil and Environmental Engineering, Virginia Polytechnic Institute and State University) contributed to experimental design and provided paper feedbacks.

Ms. Lixby A. Diaz (School of Materials Engineering, Purdue University) assisted with FTIR test.

Chapter 4

Dr. Shou Zhao (Department of Chemistry and Biochemistry, University of California, Santa Barbara) contributed to synthesize lignin derived ligand.

Dr. Mahdi Abu-Omar (Department of Chemical Engineering and Department of Chemistry & Biochemistry, University of California, Santa Barbara) help to solve technical problems during the ligand synthesis.

CHAPTER 1. CRUDE OIL CONTAMINATION OF PLASTIC AND COPPER DRINKING WATER PIPES

1.1 Introduction

Oil spills pose threats to drinking water utilities, infrastructure, and community water supplies. For the year 2016, the U.S. National Response Center estimated that there were 23,170 chemical incidents in the U.S. Of those incidents, almost half (11,937) contaminated a water resource and about 60% were related to oil products [1]. Oils and related products such as crude, diesel, No. 2 fuel, and gasoline are often transported using hazardous material pipelines, trucks, and railcars [2-4]. As spills from these transport vessels have been previously demonstrated, contaminated source water can pass through drinking water treatment plants and water distribution systems, entering premise plumbing undetected [5-7] (Table 1.1).

A literature review demonstrated that oil spills in the U.S. and Canada have contaminated both surface and ground water supplies (Table 1.1). Oil spills commonly prompted communities to shut their intake (when warning was provided), truck in clean water, and/or switch to a backup water supply. Several incidents were first detected after contaminated water had passed through treatment plants and the water distribution system, and had reached customer taps [5, 7, 8]. A wide range of delays between the spill (e.g., pipe rupture) and detection were found (immediate detection vs. after 17 hr.) [9]. To protect public health and infrastructure, preventing oil contaminated water from reaching the water distribution system and customer infrastructure is desired, but evidence shows this does not always occur [10, 11].

Plastic water pipes are being chosen for new construction and water piping, which typically contain the largest surface area for contaminant sorption in distribution infrastructure. Plastic pipes

used for drinking water conveyance include crosslinked polyethylene (PEX) types A and B, high-density polyethylene (HDPE), and chlorinated polyvinylchloride (CPVC).

A previous study conducted by Marshutz (2001) showed that copper (90%) was the most widely used plumbing material in the U.S., compared to PEX (7%) and CPVC (2%) [18]. However, a more recent survey conducted in the southeastern United States revealed that PEX (54%) was the most common material for 59 households that replumbed followed by copper (9%) and CPVC (7%) [19]. The trend implies an increasing use of plastic pipes due to their flexibility and low cost. While some studies have shown oil contaminated soil or groundwater can externally permeate plastic water pipes (over long time), a short exposure period (hours to days) caused by conveyance of contaminated water has not been studied [20-24]. Because plastic pipes chemically differ from one another, water utilities that use some or all of these materials may have quite different experiences when trying to decontaminate their piping [25-27]. Furthermore, the degree of chemical leaching from oil contaminated pipes into clean water after the contaminated water has been flushed out has not been studied. The potential for contaminants to exceed drinking water maximum contaminant levels (MCLs), taste and odor limits also deserve scrutiny. Also, an important water quality parameter, total organic carbon (TOC) has been used to characterize the treatment efficiency of oil-field and natural gas produced water [28-30]. But TOC has not been evaluated as the potential indicator under the oil contaminated drinking water scenario.

Table 1.1 Summary of select oil spills affecting surface and ground water supplies used for drinking water

Location	Year	Pop.	Spill Details					Water System Details		
			Cause	Product	Delay, hr	Est. Vol.[a], gal	Dist., mi	Alert?	Assets	Actions
Nibley, UT	15	5,000	Truck	Diesel	na	nr	nf	No	WTP, DS, PS	Water stations in nearby cites
Mt. Carbon, WV	15	2,000	Rail	Crude: Light	na	378,000	nf	Yes	nc	Ran out; Trucked-in
Greenbrier Co., WV	15	12,000	Truck	Diesel	na	4,000	nf	Yes	WTP	Ran out; Trucked-in
Longueuil, CAN	15	300,000	AST	Diesel	na	7,500	nf	No	WTP, DS, PS	Trucked-in
Glendive, MT	15	5,500	Pipe	Crude: Light	nf	30,000	nf	No	WTP, DS, PS	Trucked-in
Lynchburg, VA	14	492,900	Rail	Crude: Light	na	29,600	nf	Yes	nc	Alt source
Mayflower, AR	13	-	Pipe	Crude: Heavy	12	> 210,000	nf	Yes	nc	N/A
Sundre, CAN	12	-	Pipe	Crude: Light	2.3	12,600	25	No	WTP	Trucked-in
Marshall, MI	10	-	Pipe	Crude: Heavy	>17	>800,000	25	Yes	nc	n/a
Reston, VA	93	1,000,000	Pipe	#2 Fuel oil	> 0	477,436	60	Yes	WTP	Alt source
Simpsonville, SC	91	10,500	Pipe	#2 Fuel oil	>0	550,000	32	Yes	WTP	Alt source; Trucked-in
Pittsburgh, PA	88	23,000	AST	Diesel	na	>800,000	600	Yes	WTP	Alt source; Trucked-in
Atlanta, GA	63	625,000	Pipe	Kerosene	nf	60,000	nf	No	WTP	Trucked in

a. Volume of spilled oils are approximate values

AST = Above ground storage tank; WTP = water treatment plant; DS = Distribution system; PS = Building plumbing systems; nc = not contaminated

Crude oils and their related products are complex mixtures that contain organic, inorganic, and radionuclide compounds. Monoaromatic (MAH) and polycyclic aromatic hydrocarbons (PAH) represent the majority of oil products by mass, and their compositions vary widely by geographical location and source [31, 32]. As shown in Table 1.2, crude oil and the related products can contain high organic chemical concentration and compounds have a wide range of physiochemical properties.

For regulated drinking water contaminants, the maximum contaminant concentration present in oils can be as much as 2.2×10^6 times greater than the corresponding drinking water MCLs (e.g., benzo(a)pyrene). Even when spilled oil might is diluted in the receiving water, there is still the risk that the drinking water standards could be exceeded for some oil-related contaminants. It is noteworthy that some compounds present in oils do not have federal drinking water standards (Table 1.2). However, as the 2014 chemical spill in West Virginia made clear, contaminants without federal drinking water standards can also pose health risks [33]. Therefore, it is important for emergency responders to fully characterize which contaminants are present in the spilled oil and contaminated water so health officials can conduct the appropriate risk assessments. Once oil enters a water, the fate of oil contaminants is a function of contaminant physiochemical properties, environmental conditions, and other materials that contact the contaminants (Figure 1.1). It is well-known that volatilization is a major mass transfer pathway for gasoline and kerosene spills because these liquids contain a great amount of high volatility constituents [34, 35]. However, dissolution of volatile contaminants also occurs simultaneously and fate of these contaminants in the water column is also important.

Table 1.2 MAH and PAH composition of various crude oils and refined products

Contaminant Detected in Oil	U.S. Drinking Water Limit, mg/L	Concentration in Oil, mg/L	Max Concentration in Oil/ Drinking Water Limit Ratio	Property		
				VP at 25°C, mmHg	Cw at 25°C, mg/L	Log K_{ow} at 23°C
Monoaromatic Hydrocarbons (MAHs)						
Benzene[a]	0.005[b]	0-2866	573,200	94.8	1,790	2.13
Toluene	1[b]	136-5,928	5,928	28.4	526	2.73
Ethylbenzene	0.7[b]	58-1,319	1,884	9.6	169	3.15
Total Xylenes	10[b]	396-6,187	618	6.61	178	3.12
C_3-Benzenes	-	940-13,780	-	-	-	-
Total MAH	-	1,570-21,920	-	-	-	-
Polycyclic Aromatic Hydrocarbons (PAHs)						
Naphthalene[a]	0.02[c]	3,939-20,852	1,042,600	8.50×10^{-2}	31	3.30
Phenanthrene	-	1,296-22,779	-	1.21×10^{-4}	1.15	4.46
Dibenzothiophene	-	609-2,033	-	2.05×10^{-4}	1.47	4.38
Fluorene	0.04[c]	513-4,986	124,650	6.00×10^{-4}	1.69	4.18
Chrysene	-	167-11,887		6.23×10^{-9}	2.00×10^{-3}	5.81
Biphenyl	-	7-839	-	-	-	-
Acenaphthylene	-	7-34		6.68×10^{-3}	16.1	3.94
Acenaphthene	0.06[c]	2.86-167	2,783	2.15×10^{-3}	3.9	3.92
Anthracene	0.3[c]	0.99-217	723	6.53×10^{-6}	0.0434(24°C)	4.45
Fluoranthene	-	0.27-80	-	9.22×10^{-6}	0.26	5.16
Pyrene	0.03[c]	4.10-552	18,400	4.50×10^{-6}	0.135	4.88
Benz(a)anthracene[a]	-	0.25-551	-	-	-	-
Benzo(b)fluoranthene[a]	-	0.12-125	-	5.00×10^{-7}	1.50×10^{-3}	5.78
Benzo(k)fluoranthene[a]	-	0.12-34	-	9.65×10^{-10}	8.00×10^{-4}	6.11
Benzo(e)pyrene	-	0.12-221	-	5.70×10^{-9}	6.30×10^{-3}	6.44
Benzo(a)pyrene[a]	0.0002[b]	0.12-449	2,245,000	-	-	-
Perylene	-	0-159	-	5.25×10^{-9}	4.00×10^{-4}	6.25
Indeno(1,2,3c,d)pyrene[a]	-	0-25	-	-	-	-
Dibenz(a,h)anthracene[a]	-	0-68	-	-	-	-
Benzo(g,h,i)perylene	-	0-83	-	1.00×10^{-10}	2.60×10^{-4}	6.63

Sources: [12-14]. a. Substance defined as a known or probable human carcinogen by the IARC and NTP. [15, 16]; b. U.S. EPA Maximum Contaminant Level of Drinking Water (MCL) (mg/L) [17]; c. Reference dose proposed by U.S. EPA Drinking Water Health Advisories (mg/kg/day) [14]; VP-Vapor Pressure, mmHg; Cw-Water Solubility, mg/L; Log K_{ow}- Octanol-Water Partition Coefficient; Dash (-) represents no Drinking Water Standards or Health Advisories available for that contaminant. Reproduced with permission by the Water Research Foundation (2016).

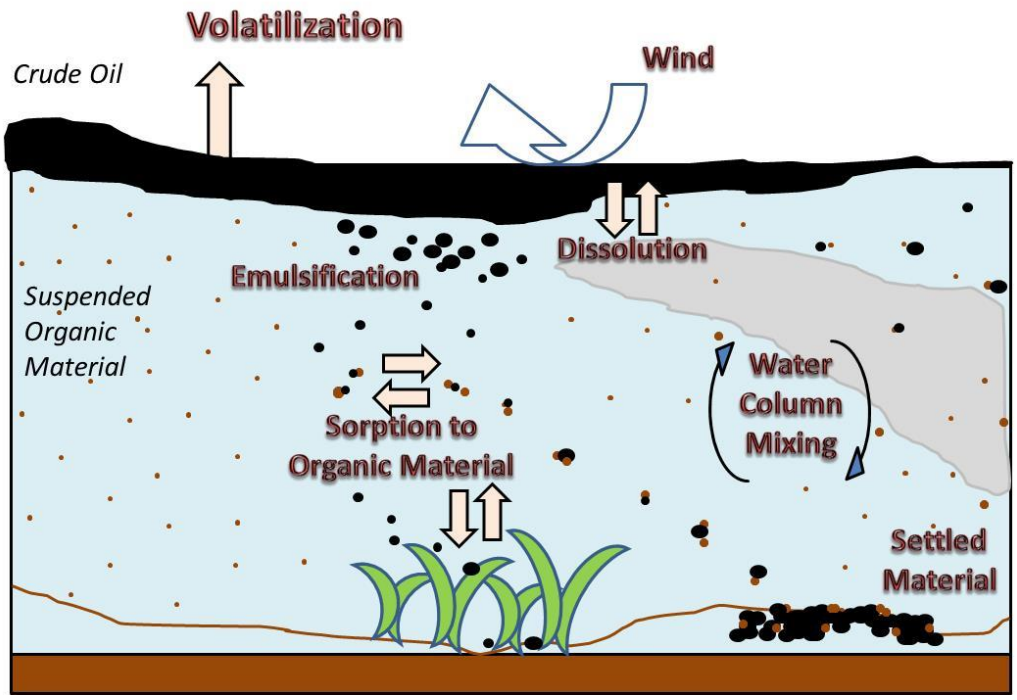

Figure 1.1 Physiochemical processes of spilled oil in the environment. Reproduced with permission by the Water Research Foundation (2016).

This study was initiated to understand the degree to which plastic and copper pipes become contaminated by oil and subsequent leaching of sorbed contaminants into the water supply. The goal of this work was to investigate which plumbing materials were more susceptible (easier to sorb and desorb contaminants) during the short duration contamination events and the duration required for contaminants in the water back to the safe level. The specific objectives were to (1) assess the potential of benzene, toluene, ethylbenzene, and xylenes from crude oil contaminated water to sorb and desorb from the PEX, HDPE, CPVC, and copper pipes over a 30-day leaching period, (2) determine if other crude oil related contaminants (e.g. MAHs and PAHs) can be sorbed and desorbed from PEX-A pipe, and (3) evaluate whether TOC concentration is a good indicator for oil contaminated water.

1.2 Experimental

1.2.1 Pipe Materials, Chemicals and Preparation

PEX-A, PEX-B, HDPE, CPVC and copper potable water pipes were purchased from regional pipe supply companies with different inner diameters: 1.70, 1.68, 2.09, 1.77 and 2.06 cm, respectively. PEX-A pipe was manufactured with a medium-density polyethylene (PE) resin while PEX-B pipe was manufactured with a high-density PE resin. HDPE pipe was also manufactured with a high-density resin. All pipes were labeled as certified for potable water with a National Sanitation Foundation International [36] logo. BTEX (e.g. benzene, toluene, ethylbenzene and total xylene) (SKU-43728) and trimethylbenzene isomer analytical standards were purchased from Sigma Aldrich. The DEP(MA)-PAH mix was obtained from AccuStandard (1000µg/mL in CH_2Cl_2). Louisiana light sweet crude (LLSC) oil used for the experiments was obtained from a crude oil processing facility in Mobile, AL.

Before pipe contamination experiments were conducted, all new pipes were tap water rinsed and disinfected similar to field protocols [37]. Pipes were flushed for 10 min. with tap water then were filled with a 200 mg/L free chlorine solution (made from 5.65-6% wt% of NaOCl, Fisher Chemical). The laboratory prepared tap water was a low alkalinity water recipe adopted from prior work, with the pH adjusted in the range of 6 to 8 [38, 39]. Teflon® wrapped silicon stoppers were used to keep the water in place and prevent leaking. After 3 hr. stagnation, pipes were drained and flushed again using tap water for 3 min.

1.2.2 Pipe Contamination

Pipes were contaminated with one of two crude oil / contaminated water solutions: (1) 0.05% v/v solution and (2) 0.3% v/v solution. The 0.3% solution was adopted from an ongoing U.S. EPA crude oil-cast iron water pipe contamination study [40]. An oil-water solution 50 times less

concentrated (i.e. 0.05%) was also examined in the present study. Oil-water solutions were prepared by 20 hr. of mixing LLSC and synthetic tap water in aspirator bottles [41]. After 5 hr. of stagnation, aliquots were removed through the bottom aspirator valve to obtain water with the soluble fraction of oil. Pre-conditioned pipe coupons were filled with oil solutions without headspace, capped and remained stagnant for 3 days. This exposure duration was based on prior Do Not Use drinking water orders which typically lasted 2 to 3 days, but for some cases the contaminated water could be remained in place for up to 30 days [42]. A control group was prepared by filling pipe coupons with synthetic tap water only. All the experiments were conducted in triplicate.

1.2.3 Pipe Decontamination

After the pipe contamination period, each pipe was drained and rinsed with about 200 mL synthetic tap water to remove any residue on the pipe inner wall. Next, pipes were filled and replaced with freshly prepared synthetic tap water. This draining and refilling procedure was repeated every three days for up to 30 days [38, 43]. At day 3, 6, 9, 15, and 30, water drained from the pipe was collected and characterized for BTEX, other MAHS, potential PAHs and TOC concentration. After sampling process on certain day, pipe segments would be refilled with clean water. Leaching results were expressed in two forms: (1) BTEX/TOC aqueous concentrations, µg/L or mg/L and (2) conversion of BTEX/TOC levels to µg/dm^2 so pipe diameter differences were considered. For more details, BTEX/TOC leaching data were calculated by multiplying measured concentration (µg/L) by volume of the pipe coupon (L) and divided by pipe inner surface area (dm2).

1.2.4 Water Quality and Statistical Analysis

Headspace solid phase microextraction-gas chromatography/mass spectrometry (HS-SPME-GC/MS) was used to quantify aqueous BTEX (benzene, toluene, ethylbenzene and xylene, total)

concentration [44, 45] (Table 1.3). Method details are shown elsewhere [11]. A Supelco SPME fiber assembly (100 µm PDMS, fused silica 23 Ga) was selected to extract the volatile compounds. The fiber was pre-conditioned with a hot injector inlet (250 ^{o}C) for 30 min. The GC column was Zebron ZB-WAX from Phenomenex (diameter 0.32 mm, length 30 m, film 0.5 µm) coupled with multipurpose MS detector. BTEX standard and synthetic tap water were used to make standard solutions. Calibration curves were developed for both low (0.2-10 µg/L) and high range (50-2,000 µg/L) of BTEX solutions with the correlation coefficient of 0.99 or greater. The total xylene concentration was calculated as counting o-, m-, and p-xylene isomers and reported in this study. The liquid-liquid extraction technique was performed as described from a past study and the concentrate was analyzed by GC-MS [46]. Peaks detected from concentrates were confirmed with BTEX, trimethylbenzene and PAHs standards (e.g. retention time and parent ion), coupled with mass spectral library. TOC concentration was determined using a Shimadzu TOC-L CPH analyzer with a calibration standard curve ranging up to 10 mg/L (USEPA method 415.1) [47, 48]. NCSS software was applied to perform single and multi-variate analysis of variance (ANOVA) with a $\alpha = 0.05$ significance level.

Table 1.3 SPME-GC/MS target compounds

Compounds	**RT (min)**	**Quantification ions (m/z)**	**MDL[b] (µg/L)**
Benzene	2.84	78, 77, 52	0.24
Toluene	4.38	91, 92, 65	0.18
Ethyl benzene	5.98	91, 106, 51	0.16
Xylene, total	Various [a]	91, 106, 105	0.44

a. RT, retention time for *o*-, *m*-Xylene and *p*-Xylene ranged from 6.10 to 7.40 min.; b. MDL, minimum detection limit for each compound was calculated based on 7 replicates, MDL = Std. dev * $t_{(n-1).}$

1.3 Results and Discussion

1.3.1 BTEX Fate in Contact with Plastic and Copper Pipe Materials

After oil contaminated water contacted pipes for three days, aqueous MAH concentration was significantly reduced (Table 1.4) ($p < 0.01$). The initial BTEX concentrations for the crude oil water were: benzene (935 ± 41 µg/L), toluene (284 ± 13 µg/L), ethylbenzene (205 ± 3 µg/L), and total xylenes (1,139 ± 32 µg/L). After the 3 day exposure period, BTEX levels were much lower for all plastic pipe solutions compared to copper pipe solution. These results indicated that plastic pipes have more affinity to BTEX compounds than copper pipes. It is well-known BTEX compounds can permeate the plastic pipes studied, but this short duration exposure and head-to-head experiment underscores how different the materials perform under a similar contamination scenario. Additional experiments were conducted to evaluate pipe decontamination and leaching for a 30 day period.

Table 1.4 BTEX concentration for PEX-A, PEX-B, HDPE, and copper pipes exposed in the 0.05% oil mixture for 3 days

Pipe	**Concentration (µg/L)**			
Material	**B**	**T**	**E**	**X**
PEX-A	255 ± 35	21 ± 4	95 ± 1	384 ± 3
PEX-B	269 ± 35	24 ± 5	96 ± 1	389 ± 4
HDPE	214 ± 10	17 ± 0	95 ± 2	378 ± 9
Copper	397 ± 74	107 ± 23	141 ± 7	718 ± 33

Data shown represents the mean (standard deviation) for triplicate pipe samples. Results for CPVC initial and after 3 days BTEX levels in the crude oil mixture were not able to be measured.

As expected, the greatest BTEX concentrations were detected for all pipes on day 3, but BTEXs were only detected on day 3 for copper pipes (Table 1.5). Absence of BTEX on subsequent testing days is likely due to residual contaminants that had adhered to the copper pipe surface and were not removed during contaminated pipe tap water rinsing. For all plastic pipes, benzene and

toluene were detected in water for up to 15 days. This result indicated that those contaminants had permeated and were desorbing from the plastic pipes. Except for CPVC pipe, benzene and toluene were detected for all PE pipes for 30 days. 3. Copper drinking water pipe is a common material used to replacement plastic pipes that have been externally permeated due to petroleum product spills [26, 49].

As simulated water use continued, lower concentrations of BTEXs were found. PEX-A pipe was the most susceptible to contamination as reflected by the greatest amount of BTEX desorbed during the study. This finding indicates that the type of water pipe even within the same water distribution system or building plumbing could influence why different drinking water contaminant levels are detected during after contaminated drinking water has been flushed out. Water utilities and health officials should consider the type of water pipe material in contact with contaminated drinking water when determining the time needed to return infrastructure to safe use. A review of drinking water contamination incidents indicated this phenomenon has not been incorporated into water distribution and building plumbing decontamination procedures [42].

During the 30 day decontamination study for the plastic and copper pipes examined, benzene was the only compound found to exceed its MCL. For the 0.3% oil mixture condition, all four plastic pipes exceeded the benzene MCL on day 9 (Table 1.5). Even on day 15, all polyethylene pipes leached benzene above its corresponding MCL. Copper pipe was the least affected (MCL only exceeded on day 3). PEX-A pipe consistently resulted in the greatest benzene concentration throughout the 30 day study. For the less concentrated oil water mixture (0.05%) condition, the detected benzene concentration was much lower, but still exceeded its MCL for 11 of 25 pipe-exposure duration pairs. Again, benzene levels from PEX-A pipe were markedly greater than for PEX-B, HDPE, and CPVC pipes. MCLs for toluene (1,000 µg/L), ethylbenzene (700 µg/L), and

total xylene (10,000 µg/L) were not exceeded or approached for either oil-water condition. However, on day 3 TEX compounds exceeded their taste and odor thresholds for the 0.3% crude oil contamination scenario (Table 1.5). Even though TEX compounds were below their health based MCLs, their presence would have contributed to taste and odor problems for polyethylene materials. In contrast, for the 0.3% oil mixture condition TEX levels for CPVC and copper pipes slightly exceeded taste and odor thresholds for day 3 only.

Table 1.5 BTEX concentration during 30 day decontamination study for PEX-A, PEX-B, HDPE, CPVC, and Copper pipes

Material	Mean Desorbed Concentration (µg/L)							
	B	**T**	**E**	**X[a]**	**B**	**T**	**E**	**X**
		0.3% oil mixture Day 3				*0.05% oil mixture Day 3*		
PEX-A	**1,434.4**	140.2 ^{OT}	2.43 ^{O}	73.00 ^{O}	**77.0**	12.6	-	-
PEX-B	**1,167.9**	116.8 ^{OT}	1.68	66.80 ^{O}	**36.0**	3.53	-	-
HDPE	**1,274.1**	129.0 ^{OT}	2.07 ^{O}	58.50 ^{O}	**39.6**	1.61	-	-
CPVC	**81.03**	38.88 ^{O}	2.42 ^{O}	10.36	**9.22**	0.76	-	
Copper	**5.45**	7.90	2.18 ^{O}	22.60 ^{O}	0.46	0.85	-	-
		0.3% oil mixture Day 6				*0.05% oil mixture Day 6*		
PEX-A	**121.1**	9.10	1.09	8.72	**56.7**	4.61	-	-
PEX-B	**80.2**	2.89	0.47	3.68	**25.4**	3.03	-	-
HDPE	**100.5**	1.56	-	2.38	**24.2**	2.02	-	-
CPVC	**10.63**	0.98	-	-	2.38	0.51	-	
Copper	-	-	-	-	-	-	-	-
		0.3% oil mixture Day 9				*0.05% oil mixture Day 9*		
PEX-A	**51.3**	11.1	-	-	**25.4**	0.61	-	-
PEX-B	**37.6**	9.82	-	-	**5.33**	0.28	-	-
HDPE	**47.4**	9.13	-	-	**5.03**	0.33	-	-
CPVC	**5.12**	0.42	-	-	1.26	0.43	-	-
Copper	-		-	-	-	-	-	-
		0.3% oil mixture Day 15				*0.05% oil mixture Day 15*		
PEX-A	**21.0**	9.46	-	-	**6.14**	-	-	-
PEX-B	**16.5**	5.33	-	-	3.01	-	-	-
HDPE	**18.5**	7.63	-	-	2.10	-	-	-
CPVC	1.74	0.28	-	-	0.70	0.37	-	-
Copper	-	-	-	-	-	-	-	-
		0.3% oil mixture Day 30				*0.05% oil mixture Day 30*		
PEX-A	0.23	0.48	-	-	0.79	-	-	-
PEX-B	0.34	0.20	-	-	0.54	-	-	-
HDPE	0.28	0.26	-	-	0.25	-	-	-
CPVC	-	-	-	-	-	-	-	-
Copper	-	-	-	-	-	-	-	-

a Xylene represents total xylene, which counts for o-, m-, p-isomers; - represents the value is less than detection limit or not detectable; Red and bolded text represents a concentration that exceeds an MCL; o Concentration is greater than the odor threshold; ^{T} Concentration is greater than the taste threshold.

MDL	0.24	0.18	0.16	0.44
EPA MCL	5	1,000	700	10,000
^{O}Odor [50, 51]	2,000	24	2	20
*Taste [50, 51]	500	40	72	300

1.3.2 The Role of Pipe Type on MAH Concentration

To determine the role of pipe type on leaching performance, BTEX concentrations were normalized using each pipe's inner wall surface area (μg/dm^2-time). MAH flux, mass/surface area-time, from PE materials was initially orders of magnitude greater than flux from CPVC and copper pipes (Figures 1.2 and 1.3). Differences were less noticeable by day 30. When the inner pipe wall surface area exposed to contaminated water was normalized across pipes, the PEX-A material was still the most susceptible to BTEX permeation and leaching. For the 0.05% oil contamination scenario, the rank of most to least contaminated pipe materials was PEX-A > HDPE > PEX-B > CPVC > copper ($p < 0.01$) (Table 1.6).

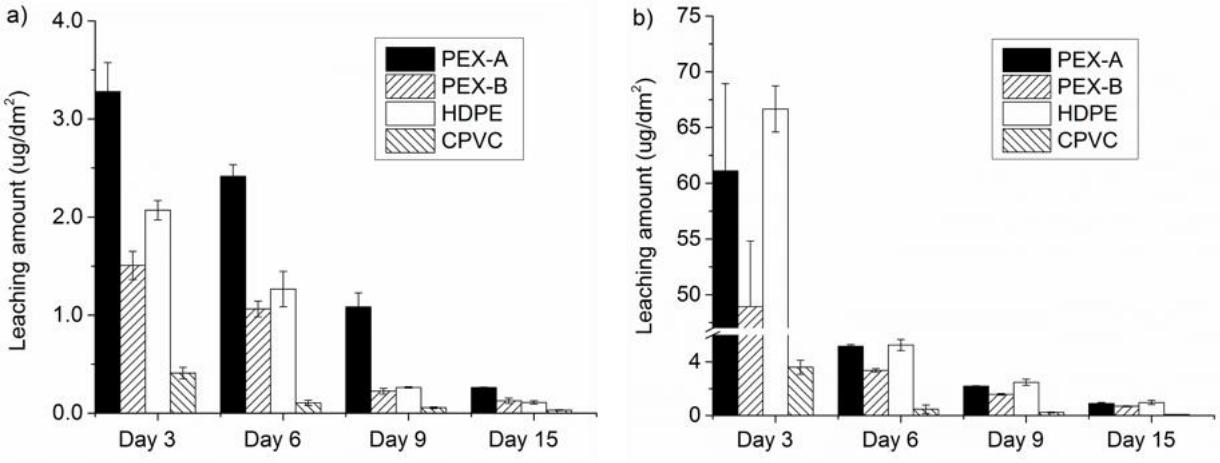

Figure 1.2 Benzene leaching data from different pipe materials, presented as mass per unit surface area, during decontamination process from two contamination scenarios: a) 0.05% oil mixture contamination scenario and b) 0.3% oil mixture contamination scenario.For each pipe material, 3 pipe coupon replicates were adopted to measure the consistency. Column height is the average and the error bars show the standard deviation. Reproduced with permission by the Water Research Foundation (2016).

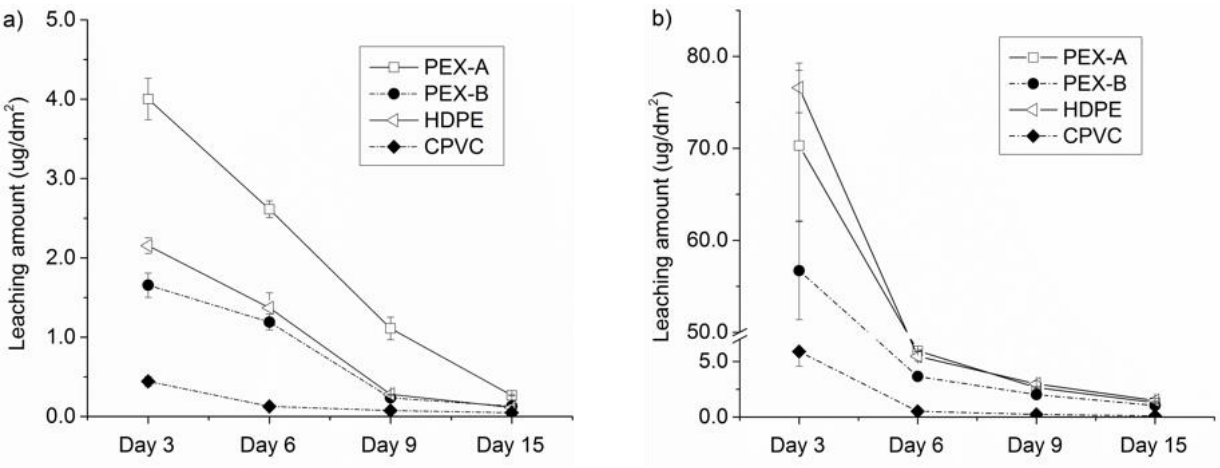

Figure 1.3 Total BTEX leaching from different pipe materials, presented as mass per unit surface area, during decontamination process from two contamination scenarios: a) 0.05% oil mixture contamination scenario; b) 0.3% oil mixture contamination scenario.For each pipe material, three pipe coupon replicates were adopted to measure the consistency. Symbols represent the average and the error bars show the standard deviation. Reproduced with permission by the Water Research Foundation (2016).

BTEX leaching from pipe materials depended on the initial drinking water oil exposure concentration, the type of plumbing materials, as well as the exposure duration after contamination occurred (Table 1.6). When the oil concentration was increased to 0.3% v/v, no difference was found between PEX-A and HDPE pipes (p = 0.896). The remaining materials had lower fluxes than both PEX-A and HDPE pipes during the study period: PEX-B > CPVC > Copper ($p < 0.05$). Copper pipe sorbed and desorbed much less contaminant compared to all plastics studied (Table 1.5).

1.3.3 Leaching of Oil Related Contaminants other than BTEX

Because PEX-A pipe was the most susceptible material to BTEX contamination, leaching from this pipe was studied in greater detail. Analytical standards were used to identify the tentatively identified compounds in both the crude oil/water mixture and water samples exposed to contaminated pipes (Figure 1.4). After the simulated 3 day Do Not Use drinking water condition with the 0.3% v/v crude oil-water mixture, PEX-A pipe on day 3 leached a variety of oil related

compounds (Figure 1.5). In addition to BTEX several other MAHs and PAHs had sorbed and desorbed into drinking water. Contaminants that were confirmed include 1,3,5-trimethylbenzene, 1,2,4-trimethylbenzene, 1,2,3-trimethylbenzene, naphthalene, 2-methylnaphthalene and 1-methylnaphthalene. None of these contaminants have drinking water MCLs [17]. A limitation of this study is that drinking water disinfectants were not present in the test water for this experiment. Although, analytical methods oil constituents are susceptible to halogenation during water treatment [52], and could be transformed into other compounds also not routinely screened for during standard analytical methods. Results show that once contaminated water is suspected, chemical analysis is needed to thoroughly identify the compounds present [11]. Negative emergency response, public health, and public confidence consequences of issuing water safety guidance without appropriately identifying chemicals in the contaminated drinking water can be found elsewhere [54].

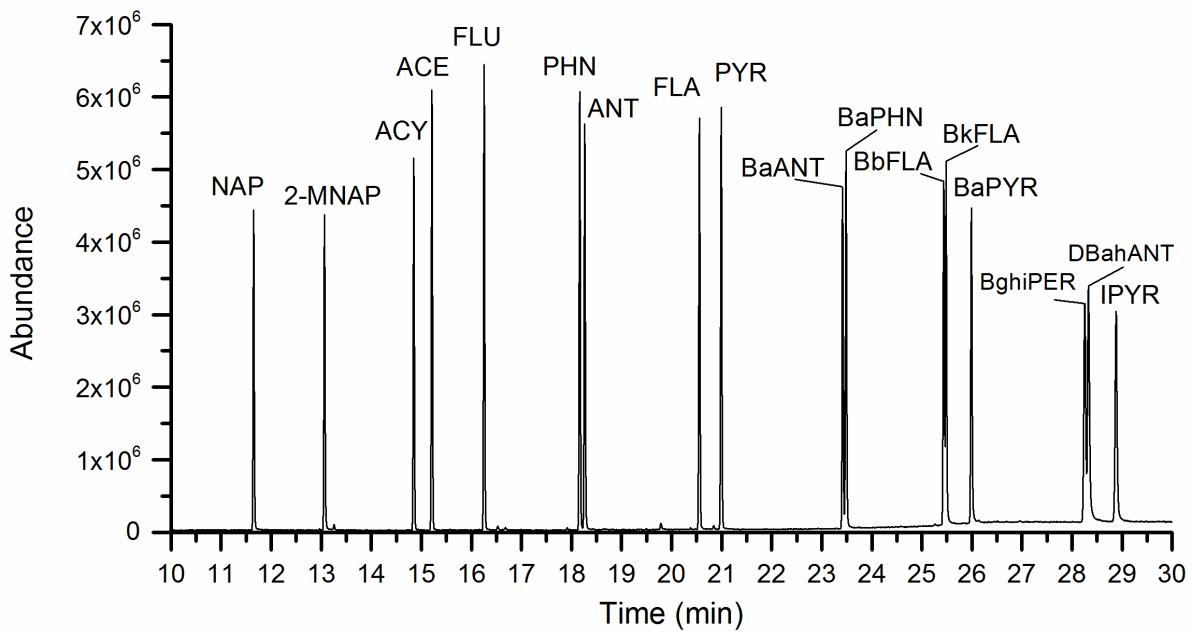

Figure 1.4 Total ion chromatogram (TIC) of PAH standards containing 17 PAHs with peaks labeled as: NAP: naphthalene (rt=11.65, m/z=128); 2-MNP: 2-methylnaphthalene (rt=13.07, m/z=142); ACY: acenaphthylene (rt=14.85, m/z=152); ACE: acenaphthene (rt=15.21, m/z=154); FLU: fluorene (rt=16.25, m/z=165); PHN: phenanthrene (rt=18.17, m/z=178); ANT: anthracene (rt=18.27, m/z=178); FLA: fluoranthene (rt=20.56, m/z=202); PYR: pyrene (rt=20.99, m/z=202); BaANT: benzo(a)anthracene (rt=23.42, m/z=228); BaPHN: benzo(a)phenanthrene (rt=23.49, m/z=228); BbFLA: benzo(b)fluoranthene (rt=25.44, m/z=252); BkFLA: benzo(k)fluoranthene (rt=25.49, m/z=252); BaPYR: benzo(a)pyrene (rt=25.99, m/z=252); BghiPER: Benzo(g,h,i)perylene (rt=28.25, m/z=276); DBahANY: Dibenzo(a,h)anthracene (rt=28.33, m/z=278)and IPYR: Indeno(1,2,3-cd)pyrene (rt=28.88, m/z=276). rt stands for retention time. m/z is the parent ion for the contaminant.

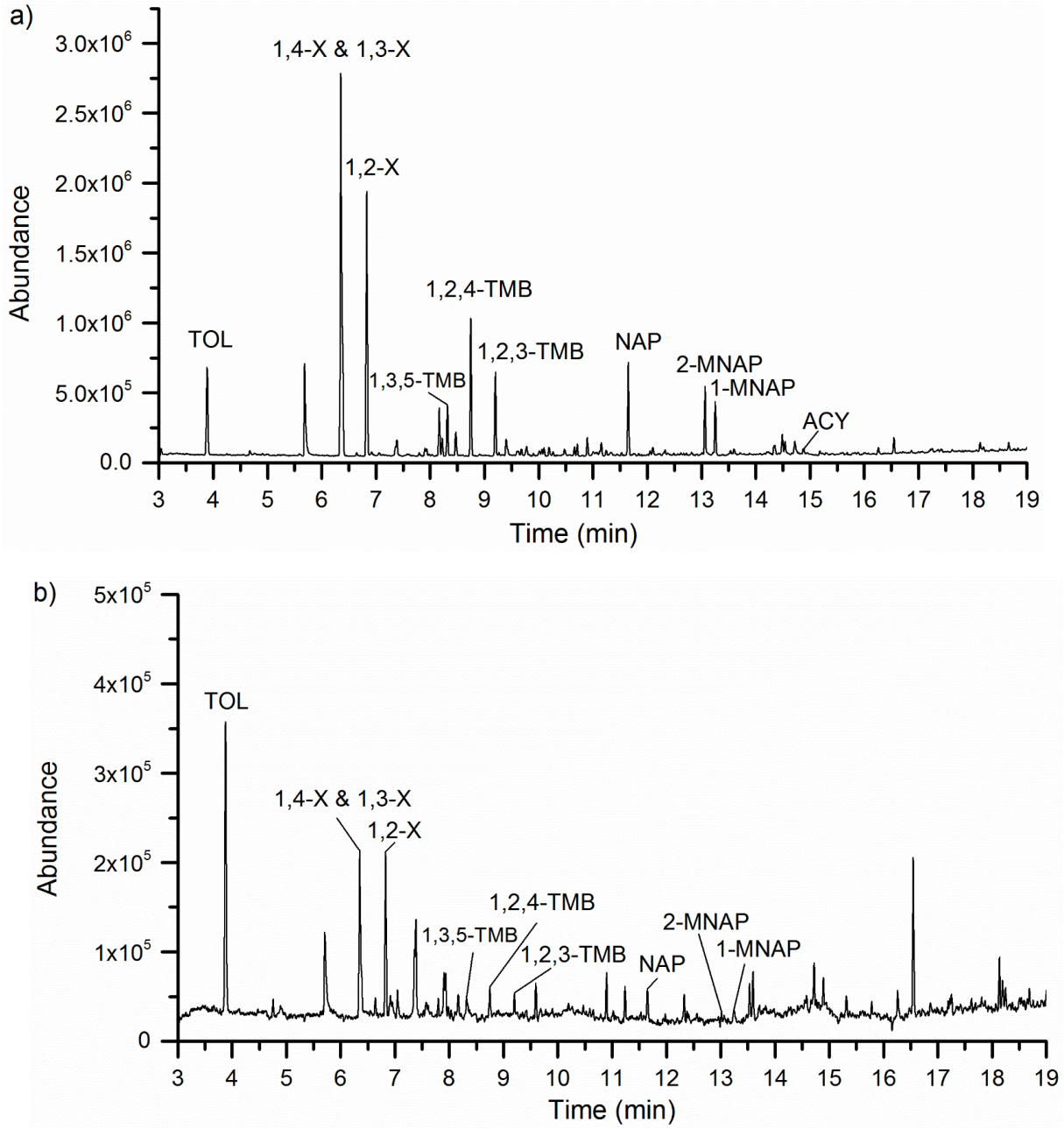

Figure 1.5 Total ion chromatogram (TIC) of a) 0.3% crude oil mixture and b) on day 3 contaminated PEX-A pipe leaching water sample with peaks labeled as: TOL: toluene (rt = 3.89 min); 1,4-X: 1,4-xylene (rt = 6.35 min); 1,3-X: 1,3-xylene (rt = 6.38 min); 1,2-X: 1,2-xylene (rt = 6.83 min); 1,3,5-TMB: 1,3,5-trimethylbenzene (rt = 8.32 min); 1,2,4-TMB: 1,2,4-trimethylbenzene (rt = 8.75 min); 1,2,3-TMB: 1,2,3-trimethylbenzene (rt = 9.20 min); NAP: naphthalene (rt = 11.65 min); 2-MNAP: 2-methylnaphthalene (rt = 13.07 min); 1-MNAP: 1-methylnaphthalene (rt = 13.25 min) and ACY: acenaphthylene (rt = 14.85 min). These contaminants were not detected from new PEX-A pipe leaching water sample. Benzene not shown as it eluted before the solvent cut off time. rt stands for retention time.

1.3.4 The Value of TOC Monitoring

Due to high background organic carbon released from the plastic pipes, TOC monitoring was not effective for estimating MAH reductions. TOC concentrations in control groups were greatest for new PEX-A pipes (> 6.5 mg/L), while other types of piping materials had TOC levels less than 1 mg/L. This finding agreed well with the past study, where PEX-A pipes also founds leached more TOC than other pipe materials (e.g. PEX-B and PEX-C) [38]. The normalized TOC leaching data failed to differentiate the 0.3% and 0.05% oil mixture contamination scenario from control groups (Table 1.6).

Table 1.6 Statistical analysis of multi-variant parameters

Parameters	**BTEXs (μg/dm^2)**		**TOC (μg/dm^2)**	
	p value	*Significant or not?*	*p value*	*Significant or not?*
Main effect				
Oil concentration	<0.05	Yes	0.73	No
Pipe Material	<0.05	Yes	<0.05	Yes
Exposure duration	<0.05	Yes	0.15	No
Interaction effect				
Conc. and material	<0.05	Yes	0.30	No
Conc. and time	<0.05	Yes	0.13	No
Material and time	<0.05	Yes	<0.05	Yes

Reproduced with permission by the Water Research Foundation (2016).

1.3.5 Future Work

To effectively recover water distribution system assets and building plumbing, results show the following information is important: the type of pipe/materials exposed, chemicals present, their initial concentration, and the duration of contaminated water exposure. These factors will influence the time needed to desorb chemicals and return infrastructure to safe use. Other factors not examined in this study but likely would influence the time needed to desorb chemicals from infrastructure include water temperature, pipe scales, biofilms, other materials such as gaskets, fixtures, valves, appliances, and water heaters in the plumbing system. As reported by others,

flushing is a commonly applied pipe cleaning method, but sometimes infrastructure replacement was conducted [35]. Surfactants have shown to be inefficient for removing BTEX from copper and PEX-A pipe [53]. Also found was that some surfactant solutions can damage plastics. It is recommended that additional work be conducted to determine what actions are needed to safely decontaminate oil contaminated distribution and plumbing infrastructure.

1.4 Conclusion

The goal of this study was to investigate the susceptibility of plastic and copper service lines to short-term oil contamination and assess their subsequent ability to leach contaminants into the water supply. Results showed that copper was the least susceptible to contamination, but did desorb BTEX compounds during the first 3 day leaching period. PEX, HDPE, and CPVC pipe materials sorbed and desorbed much greater levels of BTEXs into drinking water than copper pipe. PEX-A and HDPE pipes were more vulnerable to contamination than PEX-B pipe, while CPVC exhibited the least susceptibility among the plastics. Benzene accounted for the majority of the total leached MAHs for all types of pipe materials and often exceeded the MCL; taste and odor thresholds were also exceeded. Non-BTEX compounds like trimethylbenzene isomers and PAH contaminants were also found desorbing from a PEX-A pipe.

The ability of a water distribution system to return contaminated pipes to service will be influenced by several factors. These include the type of pipe contaminated, the composition of crude oil contaminated water, aqueous concentration of contaminants, and the time since the contaminated water was removed from the pipe. A drinking water's TOC concentration was not a good indicator of oil contaminated water. Other water characterization techniques (e.g. GC-MS) were needed to better characterize the target contaminants and the levels in the water. Tentative

identification of compounds enabled the authors to then purchase analytical standards and confirm the presence of MAHs and PAHs.

Results of this study are specific to the crude oil tested. Difference composition of oils could result in different aqueous concentrations. Considering the complex composition of oil products (i.e., MAHs, PAHs, metals and radionuclides), other contaminants should also be monitored and studied. Future work is recommended to examine the short-term interaction of contaminants with water distribution system materials under different water hydraulic conditions (i.e., various flow and pressure conditions).

1.5 References

[1] J.L. Weidhaas, A.M. Dietrich, N.J. DeYonker, R. Ryan Dupont, W.T. Foreman, D. Gallagher, J.E. Gallagher, A.J. Whelton, W.A. Alexander, Enabling Science Support for Better Decision-Making when Responding to Chemical Spills, J. Environ. Quality, 45 (2016) 1490-1500.

[2] C.E. Restrepo, J.S. Simonoff, R. Zimmerman, Causes, cost consequences, and risk implications of accidents in US hazardous liquid pipeline infrastructure, Int. J. Crit. Infr. Protect., 2.1 (2009): 38-50.

[3] D. Yuhua, Y. Datao, Estimation of failure probability of oil and gas transmission pipelines by fuzzy fault tree analysis, J. Loss Prevent. Process Ind., 18.2 (2005): 83-88.

[4] Pipeline and Hazardous Materials Safety Administration (PHMSA), Pipeline Safety: Hazardous Liquid Pipelines Transporting Ethanol, Ethanol Blends, and other Biofuels. http://www.phmsa.dot.gov/staticfiles/PHMSA/DownloadableFiles/Files/EthanolNotice7.07%20(Policy%20Statement%20to%20convert).pdf, 2007 (accessed 15.08.06).

[5] A. Anselmo, J. Sullivan, DME: The Best Fuel, Period, ChemBioPower . http://static1.squarespace.com/static/54a07d7ae4b093269b63ac5c/t/54e514a3e4b0773025013b38/1424299171380/CBP-WhitePaper-v5.pdf, 2015 (accessed 15.10.13).

[6] Montana Department of Environmental Quality (DEQ), Bridge Pipeline's Oil Spill on the Yellowstone River near Glendive. http://www.deq.mt.gov/yellowstonespill2015.mcpx#Updates, 2015 (accessed 15.02.03).

[7] D. Luther, Another American Water Emergency: Utah Municipal Water Supply Tainted by Chemical Spill, Freedomoutpost. http://freedomoutpost.com/2015/04/another-american-water-emergency-utah-municipal-water-supply-tainted-by-chemical-spill/, 2015 (accessed 15.05.01).

[8] Agency for Toxic Substance & Disease Registry (ATSDR), 2015 Yellow River Oil Spill, http://www.atsdr.cdc.gov/yellowstone_river.html, 2015 (accessed 15.01.20).

[9] National Transportation Safety Board (NTSB), Enbridge Incorporated Hazardous Liquid Rupture and Release. http://www.ntsb.gov/investigations/AccidentReports/Reports/PAR1201.pdf, 2010 (accessed 15.04.15).

[10] T.M. Brody, P.D. Bianca, J. Krysa, Analysis of inland crude oil spill threats, vulnerabilities, and emergency response in the midwest United States, Risk Anal., 32 (2012) 1741-1749.

[11] X. Huang, A.J. Whelton, S. Andry, J. Yaputri, D. Kelly, D.A. Ladner, Interaction of Fracking and Crude Oil Contaminants with Water Distribution Pipes, EO 2014-07, Water Research Foundation (WRF), 2016.

[12] Environmental Canada, ETC Spills Technology Databases, Oil Properties Database. http://www.etc cte.ec.gc.ca/databases/oilproperties/, 2001 (accessed 15.02.21).

[13] Syracuse Research Corporation (SRC), FatePointers Search Module. http://esc.srcinc.com/fatepointer/search.asp, 2013 (accessed 15.02.10).

[14] U.S. Environmental Protection Agency (EPA), 2012 Edition of the Drinking Water Standards and Health Advisories. http://water.epa.gov/action/advisories/drinking/upload/dwstandards2012.pdf, 2012 (accessed 15.02.13).Washington, D.C.

[15] International Agency for Research on Cancer (IARC). Agents Classified by the IARC Monographs, Volumes 1–111. World Health Organization. 2015.

[16] U.S. Department of Health and Human Services, 13th Report on Carcinogens. http://ntp. niehs. nih. gov/pubhealth/roc/roc13/index. html, 2014 (accessed 15.03.02).
[17] U.S. Environmental Protection Agency (EPA), National Primary Drinking Water Regulations. http://water.epa.gov/drink/contaminants/upload/mcl-2.pdf, 2009 (accessed 15.01.10).Washington, D.C.
[18] S. Marshutz, Hooked on copper: A comparison shows the gap is narrowing with PEX gaining popularity as a preferred material in new construction and repiping work, Reeves Journal, (2001).
[19] J. Lee, E. Kleczyk, D.J. Bosch, A.M. Dietrich, V.K. Lohani, G. Loganathan, Homeowners' decision-making in a premise plumbing failure-prone area (PDF), J. Am. Water Works Assoc., 105.5 (2013): E236-E241.
[20] American Water Works Assiciation (AWWA), Permeation and Leaching. https://www.epa.gov/sites/production/files/2015-09/documents/permeationandleaching.pdf, 2002 (accessed 15.06.08).
[21] A.R. Berens, J.P. Pfau, D.E. Crum, K.E. Carns, Prediction of Organic Chemical Permeation Through PVC Pipe [with Discussions], J. Am. Water Works Assoc., (1985): 57-65.
[22] K.P. Chao, P. Wang, Y.T. Wang, Diffusion and solubility coefficients determined by permeation and immersion experiments for organic solvents in HDPE geomembrane, J. Hazard. Mater., 142.1 (2007): 227-235.
[23] T.M. Holsen, J.K. Park, D. Jenkins, R.E. Selleck, Contamination of potable water by permeation of plastic pipe, J. Am. Water Works Assoc., (1991): 53-56.
[24] F. Mao, J.A. Gaunt, C.L. Cheng, S.K. Ong, Permeation of BTEX compounds through HDPE pipes under simulated field conditions, J. Am. Water Works Assoc., 102.3 (2010): 107.
[25] A.J. Whelton, A.M. Dietrich, D.L. Gallagher, Impact of chlorinated water exposure on contaminant transport and surface and bulk properties of high-density polyethylene and cross-linked polyethylene potable water pipes, J. Environ. Eng., 137.7 (2011): 559-568.
[26] S.K. Ong, J. Gaunt, F. Mao, C.L. Cheng, L. Esteve-Agelet, C. Hurburgh, Impact of hydrocarbons on PE/PVC pipes and pipe gaskets, J. Am. Water Works Assoc., (2008).
[27] I. Skjevrak, A. Due, K.O. Gjerstad, H. Herikstad, Volatile organic components migrating from plastic pipes (HDPE, PEX and PVC) into drinking water, Water Res., 37.8 (2003): 1912-1920.
[28] X. Zhao, Y. Wang, Z. Ye, A.G. Borthwick, J. Ni, Oil field wastewater treatment in biological aerated filter by immobilized microorganisms, Process Biochem., 41.7 (2006): 1475-1483.
[29] Y.S. Li, L. Yan, C.B. Xiang, L.J. Hong, Treatment of oily wastewater by organic–inorganic composite tubular ultrafiltration (UF) membranes, Desalination, 196.1 (2006): 76-83.
[30] L.M. Jackson, J. Myers, Design and construction of pilot wetlands for produced-water treatment, in: SPE Annual Technical Conference and Exhibition, 2003.
[31] U.S. Environmental Protection Agency (EPA), Crude Oil Category: Category Assessment Document. http://www.epa.gov/hpv/pubs/summaries/crdoilct/c14858ca.pdf, 2011 (accessed 15.02.18). Washington, D.C.
[32] W.K. Seifert, J.M. Moldowan, Paleoreconstruction by biological markers, Geochim. Cosmochi,. Ac., 45.6 (1980): 783-794.
[33] A.J. Whelton, L. McMillan, M. Connell, K.M. Kelley, J.P. Gill, K.D. White, R. Gupta, R. Dey, C. Novy, Residential Tap Water Contamination Following the Freedom Industries Chemical Spill: Perceptions, Water Quality, and Health Impacts, Environ. Sci. Technol., 49.2 (2015): 813-823.

[34] W.E. Coleman, J.W. Munch, R.P. Streicher, H.P. Ringhand, F.C. Kopfler, The identification and measurement of components in gasoline, kerosene, and no. 2 fuel oil that partition into the aqueous phase after mixing, Arch. Environ. Con. Tox., 13.2 (1984): 171-178.
[35] M. Reed, The physical fates component of the natural resource damage assessment model system, Oil Chem. Pollut., 5.2-3 (1989): 99-123.
[36] National Sanitation Foundation Inernational/American National Standards Institute (NSF/ANSI), NSF/ANSI 61-2016 Drinking water system components-Health effects. http://www.nsf.org/newsroom_pdf/NSF-ANSI_61_watemarked.pdf, 2016 (accessed 16.10.12). Ann Arbor, MI.
[37] K.M. Kelley, A.C. Stenson, R. Cooley, R. Dey, A.J. Whelton, The cleaning method selected for new PEX pipe installation can affect short-term drinking water quality, J. Water Health, 13.4 (2015): 960-969.
[38] K.M. Kelley, A.C. Stenson, R. Dey, A.J. Whelton, Release of drinking water contaminants and odor impacts caused by green building cross-linked polyethylene (PEX) plumbing systems, Water Res., 67 (2014): 19-32.
[39] Y. Zhang, M. Edwards, Accelerated chloramine decay and microbial growth by nitrification in premise plumbing, J. Am. Water Works Assoc., 101.11 (2009): 51.
[40] H. John, Methods used by EPA to create crude oil contaminated drinking water for contamination studies. 2016, February 11. Personal Communication.
[41] J. Anderson, J. Neff, B. Cox, H. Tatem, G.M. Hightower, Characteristics of dispersions and water-soluble extracts of crude and refined oils and their toxicity to estuarine crustaceans and fish, Mar. Biol., 27.1 (1974): 75-88.
[42] K.S. Casteloes, R.H. Brazeau, A.J. Whelton, Decontaminating chemically contaminated residential premise plumbing systems by flushing, Environ. Sci.: Water Res. Technol., 1.6 (2015): 787-799.
[43] E.J. Kim, J.E. Herrera, D. Huggins, J. Braam, S. Koshowski, Effect of pH on the concentrations of lead and trace contaminants in drinking water: A combined batch, pipe loop and sentinel home study, Water Res., 45.9 (2011): 2763-2774.
[44] J. Pawliszyn, Applications of solid phase microextraction, Roy. Soc. Chem., 1999.
[45] I. Arambarri, M. Lasa, R. Garcia, E. Millán, Determination of fuel dialkyl ethers and BTEX in water using headspace solid-phase microextraction and gas chromatography–flame ionization detection, J. Chromatogr. A, 1033.2 (2004): 193-203.
[46] M.L. Tabor, D. Newman, A.J. Whelton, Stormwater chemical contamination caused by cured-in-place pipe (CIPP) infrastructure rehabilitation activities, Environ. Sci. Technol., 48.18 (2014) 10938-10947.
[47] J. Aitkenhead-Peterson, M.K. Steele, N. Nahar, K. Santhy, Dissolved organic carbon and nitrogen in urban and rural watersheds of south-central Texas: land use and land management influences, Biogeochemistry, 96.1-3 (2009): 119-129.
[48] R.J. Miltner, H.M. Shukairy, R.S. Summers, Disinfection by-product formation and control by ozonation and biotreatment, J. Am. Water Works Assoc., (1992): 53-62.
[49] F. Goodfellow, S. Ouki, V. Murray, Permeation of Organic Chemicals Through Plastic Water-Supply Pipes, Water and Environ. J., 16.2 (2002): 85-89.
[50] World Health Organization (WHO), Guidelines for drinking-water quality, fourth edition. 2011.
[51] U.S. Department of Health and Human Services (HHS), Toxicological profile for benzene, Atlanta, GA: Agency for Toxic Substances and Disease Registry (ATSDR), (1993).

[52] H. Shiraishi, N.H. Pilkington, A. Otsuki, K. Fuwa, Occurrence of chlorinated polynuclear aromatic hydrocarbons in tap water, Environmental Sci. Technol., 19.7 (1985): 585-590.
[53] K.S. Casteloes, G.P. Mendis, H.K. Avins, J.A. Howarter, A.J. Whelton, The interaction of surfactants with plastic and copper plumbing materials during decontamination, J. Hazard. Mater., 325.5 (2016): 8-16.
[54] A.J. Whelton, L. McMillan, C.L-R. Novy, K.D. White, X. Huang. Case Study: The crude MCHM chemical spill, West Virgnia. Environ. Sci.: Wat. Res. Technol. DOI: 10.1039/C5EW00294J

CHAPTER 2. COMPETITIVE HEAVY METAL ADSORPTION ONTO NEW AND AGED POLYETHYLENE UNDER VARIOUS DRINKING WATER CONDITIONS

2.1 Introduction

During the past several decades plastic piping materials have been increasingly used to replace metal pipes (mainly galvanized steel/iron and lead) in water distribution systems [1]. According to Lucintel (2015), the plastic pipe market is expected to have an annual growth rate of 6.8% in the next two years [2], and the greater growth will happen in the infrastructure development. With the increasing installation of plastic pipes for drinking water transport for buried water distribution and building plumbing, questions have been raised regarding their degradation, leaching, and the potential health risks. Past studies have primarily focused on chlorinated water and thermally induced chemical oxidation which can lead to plastic pipe degradation and mechanical failure [3, 4]. In addition, chemical leaching has also received some scrutiny [5-7] because leached chemicals may support biofilm formation, cause taste and odor problems [5, 8, 9], or exceed drinking water health-based standards.

Studies have shown that heavy metals can deposit onto plastic drinking water pipes used for water mains [10, 11], service lines (i.e., PVC and HDPE pipes) [12, 13], and building plumbing [14]. The most common heavy metals reported on plastic water pipe surfaces included As, Cd, Cu, Fe, Mn, Ni, Zn and Pb. Lead loading has been found as high as 9,681 μg Pb per gram of scale for exhumed PVC pipes, and Cu was found with average loading of 35 μg Cu per gram of scale on exhumed PVC pipe [11, 13]. Metal deposit formation are likely influenced by source water quality variation, system operations, and upstream piping materials or fittings. Unlike recently discovered metal deposits on plastic drinking water pipes, scales on metals pipes have been extensively

studied (i.e., Cu_2O, CuO, α-FeOOH, Fe_3O_4 and MnO_2 and $PbCO_3$) [10, 15, 16]. Furthermore, the metallic piping leaching and scales' detachment were also investigated, which mainly resulted from water chemistry and hydraulic condition changes [17-19]. Due to change of water resource and no corrosion control was implemented, lead scales started to detach from plumbing in Flint, Michigan. This water crisis not only caused the elevated lead in the drinking water (as high as > 5,000 μg/L, compared with MCL is only 15 μg/L), but also threatened residents' health [19, 20]. To date, there is no clear understanding regarding the fundamental processes that control heavy metal sorption onto plastic drinking water pipe surfaces. While the ongoing replacement of metal pipes with plastic pipes could reduce heavy metal sources within the drinking water distribution systems, the lack of understanding on heavy metals accumulation or release onto or rom plastics drinking water pipes is concerning. To better understand drinking water safety in piping systems that contain plastics, factors that control heavy metal interaction with plastic drinking water materials requires immediate study.

Few studies have been published regarding metal adsorption onto plastic drinking water pipes, so metals adsorbed onto micro/macro plastics [21-23] and plastic sampling containers [24, 25] were reviewed as the potential infrastructure application. Holmes et al. (2014) found, under the estuarine conditions, aged plastic pellets (i.e., from the ocean) adsorbed more metals (i.e., Cd, Co, Cr, Cu, Ni and Pb) than new plastics during a 48 hr adsorption period [26]. With the increasing of salinity, Cd, Co, Ni and Pb loading was decreased. However, the variation of pH values (i.e., 4-10.5) did not significantly alter Cu and Pb adsorption onto aged pellets. The iron adsorption onto different types of containers was observed by Fischer et al. (2007) after 25-70 hr equilibrium period [25]. While glass and quartz materials adsorbed most of the available iron (i.e., 94-98%), polyethylene and polycarbonate adsorbed the least amount (i.e., less than 50%). By comparing the

affinity constant between metal-container wall and metal-organic complex, they indicated that organic matters should be considered during metal-plastic interaction process.

Both plastic surface characteristics and the solution conditions may affect metal adsorption process. As plastic surfaces aged, the amount of oxygen containing functional groups (i.e., >C–O, >C=O and >O-C=O) increased. This condition may induce electrostatic diploes and enhance the plastic's metal adsorption capacity [26, 27]. A recent plastic drinking water pipe investigation showed that Pb was electrostatically bound to oxidized carbon that was formed on aged low-density polyethylene (LDPE) sheets [28]. The aging process may also increase the surface's roughness, porosity and hydrophilicity and cause a greater amount of metal adsorption [21, 29]. Because metal speciation is mainly controlled by water pH, dissolve oxygen/carbon dioxide, and the presence of other constituents in water, the type and form of metal on the plastic surface may be specific due to specific drinking water quality conditions. To simplify the metal system and metal interactions with solids, others have studied pH <5 conditions [29, 30]. At pH $\leq$ 5, close to 100% of the metals will be in the ionic form, however, this pH value is not within the typical drinking water pH range (i.e., 6.5-8.5).

Past metal-plastic sorption studies have proposed several mechanisms and some directly conflict with one another. For example, (1) The plastic surface acquired a negative charged surface when immersed in fresh or salt water solution, which caused metal ion adsorption [22, 26], (2) The plastic surface became more negatively charged with increasing water pH, resulting in greater electrostatic attractions between metal species and the plastic surface, (3) Increased water pH promoted metal hydrolysis/precipitation and resulted in less metal cations available for adsorption [22]. However, to date, the mechanism of metal-plastic interaction has not been thoroughly studied. Neither the effect of organic constitutes nor the corrosion inhibitor or free chlorine on metal-plastic

interaction has been studied. Since these variables are important drinking water characteristics, they are worth a further study.

The goal of the present study was to identify factors that influence metal-plastic interactions under mixed metal drinking water conditions. Mixed metal drinking water solutions (i.e., Cu, Fe, Mn, Pb and Zn) were used throughout the study. These metals are commonly found in plumbing systems. The author's hypothesis was that both plastic properties (i.e., aging, porosity, surface roughness and wettability) and water conditions (i.e., pH, the presence of organic carbon, corrosion inhibitor and free chlorine) would affect the amount of metal adsorbed onto the plastic's surface. Since plastic pellets are often used as the raw materials to manufacture plastic piping materials (i.e., PVC, PE, PP and PEX), in the current work, low density polyethylene (LDPE) pellets were adopted. While the LDPE piping is not used in the United States, it was previously used in United Kingdom water distribution systems [31].

2.2. Materials and methods

2.2.1 Materials and reagents

Low density polyethylene (LDPE) pellets and sheets were purchased from Sigma Aldrich, MO, whereas aged plastics were obtained based on the previous work [28]. For more details, 99.5% purity oxygen was supplied as the ozone generator feeding gas. New LDPE plastics (25 g) were added into 250 ml of nanopure water in a flat-bottom three-necked flask. The aging process was conducted at 85 ^{o}C (within a water bath), with a 4 mg/min ozone mass flowrate. Aging duration was varied from 2 to 10 hrs. Before metal interaction experiments, new and aged pellets were pre-conditioned (stirring with 500 ml nanopure water) for 24 hr and air dried.

In the current study, a synthetic tap water recipe was adopted to better simulate the tap water matrix [32]. Millipore Mili-Q water (MQW) (18.2 MΩ cm) was used to prepare all solutions.

Reagents used throughout the study were analytical grade or higher. Metal stock solutions (i.e., Cu, Fe, Mn, Pb and Zn) were 1,000 ppm ICP-MS standards (Ricca Chemical, TX), and desired concentrations were achieved through series of dilutions. NaOH and HNO_3 were used to adjust solution pHs. $Na_2HPO_4.7H_2O$ (Catalog No. AC206515000) was used as the representative corrosion inhibitor, which was purchased from Fisher Scientific, NH. Whereas, sodium hypochlorite (10-15%, reagent grade) (supply part No. 425044) was obtained from Sigma-Aldrich, MO and used to test the free chlorine effect. The aquatic Suwannee River NOM (SRNOM) was purchased from the International Humic Substances Society (IHSS) (Catalog No. 2R101N). PEX-A (i.e., cross-linked medium density polyethylene) pipes with 3/4" diameter were purchased from SupplyHouse.com (product No. F1040750).

2.2.2 Characterization

The Fourier transform infrared (FTIR) spectroscopy (Perkin Elmer spectrum 100 FTIR spectrometer) was used to provide functional groups information on new and aged LDPE pellets surfaces. Past studies showed that the presence of polar functional groups (i.e., >C=O, -OH, and >C=O<) on aged plastics could be responsible for the higher metal uptake [3, 22, 28]. The FTIR spectrum was obtained in the wavelength range of 600-4000 cm^{-1}, with a 1 cm^{-1} resolution. Each type of plastic pellets (i.e., new, 2 hr, 5 hr, and 10 hr aged) were scanned in triplicate to ensure the accuracy. The surface wettability for both new and aged LDPE segments (dimension: 1×1 cm^2) was achieved through the goniometer (Rame-hart Instrument Co., NJ). During the measurement, a 2 µL DI water droplet was deposited onto the sample surface. Then the image was taken and the contact angel was measured by the DROPimage Advanced software. The surface areas of plastics were determined by the Brunauer-Emmett-Teller (BET) method. In this process, 15 pellets were adopted with the averaged weight varied from 0.48-0.52 g. And N_2 gas adsorption-desorption was conducted by the Micrometritics TriStar 3020 Analyzer system. Prior the BET test, pellets samples

were weighted in Micromeritics sample tubes and went through degassing process for 5 hr at 70 ^{o}C [27]. For the following two tests, new and aged LDPE segments (10×1×1 cm^2) were exposed to 3 mg/L metal solutions (for 24 hr) and dried in the anaerobic chamber. The morphology of the metal deposited on a plastic surface was examined by scanning electron microscopy-energy dispersive X-ray spectroscopy (SEM-EDS) (Hitachi S-4800 Field Emission SEM). To enhance each samples' conductivity, plastic segments were sputter-coated with a thin carbon film and the conductive tape was also used. The basic operational conditions were adopted from previous studies, which were at 20 keV and with a working distance of 15 mm [21]. X-ray photoelectron spectroscopy (XPS) (Kratos AXIS Ultra DLD Imaging X-ray Photoelectron Spectrometer) was used to characterize the metal deposit speciation on plastic surfaces. The measurement was conducted by using an Al Kα X-ray source (1486.7 eV of protons) and a high vacuum chamber (10^{-8} Torr). All binding energies were referred to 284.6 eV C 1s peak to compensate the surface charging effect.

2.2.3 Metal adsorption test

For the kinetic study, 50 pre-conditioned LDPE pellets (i.e., new and aged) were added into a 50 ml Teflon (PTFE) bottle. In order to simplify metal speciation in the solution, the water was purged beforehand (with N_2) to remove oxygen and all experiments were conducted within an anaerobic chamber. To initiate the metal adsorption process, 20 ml 30 µg/L of oxygen free metal solutions (i.e., Cu, Fe, Mn, Pb and Zn) were added into each bottle. The ratio of plastic pellet surface area to the solution volume (S/V) was estimated as 1.5 cm^2/ml, which was comparable to the S/V ratio for 1" diameter plastic drinking water pipes. Then the water pH was adjusted to 7.5 by using NaOH and HNO_3 solutions. Kinetic studies were conducted in duplicate for up to 24 hr, and at room temperature (22 ^{o}C) with stirring speed of 250 rpm. Although trace metal levels are varied in different drinking water conditions, overall the selected metal concentration (i.e., 30 ppb)

was comparable to drinking water in the United States [33]. Periodically, pellets were removed from the reactor and placed into a 15 ml metal-free polypropylene centrifuge tube. The plastic centrifuge tube was pre-filled with 10 ml of 2% HNO_3 and the digestion duration was the minimum of 48 hr [34]. Then digested solutions were analyzed by inductively coupled plasma-optical emission spectroscopy (ICP-OES) (Perkin Elmer). Except plastic pellets, metal solutions from the reactor were used to measure total organic carbons (TOCs) through a Shimadzu TOC-LCPH analyzer. The TOC calibration curve was built from 0.5 to 30 mg/L and the method detection limit (MDL) was determined as 0.168 mg/L from 7 replicates.

In order to study the effect of water conditions on metal-plastic adsorption process, other variables were also studied. For example, free chlorine was selected within the range of 0.5-2 mg/L as Cl_2. The role of Na_2HPO_4, working as the potential orthophosphate corrosion inhibitor, was examined from 1-5 mg/L as PO_4^{3-}. In addition, the effect of organics was examined by using the 18 mg/L (as DOC) SRNOM and plastic leaching water. The concentrated plastic leaching water was achieved by filling the clean synthetic water into a new PEX-A pipe and left at the 55 ^oC constant room for one month. Then the desired DOC level of plastic leaching solution (i.e., 18 mg/L) could be reached by dilutions. The metal loss percentage (C_b %) to PTFE bottle walls was estimated from the control group (i.e., no pellets were added). Calculations were conducted by subtracting the metals remaining in solution (i.e., at 24 hr) (C_l, µg/L) from the initial metal concentration (C_o, µg/L) ($C_b\% = \frac{C_o - C_l}{C_o} \times 100\%$).

The isotherm study was conducted in triplicate. LDPE pellets (i.e., 50) were added within 20 ml of metal solutions in an anaerobic chamber. Initial metal concentrations (i.e., Cu, Mn, Pb and Zn, respectively) were varied from 5 to 100 µg/L at pH 7.5. After 24 hr, pellets were digested and along with left over metal solutions were analyzed by ICP-OES. Effect of metal solution pH on

metal adsorption capacity was also studied in the same manner. The initial pH was adjusted from 5.5 to 10.5. At the end of the experiment (up to 24 hr), pellets were digested by using the previous method (i.e., 2% of HNO_3 for 48 hr) and metal solutions were measured by the TOC analyzer. Furthermore, dominant factors that could potentially affect metal adsorption or the organic leaching onto/from plastic pellets were studied by using the NCSS statistical software. The multivariate analysis of variance (MANOVA) test was conducted, with 95% confidence interval and α=0.05.

2.3. Results and discussion

2.3.1 Plastic surface oxidation

The aging process altered LDPE surface chemistry, increased surface hydrophilicity and surface area. ATR-FTIR results showed that the new polymer did not have oxygen-containing bonds while (-OH bend) [939 and 1411 cm^{-1}], ether (C-O-C stretch) [1105 and 1170 cm^{-1}] and ketone (C=O bend) [at 1708 cm^{-1}] bonds were present on aged LDPE (Figure A.1) [27, 35]. Aging also changed the LDPE surface from hydrophobic (θ>90^o) to hydrophilic (θ<90^o) (Figure 2.1). Aging increased surface area from 0.0493 (new LDPE pellets) to 0.1036 m^2/g (10 hr aged pellets) (Figure 2.2).

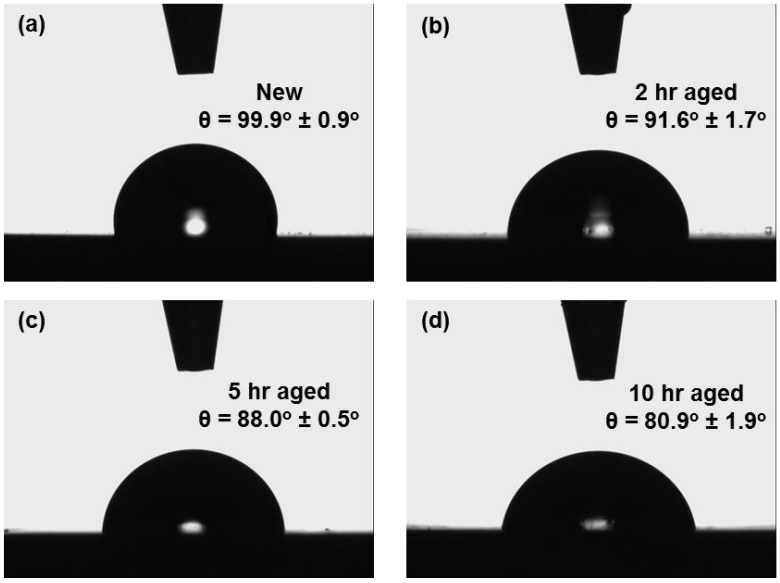

Figure 2.1 Contact angle measurement images of (a) New LDPE segment, (b) 2 hr aged LDPE segment, (c) 5 hr aged LDPE segment, and (d) 10 hr aged LDPE segment.

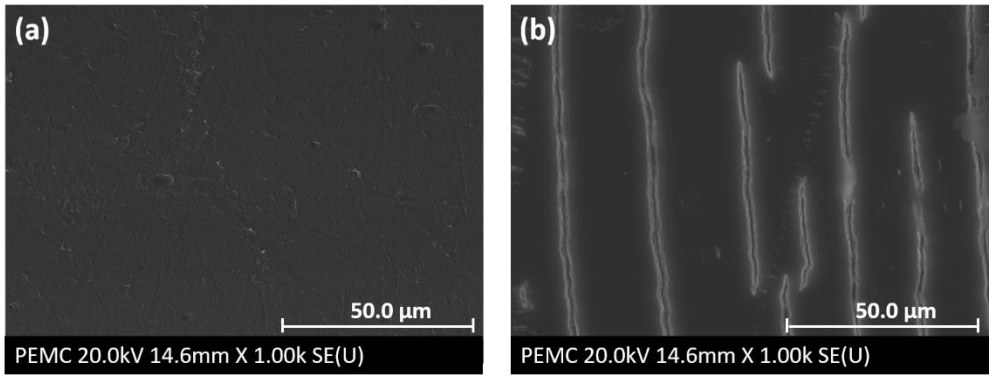

Figure 2.2 SEM images of (a) New LDPE segment and (b) 10 hr aged LDPE segment.

2.3.2 Metal adsorption was greater for aged plastic than new plastic

For the target metals (i.e., Cu, Mn, Pb and Zn), the longer the aging process, the greater abundance of metal ($\frac{Mass \text{ of adsorbed metal } (\mu g)}{Surface\ area \text{ of } plastic\ pellets\ (m^2)}$) was observed on LDPE pellets (Figure 2.3) (Figure A.2). After exposing aged plastic to mixed metal solutions for 10 hr, aged LDPE pellets adsorbed about five times more metals than new pellets. In addition, new LDPE pellets adsorption reached equilibrium within 2 hr, whereas the 5 and 10 hr aged plastics did not reach the equilibrium

until 10 hr. This difference may be due polar functional groups (i.e., -OH, C-O-C and C=O) formed on aged LDPE pellets being more favorable for metal specie attraction [22, 27], increased surface hydrophilicity and enhanced surface area [21, 36] would also promote metal adsorption.

In the mixed metal solution system, Cu was adsorbed the most followed by Pb, Zn and Mn (Figure 2.3). This result was mainly due to metal properties and the attraction between metals and plastic surfaces. Faur-Brasquet et al. (2002) used activated carbon cloth (i.e., CS-150) to remove metals from both single and mixed metal system [37]. Results showed the mixed metal system (i.e., Cu and Pb) decreased the adsorption capacity onto CS-1501 than the single metal system (i.e., Cu only or Pb only). And the initial adsorption rate of Pb(II) over Cu(II) ($\Upsilon_{Pb(II)}/\ \Upsilon_{Cu(II)}$) was 0.78 on CS-150, which indicated more Cu was absorbed than Pb. With the absence of organics, Perelomov et al. (2011) discovered the highest amount Cu was adsorbed onto goethite, followed by Pb and Zn in the mixed metal solution from pH range 4.5-7.0 [38]. This finding agreed well with the metals' electronegativity order (Cu>Pb>Zn) and affinity of metals to minerals surfaces. Here the MINEQL software was adopted to better understand metals speciation under the certain condition (Figure A.3). Starting with 30 ppb of Cu, Mn, Pb and Zn mixed metal solution, at pH 7.5, Cu^{2+} and Pb^{2+} exited at the similar level (52.8 % vs 53.2 %). But the larger ionic radius of Pb (II) (1.12 A^o) than Cu (II) (0.70 A^o) would potentially result in a faster site saturation phenomenon, in other words, the maximum adsorption capacity of Pb was reduced. Furthermore, higher electronegativity of Cu (II) (28.56 eV) > Pb (II) (26.18 eV) could also result the stronger attraction with functional groups on the LDPE surface [37, 39].

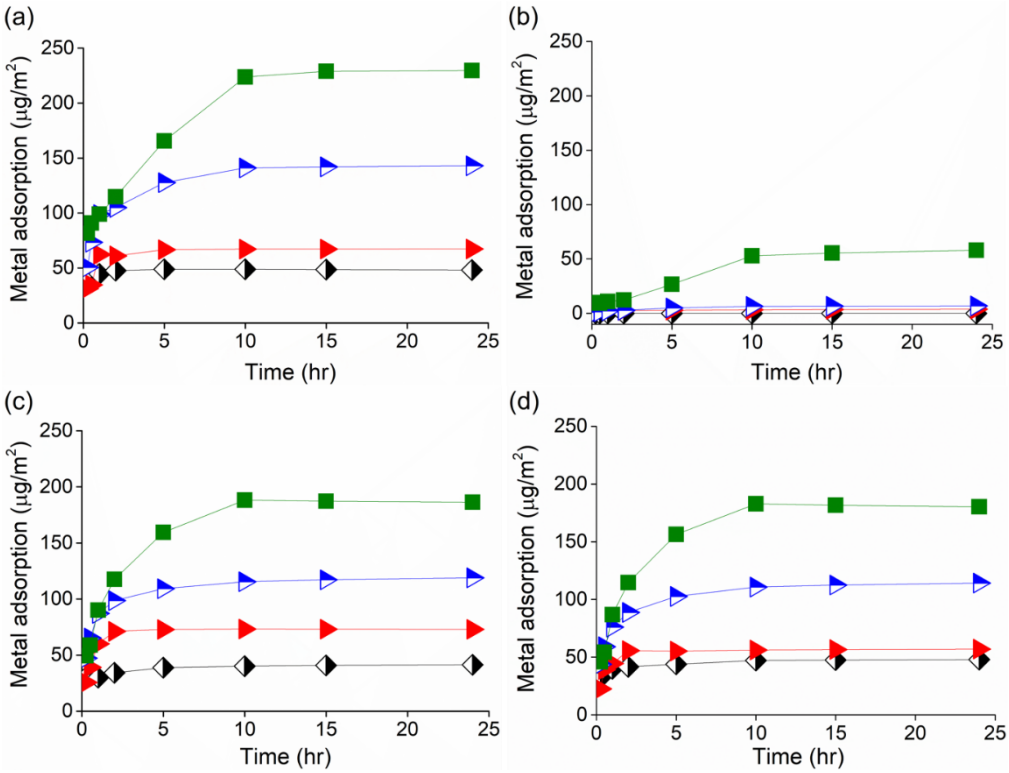

Figure 2.3 (a) Cu (b) Mn (c) Pb and (d) Zn adsorption onto New, 2 hr aged, 5 hr aged, and 10 hr aged LDPE pellets for the mixed metal system (i.e., Cu, Mn, Pb and Zn). Initial metal concentration was 30 ppb for each metal, at pH 7.5.

2.3.3 Metal solution pH influenced metal-plastic interaction

Metal adsorption behavior was significantly influenced by water pH (Figure 2.4). For most conditions examined, greater amounts of Cu and Pb adsorbed onto LDPE compared to Mn and Zn. Within the pH range of 5.5-9.5, the amount of Cu and Pb adsorbed was not significantly affected by pH change. The lack of pH dependence on metals adsorption (i.e., Cu and Pb) suggested that additional to metal ionic forms, other non-ionic forms (i.e., metal hydrolysis) were also likely able to interact with polymeric surfaces [26]. On the other hand, the amount of Mn and Zn adsorbed on the LDPE surface was significantly affected by pH. The lower amount of metal adsorbed at low pH (i.e., 5.5) could be explained as the potential competition between metal and H^+ ions. As pH increased (5.5-9.5), metal ions begin to undergo hydrolysis. Considering the charge number, the

effective hydrated radii is in the order $M^{2+} > M(OH)^{+}_{(aq)} > M(OH)_{2(aq)}$ [40]. Since metal ions with smaller effective hydrate radii could more easily diffuse into a porous structure, the increased metal adsorption was observed as the increase of pH values [26]. However, in the high pH range (i.e., pH>9.5), most of the metal ions were present in solid form $M(OH)_{2(s)}$ and would suspend/precipitate in the solution and resulted less attraction to the plastic surfaces. Except metal adsorption, organic carbon leaching was also monitored for with/without oxygen scenarios under different pH conditions (Figure A.4). Compared with control group, experimental groups showed greater organic carbon leaching as the pH increased. More specifically, the organic leaching at pH 10.5 was approximately 3 times more than that detected under pH 5.5. No significant difference was found for organic carbon leaching under with/without oxygen scenarios (*p value* = 0.15). Furthermore, it seemed there was no relation between metals adsorption (i.e., Cu, Mn, Pb and Zn) and organic carbon leaching data.

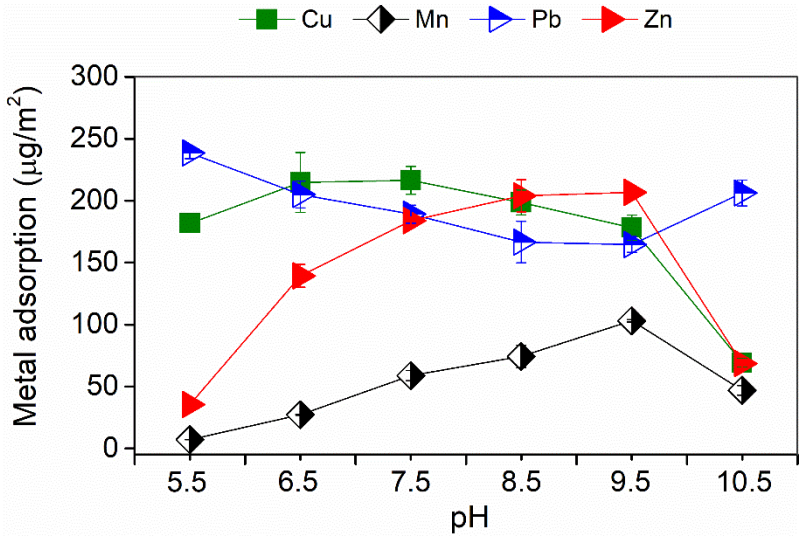

Figure 2.4 Competitive metal adsorption (■ Cu, ✳ Fe, ◆ Mn, ▶ Pb, and ▶ Zn) on 10 hr aged LDPE pellets varied with pHs. Results averaged from triplicate experimental values (with error bars showing standarized deviation). Initial metal concentration was 30 ppb for each metal.

2.3.4 Role of metals concentration on metal-plastic interaction

The Langmuir and Freundlich isotherm models were adopted to study the effect of metal concentrations on metal adsorptions. The assumption for the Langmuir isotherm was that monolayer adsorption on a homogeneous plastic surface:

$$[MP]_e = \frac{k_L[MP]_{max}[M]_e}{1 + k_L[M]_e}$$

where $[MP]_e$ ($\mu g/m^2$) is the amount of metals adsorbed onto plastics surfaces at the equilibrium status, $[MP]_{max}$ is the maximum metal adsorption capacity, $[M]_e$ is the equilibrium metal concentration in the solution, k_L ($L\ \mu g^{-1}$) is the Langmuir isotherm constant. For the Freundlich model, the assumption is that multilayer adsorption occurs:

$$[MP]_e = k_F[M]_e{}^{1/n}$$

where *n* is the measurement of linearity and k_F ($\mu g^{1-1/n}\ m^{-2}\ L^{1/n}$) is the Freundlich constant.

When plastics were exposed to varied metal levels (i.e., 5-100 ppb), as the increasing of metal concentrations in the solution, greater metal loadings were found on the plastic surface (Figure 2.5). Furthermore, as found from the previous study, experimental results fitted both models (i.e., Langmuir and Freundlich isotherm models) fairly well (Table 2.1) [29]. Among these four metals, Cu and Zn resulted the lower coefficients of determination (R^2). This result was comparable with the previous kinetic study, where Cu and Zn were also more problematic during the model fitting process. Holmes et al (2012) studied trace metals adsorption onto beached pellets (in marine environment), by adopting the Langmuir and Freundlich models, Pb adsorption had a better fit (R^2>0.9) versed poor fit for Cu (R^2<0.6) [29]. This result indicated, more complexed adsorption process was likely happening for certain metals (i.e., Cu and Zn), such as, desorption coupled with adsorption and chemisorption (i.e., metal reacted with oxidized functional groups on aged plastic

surfaces) [3, 22]. The Langmuir isotherm model predicted that the pellet's maximum metal adsorption capacity in the mixed metal solution was Cu (1,109 µg.m$^{-2)}$ > Pb (1,038 µg.m^{-2}) > Zn (893 µg.m^{-2}) > Mn (199 µg.m^{-2}). The Freundlich constant (1/*n*) revealed that the isotherms were convex (1/*n*<1) for target metals [22, 26]. When 1/*n*<1, it indicated as the increasing of metal levels in the solution, the adsorption rate decreased (with limited bonding sites) [41]. On the other hand, 1/*n*<1 showed the strong adsorption bond between metal and aged LDPE pellets surfaces.

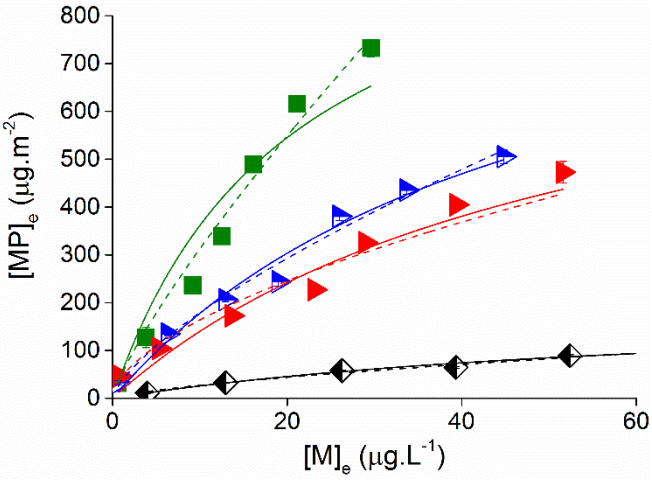

Figure 2.5 Metals competitive adsorption (■ Cu, ◆ Mn, ▶ Pb, and ▶ Zn) varied with metals concentration (onto 10 hr aged LDPE pellets). Experiments were conducted in triplicate. Solid lines represent the Langmuir isotherm model fitting, dash lines represent the Freundlich isotherm model fitting. Initial metal concentration was 30 ppb for each metal, at pH 7.5.

Table 2.1 Isotherm model fitting (Langmuir and Freundlich models) summary of competitive metal adsorption (Cu, Mn, Pb and Zn) onto 10 hr aged plastic surfaces.

	Langmuir model			***Freundlich model***		
Metal	k_L (L.µg^{-1})	$[MP]_{max}$ (µg.m^{-2})	R_L^2	k_F (µg$^{1-1/n}$ m^{-2} L$^{1/n}$)	1/n	R_F^2
Cu	0.048	1109	*0.95*	48.23	0.81	*0.99*
Mn	0.015	199	*0.98*	5.39	0.70	*0.98*
Pb	0.021	1038	*0.97*	34.92	0.71	*0.99*
Zn	0.019	893	*0.90*	42.73	0.58	*0.96*

2.3.5 Influence of dissolved organic carbons on LDPE pellets metal adsorption

SRNOM and organics leached from PEX-A pipes hindered metals adsorption to LDPE pellets (Table 2.2). In this study, the 18 mg/L (as DOC) of NOM and organics released from PEX pipes was adopted, which were in the range of NOMs found in source waters [42, 43], and the plastic pipe leaching study [44]. Among all metals, Cu loadings were affected the most, which resulted about 70 % reduction when SRNOM constitutes were present (Figure 2.6 and Table 2.2). Results also revealed that SRNOM decreased metal-plastic interaction more significantly than organic compounds leached from PEX pipes (Figure 2.6). This difference is likely due to the fact that fulvic and humic acids in SRNOM contain multiple functional groups (i.e., carboxyl, amine, and phenolic) that can potentially bond with copper. At higher water pH, organic acids can be further deprotonated and more easily to form metal complexes [37]. Sheng et al. (2010) found that, at higher pH values (pH > 7.5), majority of Cu (II) would form fulvic acid/humic acid-Cu complexes. This led to the reduction of available copper that could be adsorbed onto carbon surfaces [45]. The nature of organics released from PEX pipe has received little scrutiny [46]. But the result was likely related to the structure of PEX pipes leached organics that resulted less available metal-binding function groups under the experimental condition.

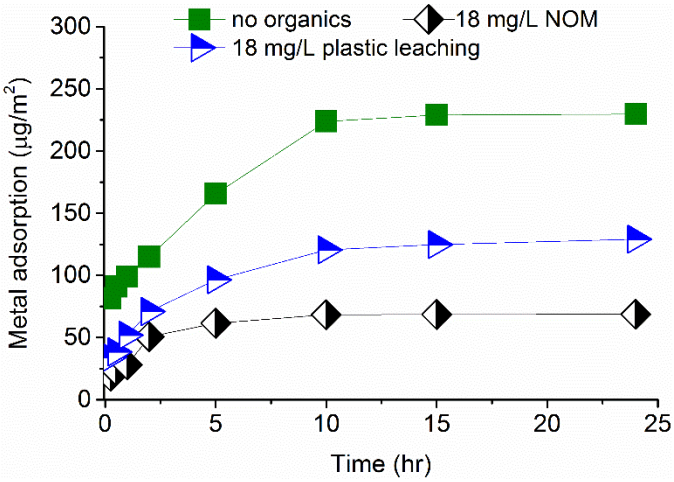

Figure 2.6 Organic constitutes effect of Cu adsorption onto 10hr aged LDPE pellets. Initial metal concentration was 30 ppb of each metal (i.e., Cu, Mn, Pb and Zn), at pH 7.5. Initial metal concentration was 30 ppb, at pH 7.5.

2.3.6 Influence of corrosion inhibitor and free chlorine on LDPE pellets metal adsorption

Under the experimental condition, the higher level of corrosion inhibitor and free chlorine resulted in less metals adsorbed onto suspended LDPE pellets (Table 2.2 and Figure 2.7). Because pellets were suspended in the solution, metal precipitates may have settled out in the water column , so "free" metal forms were more likely the driving force during metal-plastic interaction process. Cu and Pb adsorption were most affected by the presence of corrosion inhibitor and the reduction ranged from 29 to 59%. When corrosion inhibitor level was increased from 1 to 5 mg/L as PO_4^{3-}, the Pb adsorption was reduced about 2 times more (Figure 2.7 (a)). This was due to the addition of Na_2HPO_4 could potentially precipitate Pb ions in the aqueous phase. Nriagu (1974) studied the lead orthophosphate systems in the environment [47]. Except $Pb(H_2PO_4)_2$, $PbHPO_4$ and $Pb_3(PO_4)_2$, other possible lead mineral forms ($Pb_5(PO_4)_3OH$ and $Pb_5(PO_4)_3Cl$) were also discovered. Another interesting study was conducted by Cao et al. (2002), who attempted by applying phosphate to transform Pb in soils [48]. They found the phosphate treatment could be effectively turned Pb from available (for plant uptake) phase into the residual phase. And the formation of $Pb_5(PO_4)_3Cl$ was

proposed as the major mineral that was responsible for the lead immobilization. Furthermore, the lower solubility cupric phosphate scale ($Cu_3(PO4)_2$) was formed on copper surface when orthophosphate was added [49]. An interesting finding was the addition of corrosion inhibitor (i.e., Na_2HPO_4) in the current study did not influence the Mn adsorption. This was mainly due to the fact that divalent manganese phosphate compounds were often soluble at neutral pH and under room temperature [50].

Free chlorine, as a strong oxidant, could react with metals to form insoluble oxides that retarded metal-plastic interaction (Table 2.2). Compared with fairly low metal concentrations used in the current study (i.e., 30 µg/L of each metal), the lower level of chlorine (0.5 mg/L) presented could significantly affect metal adsorption (with reduction of 12-33.7%). Lytle et al. (2005) studied the long term lead precipitation within chlorinated water (1-3 mg/L Cl_2, at pH 6.65-10), in which they discovered the Pb (IV) dioxide (i.e., β-PbO_2 and α-PbO_2) formed under the high oxidation-reduction potential (ORP) scenario [51]. In addition, $PbCO_3$ could also form and coexist with PbO_2 under pH 6.5-8. The formation of lead precipitation would reduce the available lead within the solution, in such a way that led to the reduced metal uptake by plastic surfaces (Figure 2.7 (b)). Free chlorine could also react with Cu^{2+} to form Cu $(OCl)_{2(S)}$ and further oxidize cupric hydroxide to the less soluble oxide form (i.e., CuO) [52]. While Zn^{2+} may precipitate as $Zn(OH)_2$ or $ZnCO_3$, Mn^{2+} could be oxidized in the form as MnO_2 (s) after the excess chlorine addition [53, 54]. Because the free chlorine concentration used in the current study was fairly low (i.e., ≤ 2 mg/L) and experiments were conducted in a short duration (i.e., 24 hrs, at room temperature), the plastic surface degradation was negligible.

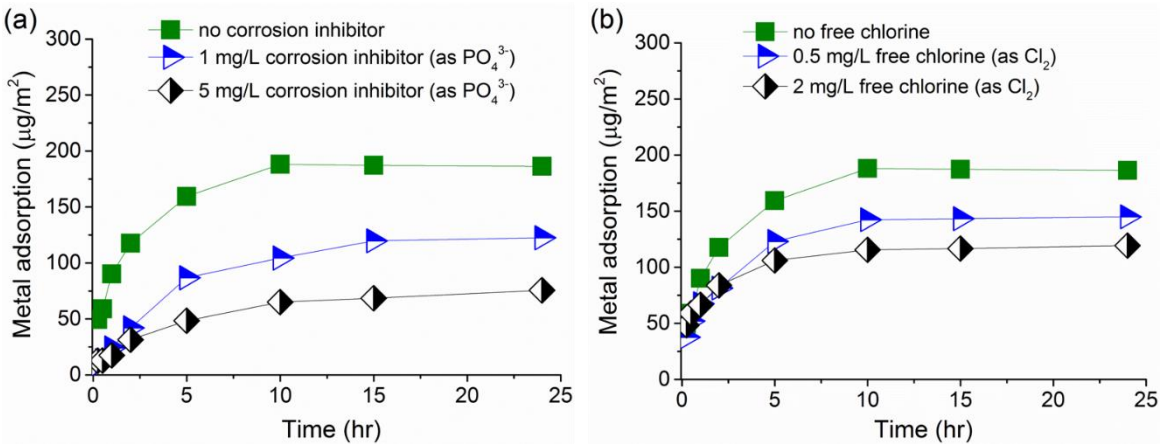

Figure 2.7 The presence of the (a) corrosion inhibitor and (b) free chlorine reduced metal adsorption onto suspended 10 hr aged LDPE pellets. Initial metal concentration was 30 ppb of each metal (i.e., Cu, Mn, Pb and Zn) at pH 7.5.

Table 2.2 Metal adsorption to suspended LDPE pellets was affected by the presence of dissolvd organic carbon, corrosion inhibitor and free chlorine .

Target metals	***Water conditions (adsorbed metal/plastic surface area) (μg/m²)***						
	LDPE only	18 mg/L NOM	18 mg/L Plastic leaching[a]	1 mg/L PO_4^{3-}	5 mg/L PO_4^{3-}	0.5 mg/L Cl_2	2 mg/L Cl_2
Cu	230	69 (***-70.1%***)	129 (***-43.8%***)	161 (*-29.8%*)	152 (*-34.0%*)	152 (*-33.7%*)	143 (*-38.0%*)
Mn	58	43 (*-26.7%*)	54 (*-6.5%*)	60 (ND)	57 *(-1.3%*)	43 (*-26.4%*)	41 (*-29.6%*)
Pb	186	163 (*-12.4%*)	176 (*-5.7%*)	123 (***-34.2%***)	76 (***-59.4%***)	145 (***-22.1%***)	119 (***-36.0%***)
Zn	180	148 (*-17.8%*)	164 (*-9.1%*)	164 (*-8.9%*)	139 (*-22.8%*)	159 (*-12.0%*)	146 (*-18.9%*)

a. Organics leaching solution was obtained from new PEX-A pipes at 55°C constant temperature room.
ND represents the there was no reduction be found.
Bold number stands for the reduction percentage of the representative metals (i.e., Cu and Pb).

2.3.7 Influence of iron addition on metal-plastic interaction

Iron was often found as the most abundant element in piping scales and suspected that could co-precipitate with other trace metals [11, 13]. So the impact of iron on metals (i.e., Cu, Mn, Pb and Zn) adsorption to LDPE pellets was also examined in the current study. Here the pseudo-first-order model and the intraparticle diffusion model were adopted to help understand the metals adsorption processes.

The pseudo-first-order model has been applied to study the interaction of metals with microplastics [22]:

$$\mathrm{M} + \mathrm{P} \xrightarrow{k_1} \mathrm{MP}$$

In which, M stands for metals in the solution, P represents the plastic surface, and MP is metal adsorbed onto plastic surfaces.

The reaction rate expression:

$$\frac{d[MP]}{dt} = k_1([MP]_e - [MP]_t)$$

Where k_1 is the pseudo-first order reaction constant, with unit hr^{-1}. $[MP]_e$ and $[MP]_t$ ($\mu g/m^2$) are amount of metals adsorbed onto plastic surfaces at the equilibrium status, and at time t (hr), respectively.

Apply the boundary condition, when t=0, $[MP]_0$=0:

$$\ln([MP]_e - [MP]_t)_{[MP]_0}^{[MP]_t} = -k_1 t$$

Final equation used for curve fitting as:

$$[MP]_t = [MP]_e(1 - e^{-k_1 t})$$

The first-order reaction half- life, $t_{1/2}$ (hr), is defined as when $[MP]_t$=1/2 $[MP]_e$. So

$$t_{1/2} = \frac{ln2}{k_1}$$

Refer to the theory proposed by Weber and Morris, the intraparticle diffusion model is shown as below [55]:

$$[MP]_t = k_p t^{1/2} + C$$

In which k_p is the intraparticle diffusion rate constant ($\mu g.m^{-2}.hr^{-1/2}$). The good fitting with this model could justify the multi-linearity adsorption mechanisms, which are often involving three steps: instantaneous external adsorption, gradual adsorption, and the equilibrium stage [56].

Compared with no Fe addition, when Fe was present in mixed metal solutions, the amount of Cu, Pb, and Zn all reduced (Figure 2.8). In the addition, for Mn and Pb, the adsorption first-order reaction half- life ($t_{1/2}$, hr) was also decreased after adding Fe in the solution (Table 2.3). For example, Pb adsorption $t_{1/2}$ value was 1.06 hr without iron and when Fe was present the value increased to 1.22 hr. For most studied metals (except Mn), the first-order half-life ($t_{1/2}$) was within 2 hr. In addition, different metals exhibit diverse behaviors. Mn and Pb were fitted better to the pseudo-first-kinetic model ($R_1^2 > R_p^2$), whereas, Cu, Fe and Zn showed a better fit to the intraparticle diffusion model ($R_1^2 < R_p^2$). A past study of trace metals adsorption with micro plastics also found poor fittings of Cu and Zn by using the first-order-kinetic model [22, 29]. They proposed the possible mechanism of this phenomenon was related to higher affinity of Cu and Zn to plastic surfaces. And the aged pellets characteristics (i.e., greater heterogeneity and porosity) that resulted the metal adsorption (i..e, Cu and Zn) equilibrium did not fully attain at the end of the experimental period. The formation of oxygen contained functional groups on aged plastic surfaces may have stronger attraction to Cu, Fe and Zn, which failed the pseudo-first-order model assumption as physical adsorption.

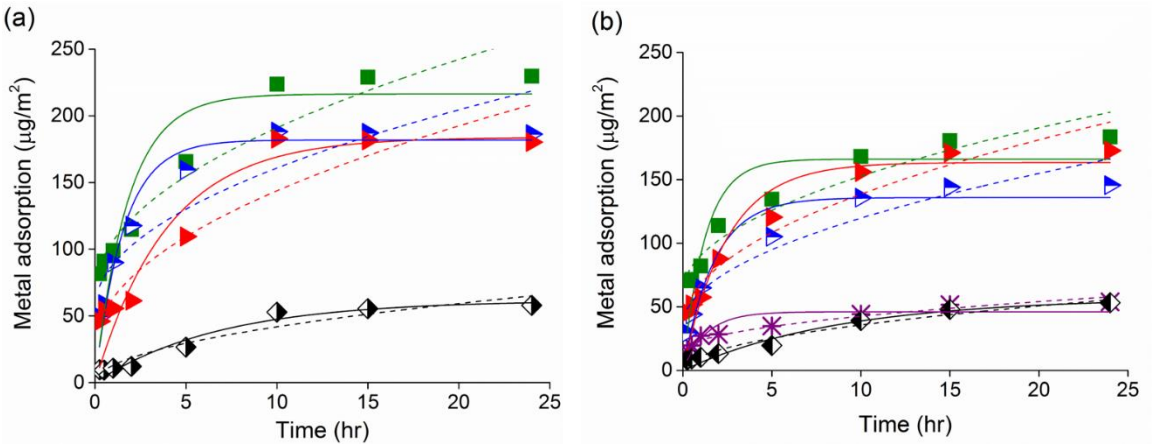

Figure 2.8 Kinetics of competitive metal adsorption (■ Cu, ✳ Fe, ◆ Mn, ▶ Pb, and ▶ Zn) onto 10 hr aged LDPE pellets surface under (a) without Fe and (b) with Fe scenarios. Solid lines stand for the pseudo-first-order kinetic model fitting, dash lines represent the intraparticle diffusion model fitting. Initial metal concentration was 30 ppb for each metal, at pH 7.5.

Table 2.3 Kinetic model fitting (pseudo-first-order and intraparticle diffusion models) summary a metals (Cu, Fe, Mn, Pb and Zn) competitive adsorption onto plastic surfaces.

	Without Fe scenario					***With Fe scenario***				
Metal	k_1 (hr^{-1})	$t_{1/2}$ (hr)	R_1^2	k_p ($\mu g.m^{-2}.hr^{-1/2}$)	R_p^2	k_1 (hr^{-1})	$t_{1/2}$ (hr)	R_1^2	k_p ($\mu g.m^{-2}.hr^{-1/2}$)	R_p^2
Cu	0.55	1.26	*0.73*	39.13	*0.91*	0.79	0.88	*0.74*	28.94	*0.92*
Fe	-	-	-	-	-	0.76	0.91	*0.73*	8.76	*0.95*
Mn	0.15	4.62	*0.95*	13.31	*0.92*	0.11	6.30	*0.94*	11.38	*0.96*
Pb	0.64	1.08	*0.95*	33.30	*0.81*	0.57	1.22	*0.92*	26.81	*0.88*
Zn	0.25	2.77	*0.86*	37.14	*0.88*	0.41	1.69	*0.89*	32.66	*0.93*

- represents the data is not available.

2.3.8 Metal accumulation and speciation on the LDPE surface

SEM-EDS analysis revealed that particulates and aggregates were found on LDPE surfaces that exposed to the mixed metal solutions. SEM-EDS spectra indicated that a variety of elements/metals (i.e., Ca, Mg, Cu, Fe, Mn, Pb and Zn) had adsorbed onto the LDPE. No particles were found when LDPE exposed to the control solution (i.e., water only, no metals) and only Ca and Mg were found through the EDS measurement (Figure A.5).

Cu, Pb and Zn were detected on LDPE surfaces, and the addition of Fe reduced other metals adsorption (Figure 2.9 and Table 2.4). Due to the fairly low level of Fe and Mn that were on LDPE pellets, these two metals were not concentrated enough to be detected by XPS (results not shown). When Fe was added, Cu, Pb and Zn element composition (%) all decreased (i.e., Cu 66.7%, Pb 50% and Zn 69.2% reduction). Within the XPS wide scan spectra, the C 1s (285 eV), O 1s (531 eV), Cu 2p (930-970 eV), Pb 4f (135-145 eV) and Zn (1010-1025 eV) characteristic peaks were detected on new LDPE pellets that exposed to mixed metal solutions (i.e., without Fe and without Fe) (Figure 2.9 (a)). Results confirmed Cu, Pb and Zn adsorption on LDPE surfaces. The high resolution of Cu 2p, Pb 4f and Zn 2f XPS spectra are also presented and studied in detail that showed reduced peaks after adding Fe (Figure 2.9 (b)-(d)). The Cu $2p_{3/2}$ and Cu $2p_{1/2}$ shake-up satellites were observed at 944 eV and 964, respectively (Figure 2.9 (b)). In addition, the Cu $2p_{3/2}$ characteristic peak located at 934.9 eV indicated the presence of Cu (II) oxides (Cu $2p_{3/2}$ at 934.6 eV) and Cu (II) hydroxides (Cu $2p_{3/2}$ at 935.1 eV) [57, 58]. An interesting fact is that the addition of disinfection product (i.e., free chlorine) in the real drinking water system could convert relatively soluble $Cu(OH)_2$ to less soluble tenorite (CuO). This catalyzed Cu aging process also coupled with rapid free chlorine decay effect ($2Cu(OH)_2 + HCl + OH^- \rightarrow 2CuO + Cl^- + \frac{1}{2}O_2 + 3H_2O$) [59]. Except free chlorine, other water conditions, such as pH, temperature, alkalinity, organic (i.e., NOM) and inorganic compounds (i.e., corrosion inhibitor and minerals) could also alter the copper transition process as stated above. The high resolution of Pb 4f spectrum shows two distinguishable peaks that located at 138.4 eV (Pb $4f_{7/2}$) and 143.2 eV (Pb $4f_{5/2}$), with an energy separation of 4.8 eV (Figure 2.9 (d)). From which the lead speciation could be attributed to PbO (Pb $4f_{7/2}$ at 138.3 eV) and $Pb(OH)_2$ (Pb $4f_{7/2}$ at 138.6 eV), respectively [60, 61]. Lead scales from drinking water systems are typically composed of Pb(II) and Pb(IV) oxides or hydroxides. In

addition, hydrocerussite [$Pb_3(CO_3)_2(OH)_2$] and carbonates ($PbCO_3$) are also often found [16, 62]. Last but not the least, the Zn $2p_{3/2}$ peak in this study was found at 1021.8 eV that corresponded well with ZnO (Zn $2p_{3/2}$ at 1021.7 eV) [57].

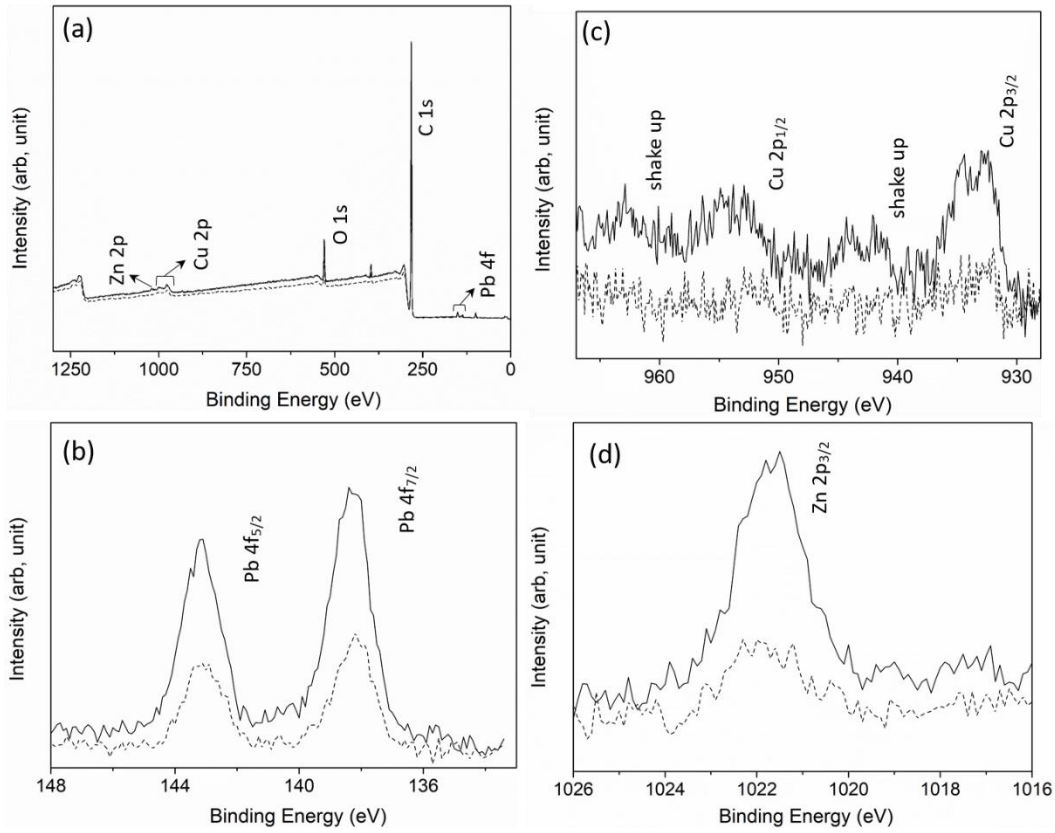

Figure 2.9 Comparison —— without Fe and ····· with Fe XPS spectra of (a) wide scan (b) Cu 2p (c) Pb 4f and (d) Zn 2p on plastic surfaces.

Table 2.4 Elemental atomic concentration % from LDPE pellets

Sample name	*Element composition (%)*					
	C 1s %	N 1s %	O 1s %	Cu 2p %	Pb 4f %	Zn 2p3/2 %
without Fe	91.34	2.03	6.30	0.15	0.06	0.13
with Fe	92.46	2.13	5.30	0.05	0.03	0.04

2.4 Conclusion

Plastic materials are increasingly used in the drinking water piping networks and to understand drinking water quality, and there is a need to better understand how plastics can influence drinking water quality. Few studies are available that describe heavy metal interaction with plastic drinking water materials.

In the present work, Cu, Fe, Mn, Pb and Zn competitive metal adsorption onto new and aged LDPE was studied under various drinking water conditions. In the absence of corrosion inhibitor and free chlorine disinfectant, aged LDPE had dramatically different metal adsorption behavior than new LDPE (i.e., 5 times greater metal loadings for Cu and Pb). Results showed that Mn and Pb has a better fit to the pseudo-first-order kinetic model (R^2>0.92). And intraparticle diffusion model turned out a better fit to Cu, Fe and Zn (R^2>0.88). In addition, both Langmuir and Freundlich isotherm models fitted fairly well to the experimental data. The maximum metal adsorption by fitting Langmuir isotherm model were Cu (1109 $\mu g.m^{-2}$) > Pb (1038 $\mu g.m^{-2}$) > Zn (893 $\mu g.m^{-2}$) > Mn (199 $\mu g.m^{-2}$) at pH 7.5.

Water pH, dissolved organic carbon from NOM and plastic pipe leaching, as well as the presence of corrosion inhibitor and free chlorine affected metal adsorption to LDPE. At lower pH (i.e., 5.5), lower metal loading was often observed, and metal loading increased with increased pH (5.5 to 9.5). At the high pH (i.e., 9.5), it is likely that most metals precipitated and resulted less attraction and loading to the LDPE surface. The presence of dissolved organic carbon reduced metal sorption sometimes markedly (i.e., Cu by 70.1%). When organic carbon solution from a commonly brand of PEX drinking water pipe was used as the experiment matrix, 43.8% less Cu absorption was observed. The corrosion inhibitor (i.e., Na_2HPO_4) and free chlorine (NaOCl) disinfectant likely caused metal precipitation (i.e., $Pb(H_2PO_4)_2$, $PbHPO_4$ and PbO_2) and therefore

reduced the amount of metals that could adsorption to the suspended LDPE pellets. SEM-EDS analysis revealed that metal deposits were present on LDPE surface in particulate and aggregate form. XPS analysis confirmed metals adsorption and the addition of Fe decreased Cu, Pb and Zn adsorption up to 66.7%. Furthermore, copper, lead and zinc deposits were primarily Cu (II), Pb (II) and Zn (II) hydroxides and oxides.

This bench-scale study provides insight into the factors that influence metal adsorption onto LDPE, and expanded investigations are recommended. Additional work should be carried-out using commercial plastic drinking water pipes, different water quality conditions, temperatures, and hydraulic conditions. Because different plastic pipes can leach different amounts and types of organic material, organic leaching from plastic drinking water pipes should be further examined. Since an oxidized plastic surface (by UV light exposure) was found to influence metal adsorption, future studies should investigate if this holds for drinking water applications where free chlorine, chloramines, chlorine dioxide, potassium permanganate, and other oxidants are applied. Because of the complexity of the experiments conducted, the role of biofilms in mediating metal-plastic interactions was not investigated in the short time exposure test (i.e., 24 hr). The release of deposited metals from plastic drinking water pipe surfaces into bulk water should also be investigated. Results presented here, combined with previous studies, indicate work is needed to better understand the fundamental processes that control heavy metal-plastic interactions in the drinking water domain.

2.5 References

[1] N.S. Grigg, Assessment and renewal of water distribution systems, American Water Works Association. Journal, 97 (2005) 58.
[2] Lucintel, Growth Opportunities in Global Plastic Pipe Market 2015-2020: Trends, Forecasts and Market Analysis, in, 2015.
[3] J.C. Montes, D. Cadoux, J. Creus, S. Touzain, E. Gaudichet-Maurin, O. Correc, Ageing of polyethylene at raised temperature in contact with chlorinated sanitary hot water. Part I–Chemical aspects, Polymer degradation and stability, 97 (2012) 149-157.
[4] K. Martel, K. Klewicki, State of the Science: Plastic Pipe, Water Research Foundation, (2016).
[5] K.M. Kelley, A.C. Stenson, R. Dey, A.J. Whelton, Release of drinking water contaminants and odor impacts caused by green building cross-linked polyethylene (PEX) plumbing systems, Water research, 67 (2014) 19-32.
[6] T.H. Heim, A.M. Dietrich, Sensory aspects and water quality impacts of chlorinated and chloraminated drinking water in contact with HDPE and cPVC pipe, Water research, 41 (2007) 757-764.
[7] V. Lund, M. Anderson-Glenna, I. Skjevrak, I.-L. Steffensen, Long-term study of migration of volatile organic compounds from cross-linked polyethylene (PEX) pipes and effects on drinking water quality, Journal of water and health, 9 (2011) 483-497.
[8] M.J. Lehtola, M. Laxander, I.T. Miettinen, A. Hirvonen, T. Vartiainen, P.J. Martikainen, The effects of changing water flow velocity on the formation of biofilms and water quality in pilot distribution system consisting of copper or polyethylene pipes, Water research, 40 (2006) 2151-2160.
[9] J. Yu, D. Kim, T. Lee, Microbial diversity in biofilms on water distribution pipes of different materials, Water Science and Technology, 61 (2010) 163-171.
[10] J.M. Cerrato, L.P. Reyes, C.N. Alvarado, A.M. Dietrich, Effect of PVC and iron materials on Mn (II) deposition in drinking water distribution systems, Water Research, 40 (2006) 2720-2726.
[11] D.A. Lytle, T.J. Sorg, C. Frietch, Accumulation of arsenic in drinking water distribution systems, Environmental science & technology, 38 (2004) 5365-5372.
[12] M. Friedman, A. Hill, S. Reiber, R. Valentine, G. Larsen, A. Young, G. Korshin, C. Peng, Assessment of inorganics accumulation in drinking water system scales and sediments, Water Research Foundation, Denver, (2010).
[13] J. Liu, H. Chen, Q. Huang, L. Lou, B. Hu, S.-D. Endalkachew, N. Mallikarjuna, Y. Shan, X. Zhou, Characteristics of pipe-scale in the pipes of an urban drinking water distribution system in eastern China, Water Science and Technology: Water Supply, 16 (2016) 715-726.
[14] M. Salehi, X. Li, A.J. Whelton, Metal Accumulation in Representative Plastic Drinking Water Plumbing Systems, Journal: American Water Works Association, 109 (2017).
[15] P. Sarin, V. Snoeyink, D. Lytle, W. Kriven, Iron corrosion scales: model for scale growth, iron release, and colored water formation, Journal of Environmental Engineering, 130 (2004) 364-373.
[16] E.J. Kim, J.E. Herrera, Characteristics of lead corrosion scales formed during drinking water distribution and their potential influence on the release of lead and other contaminants, Environmental science & technology, 44 (2010) 6054-6061.
[17] B.N. Clark, S.V. Masters, M.A. Edwards, Lead release to drinking water from galvanized steel pipe coatings, Environmental Engineering Science, 32 (2015) 713-721.

[18] M. Lasheen, C. Sharaby, N. El-Kholy, I. Elsherif, S. El-Wakeel, Factors influencing lead and iron release from some Egyptian drinking water pipes, Journal of hazardous materials, 160 (2008) 675-680.
[19] K.J. Pieper, M. Tang, M.A. Edwards, Flint water crisis caused by interrupted corrosion control: Investigating "ground zero" home, Environmental science & technology, 51 (2017) 2007-2014.
[20] M. Del Toral, High lead levels in Flint, Michigan-interim report, Flint Water Study, (2015).
[21] K. Ashton, L. Holmes, A. Turner, Association of metals with plastic production pellets in the marine environment, Marine pollution bulletin, 60 (2010) 2050-2055.
[22] A. Turner, L.A. Holmes, Adsorption of trace metals by microplastic pellets in fresh water, Environmental Chemistry, 12 (2015) 600-610.
[23] C.M. Rochman, B.T. Hentschel, S.J. Teh, Long-term sorption of metals is similar among plastic types: implications for plastic debris in aquatic environments, PLoS One, 9 (2014) e85433.
[24] D.E. Robertson, The adsorption of trace elements in sea water on various container surfaces, Analytica Chimica Acta, 42 (1968) 533-536.
[25] A. Fischer, J. Kroon, T. Verburg, T. Teunissen, H.T. Wolterbeek, On the relevance of iron adsorption to container materials in small-volume experiments on iron marine chemistry: 55 Fe-aided assessment of capacity, affinity and kinetics, Marine Chemistry, 107 (2007) 533-546.
[26] L.A. Holmes, A. Turner, R.C. Thompson, Interactions between trace metals and plastic production pellets under estuarine conditions, Marine Chemistry, 167 (2014) 25-32.
[27] K.N. Fotopoulou, H.K. Karapanagioti, Surface properties of beached plastic pellets, Marine environmental research, 81 (2012) 70-77.
[28] M. Salehi, C.T. Jafvert, J.A. Howarter, A.J. Whelton, Investigation of the Factors that Influence Lead Accumulation onto Polyethylene: Implication for Potable Water Plumbing Pipes, Journal of Hazardous Materials, (2017).
[29] L.A. Holmes, A. Turner, R.C. Thompson, Adsorption of trace metals to plastic resin pellets in the marine environment, Environmental Pollution, 160 (2012) 42-48.
[30] C. Liu, R. Bai, Q. San Ly, Selective removal of copper and lead ions by diethylenetriamine-functionalized adsorbent: Behaviors and mechanisms, Water Research, 42 (2008) 1511-1522.
[31] A.J. Whelton, T. Nguyen, Contaminant migration from polymeric pipes used in buried potable water distribution systems: a review, Critical reviews in environmental science and technology, 43 (2013) 679-751.
[32] Y. Zhang, M. Edwards, Accelerated chloramine decay and microbial growth by nitrification in premise plumbing, American Water Works Association. Journal, 101 (2009) 51.
[33] J. Duruibe, M. Ogwuegbu, J. Egwurugwu, Heavy metal pollution and human biotoxic effects, International Journal of physical sciences, 2 (2007) 112-118.
[34] X. Huang, S. Zhao, M. Abu-Omar, A.J. Whelton, In-situ cleaning of heavy metal contaminated plastic water pipes using a biomass derived ligand, Journal of Environmental Chemical Engineering, 5 (2017) 3622-3631.
[35] J. Coates, Interpretation of infrared spectra, a practical approach, Encyclopedia of analytical chemistry, (2000).
[36] Y. Mato, T. Isobe, H. Takada, H. Kanehiro, C. Ohtake, T. Kaminuma, Plastic resin pellets as a transport medium for toxic chemicals in the marine environment, Environmental science & technology, 35 (2001) 318-324.

[37] C. Faur-Brasquet, K. Kadirvelu, P. Le Cloirec, Removal of metal ions from aqueous solution by adsorption onto activated carbon cloths: adsorption competition with organic matter, Carbon, 40 (2002) 2387-2392.
[38] L. Perelomov, D. Pinskiy, A. Violante, Effect of organic acids on the adsorption of copper, lead, and zinc by goethite, Eurasian Soil Science, 44 (2011) 22-28.
[39] R.G. Pearson, Absolute electronegativity and hardness: application to inorganic chemistry, Inorg. Chem.;(United States), 27 (1988).
[40] B. Xiao, K. Thomas, Competitive adsorption of aqueous metal ions on an oxidized nanoporous activated carbon, Langmuir, 20 (2004) 4566-4578.
[41] H.A. Aziz, M.S. Yusoff, M.N. Adlan, N.H. Adnan, S. Alias, Physico-chemical removal of iron from semi-aerobic landfill leachate by limestone filter, Waste management, 24 (2004) 353-358.
[42] L. Fan, J.L. Harris, F.A. Roddick, N.A. Booker, Influence of the characteristics of natural organic matter on the fouling of microfiltration membranes, Water Research, 35 (2001) 4455-4463.
[43] E. Sharp, S. Parson, B. Jefferson, Coagulation of NOM: linking character to treatment, Water Science and Technology, 53 (2006) 67-76.
[44] A. Koch, Gas chromatographic methods for detecting the release of organic compounds from polymeric materials in contact with drinking water, in, Hygiene-Inst. des Ruhrgebiets, 2004.
[45] G. Sheng, J. Li, D. Shao, J. Hu, C. Chen, Y. Chen, X. Wang, Adsorption of copper (II) on multiwalled carbon nanotubes in the absence and presence of humic or fulvic acids, Journal of Hazardous Materials, 178 (2010) 333-340.
[46] M. Connell, A. Stenson, L. Weinrich, M. LeChevallier, S.L. Boyd, R.R. Ghosal, R. Dey, A.J. Whelton, PEX and PP water pipes: assimilable carbon, chemicals, and odors, Journal - American Water Works Association, 108 (2016) E192-E204.
[47] J.O. Nriagu, Lead orthophosphates—IV Formation and stability in the environment, Geochimica et cosmochimica acta, 38 (1974) 887-898.
[48] X. Cao, L.Q. Ma, M. Chen, S.P. Singh, W.G. Harris, Impacts of phosphate amendments on lead biogeochemistry at a contaminated site, Environmental Science & Technology, 36 (2002) 5296-5304.
[49] M. Edwards, L. Hidmi, D. Gladwell, Phosphate inhibition of soluble copper corrosion by-product release, Corrosion science, 44 (2002) 1057-1071.
[50] F. Boyle, W. Lindsay, Diffraction Patterns and Solubility Products of Several Divalent Manganese Phosphate Compounds 1, Soil Science Society of America Journal, 49 (1985) 761-766.
[51] D.A. Lytle, M.R. Schock, Formation of Pb (IV) oxides in chlorinated water, Journal (American Water Works Association), 97 (2005) 102-114.
[52] C.K. Nguyen, Interactions between copper and chlorine disinfectants: chlorine decay, chloramine decay and copper pitting, in, Virginia Tech, 2005.
[53] P. Bose, M.A. Bose, S. Kumar, Critical evaluation of treatment strategies involving adsorption and chelation for wastewater containing copper, zinc and cyanide, Advances in Environmental Research, 7 (2002) 179-195.
[54] O.J. Hao, A.P. Davis, P.H. Chang, Kinetics of manganese (II) oxidation with chlorine, Journal of Environmental Engineering, 117 (1991) 359-374.
[55] W. Weber, J. Morris, Advances in water pollution research, in: Proceedings of the First International Conference on Water Pollution Research, Pergamon Press Oxford, 1962, pp. 231.

[56] F.-C. Wu, R.-L. Tseng, R.-S. Juang, Kinetic modeling of liquid-phase adsorption of reactive dyes and metal ions on chitosan, Water Research, 35 (2001) 613-618.
[57] M.C. Biesinger, L.W. Lau, A.R. Gerson, R.S.C. Smart, Resolving surface chemical states in XPS analysis of first row transition metals, oxides and hydroxides: Sc, Ti, V, Cu and Zn, Applied Surface Science, 257 (2010) 887-898.
[58] A.V. Naumkin, A. Kraut-Vass, S.W. Gaarenstroom, C. Powell, NIST X-ray Photo-electron Spectroscopy Database, NIST Standard Reference Database 20, Version 4.1, 2012, Google Scholar.
[59] C.K. Nguyen, K.A. Powers, M.A. Raetz, J.L. Parks, M.A. Edwards, Rapid free chlorine decay in the presence of Cu (OH) 2: Chemistry and practical implications, Water research, 45 (2011) 5302-5312.
[60] V. Nefedov, Y.V. Salyn, P. Solozhenkin, G.Y. Pulatov, X‐ray photoelectron study of surface compounds formed during flotation of minerals, Surface and Interface Analysis, 2 (1980) 170-172.
[61] C. Xiong, W. Wang, F. Tan, F. Luo, J. Chen, X. Qiao, Investigation on the efficiency and mechanism of Cd (II) and Pb (II) removal from aqueous solutions using MgO nanoparticles, Journal of hazardous materials, 299 (2015) 664-674.
[62] M.R. Schock, Understanding corrosion control strategies for lead, Journal‐American Water Works Association, 81 (1989) 88-100.

CHAPTER 3. CORROSION OF UPSTREAM METAL PLUMBING COMPONENTS INFLUENCES DOWNSTREAM HEAVY METAL SURFACE LOADINGS ON PLASTIC PIPE

3.1. Introduction

Plastic pipes are increasingly being installed for new building water service lines and indoor plumbing systems and renovations. These materials are reportedly lower cost than their metal counterparts and soldering can be avoided[1]. In 2013, a 59 household survey that 54% preferred crosslinked polyethylene (PEX) pipe for replumbing their homes, followed by an epoxy lining (15%), copper pipe (9%) and CPVC (7%) pipe [2]. Plastic pipe is expected to continue to be installed with market expansion at about 6.8%/year [3]. When buildings are renovated or expanded, sometimes new plastic plumbing is added to the end of the old metal plumbing components. On a community scale, plastic pipes coexist with old metal plumbing (i.e., in the service line and water main) [4-6]. One example is that a newly renovated and low-water use PEX plumbing system that contained brass valves[5]. Before water reached the indoor piping, water traveled from the water treatment plant PVC and ductile iron pipe and a copper service line.. It is not unexpected plastic pipes are downstream of metal plumbing components, and metal components can release heavy metals into drinking water.

Some heavy metals, which have health-based and aesthetic-based drinking water limited and standards, have been detected in plastic plumbing systems. Past investigators have found elevated metal concentrations likely originated from metalc components in plastic plumbing (i.e., metal pipes, fittings and fixtures) [5-8]. Kimbrough et al (2007) compared drinking water quality from both traditional (i.e., with galvanized steel and copper pipes) and all-plastic plumbing (i.e., from the meter to the tap) in Southern California [6]. Both traditional and plastic plumbing systems

received drinking water from the same water source. No significant difference (i.e., Cu, Ni, Pb and Zn) was found between the traditional and plastic plumbing systems. The researchers concluded that brass corrosion was the major cause of lead and copper contributor in first-draw water samples. However, the role of plastic piping materials within the plumbing system corrosion process received little scrutiny.

It is well-known that metal plumbing components can release heavy metals (i.e., Cu, Ni, Pb and Zn) into drinking water [8-13], but the fate of those metals on plastic plumbing pipes has received limited study. Brass valves are a common component of PEX plumbing and can influence water quality. Factors that influence brass fixture leaching include the brass's composition (i.e., lead content), drinking water properties (i.e. pH, alkalinity, organic and corrosion inhibitor levels), galvanic connection (i.e., connect to copper pipe), and hydraulic conditions (i.e., stagnation time, water flow, and pressure) [8, 14-20]. Lytle and Schock (1996) found that the amount of lead released from brass corresponded well with the brass alloy's lead content but depended on the type of brass. It was reported lead levels could differ by as much as 50 µg/L [21]. The stagnation time (24 vs 72 hr) showed little effect on lead leached from yellow brass (C84500), whereas a higher level of lead (25 µg/L) was observed for red brass (C84500) when exposed to longer period (i.e., 72 hr). Pieper et al. (2016) found that pH and alkalinity can influence lead leaching from brass [15]. Specifically, while NSF/ANSI Standard 61 test protocol used high pH and alkalinity water (i.e., pH 8 and 500 mg/L alkalinity as $CaCO_3$), the most aggressive water scenario (i.e., pH 4 and no alkalinity) resulted about 17 times more lead leaching (from C36000) during the 19 day study. Nitrate-ammonia and disinfectants (chlorine and chloramine) can also influence lead leaching from brass devices [18]. Dudi (2004) discovered that greater Cl^-:$SO4^{2-}$ ratios resulted in a greater galvanic current (i.e., 240%), which corresponded with increased lead leaching (i.e., 240%) [19].

It was also reported that the galvanic connection with copper pipes largely enhanced lead leaching in every case. Tam et al. (2009) found orthophosphate (0.8 mg/L as P) remarkably reduced lead and copper leaching from brass fittings [11]. When pH was 7.5 or higher, as the leaching of Cu and Pb was reduced by about 70%. A higher flow velocity appeared promote the brass's corrosion rate, but flow did not change the corrosion mechanism [22]. A higher temperature often resulted in a greater amount of Zn and Pb leaching from brass plumbing devices. However, none of above mentioned works investigated the influence of metals leaching (from brass fittings) on nonmetallic materials (i.e., plastic drinking water pipes). Especially the potential of leached metals that could deposit onto plastic pipe surfaces or the effect on plastic piping degradation.

The accumulation and impact of heavy metals on plastic pipe surfaces has received limited scrutiny. Metal scales characterized from exhumed water pipes revealed a variety of heavy metals could accumulate onto water distribution HDPE and PVC piping surfaces [23-26]. Lytle et al. (2004) analyzed pipe section solids collected from 15 drinking water utilities in the United States (i.e., Ohio, Michigan and Indiana) [24]. Exhumed PVC pipe section solids were digested and results showed most abundant metals were Fe, Ca, Zn and P. Another increasing study was conducted by Cerrato et al. (2006), who found manganese (Mn) composition was about 1.8 times more in PVC scales than iron pipe scales [23]. This difference could be explained from the non-polarity and no electron exchangeable PVC surfaces properties, which provided favorable environment for Mn precipitation. Fewer studies have been conducted that described heavy metals present on plastic plumbing pipes/well casing [27-29]. By analyzing metal deposits from the one year old PEX plumbing pipe through the acid solution digestion method [30], Salehi et al (2018) discovered metal deposits variation at different locations, and as well as cold vs hot water [29]. Fe was also found as the most abundant element in PEX scales and temperature effect was

inconclusive on metal-plastic interaction. Metals that deposited onto plastic drinking water pipes could be originated from the drinking water source (i.e., Ca), water distribution system pipes (i.e., Fe, Ni and Pb), and could also from added chemicals during water treatment (i.e., $KMnO_4$) [5, 24].

Information about heavy metal associated plastic pipe degradation is limited and there is evidence that metal deposits may contribute to plastic degradation and failure. Few studies were found that evaluatd heavy metal induced plastic degradation [31-33]. Tanemura et al. (2014) found that in the presence of copper at high water temperature (i.e., > 60^oC), crystallization and increased surface roughness were observed for polyethylene raised temperature (PE-RT) pipe [31]. PE-RT specimens that indicated plastic oxidation/accelerated degradation. Other factors, such as thermal, chlorinated water, and ozone exposure in high temperature could has shown to accelerate polyethylene degradation [34-36]. Montes et al. (2012) studied the degradation of a multilayer pipe called PERT/aluminum/PERT exposed to chlorinated water (0 to 100 ppm as Cl_2) at 70^oC [35]. No pipe degradation was detected for the low chlorine concentration (1 mg/L), whereas, the higher concentrations (i.e., 25 vs 100 mg/L) demonstrated equivalent degradation. After pipes had been aged for 270 days at 70^oC, new functional groups, such as >C=H_2, -OH and >C-OC< were detected on the inner surface. While the elevated temperature (i.e., hot water) can accelerate plastic pipe degradation, water conditions (i.e., pH and alkalinity) and release of metals from upstream plumbing materials (i.e., pipes, valves, fittings) might also influence downstream plastic pipe integrity.

In the current work, the influence of metal and plastic piping on metal leaching/deposition on downstream PEX pipes was studied. Both field and bench scale tests were adopted for cold and hot water plumbing. The specific objectives were to (i) characterize scales from galvanized and connected PEX drinking water pipes that exhumed from the residential housing (ii) examine the

influence of water conditions, temperature and pipe apparatus on metal leaching from brass fitting valve and (iii) evaluate metal deposition onto plastic pipe surfaces and the potential plastic degradation phenomenon. Results from this study may be used to better design plumbing, limit premature failure of downstream plastic pipe, help avoid heavy metal drinking water problems, and predict drinking water quality at building fixtures.

3.2. Materials and methods

3.2.1 Filed study about exhumed pipe scales

On May 10, 2018, twelve galvanized iron and six PEX plumbing pipes were exhumed from a 4 bedroom, 1.5 bath, 204 m^2 area single-family home in West Lafayette, Indiana USA. The pipes conveyed water from a copper service line to various first floor fixtures. Six months prior to pipe removal, the PEX plumbing was installed. The six PEX pipes were connected to the existing galvanized plumbing pipes. The exhumed pipes were covered with Parafilm to prevent drying out and transported to the lab for analysis. Characteristics of the municipal water that entered the building has been described elsewhere [29]. In summary, the drinking water source was a well field, followed by chemical treatment that included $KMnO_4$, free chlorine as the residual disinfectant, and corrosion inhibitor (70% orthophosphate and 30% polyphosphate). The water that entered the residential housing was still fairly hard (i.e. Ca: 104 mg/L and Mg: 34 mg/L).

Metal constituents on the exhumed galvanized iron and PEX pipes were examined. Metal solids from the galvanized pipes (i.e., 0.2-0.4 g) were scraped off and weighted before digestion. About 0.02 g pre-weighted metal solids were placed in 40 ml solution (2% nitric acid + 2% hydroxylamine) with a method similar to others [10, 16, 30]. The metal- free concentrated nitric acid (67%-70%) was purchased from Fisher Scientific (Catalog No. A509-P212), which used for metal solids digestion and preparation for ICP-OES analysis. The digestion process was conducted

under 55^{o}C temperature (with slow mixing) for a minimum of 48 hr or until metals debris were dissolved. Next, a 100 µL aliquot was withdrawn and diluted to 10 ml for analysis on an Inductively Coupled Plasma-Optical Emission Spectroscopy (ICP-OES) (Perkin Elmer). To determine the metal deposits composition on PEX pipes, the exhumed PEX pipes were filled with 2% nitric acid and 2% hydroxylamine, plugged with PTFE wrapped silicon stoppers, and mixed for minimum of 48 hr. Then a 100 µL of digested solution was extracted and diluted to 10 ml before ICP-OES measurement. In order to examine variations in scale composition/metal deposition distribution along the same length of plastic pipe (i.e., PEX pipe that connected to the refrigerator), three 6 inch pipe coupons were cut and digested for metal analysis.

3.2.2 Bench-scale experiments

3.2.2.1 Materials and pipe apparatus

To study metallic and non-metallic piping connection effects on metal leaching and the potential deposition onto plastic materials, four plumbing configurations were assembled (Figure 3.1): (1) PEX piping only (3/4” diameter, 12” length), (2) Copper piping only (3/4” diameter, 12” length), (3) PEX piping (3/4” diameter, 6” length) + Brass valve + PEX (3/4” diameter, 6” length) (PBP) and (4) Copper (3/4” diameter, 6” length) + Brass valve + PEX (3/4” diameter, 6” length) (CBP). Lead-free (<0.25% of lead by weight) ball valves (3/4”) were purchased from a local plumbing supplier and 3/4" PEX-A (i.e., cross-linked medium density polyethylene) pipes were purchased from SupplyHouse.com (product No. F1040750). Pipe ends were sealed with PTFE wrapped silicone stoppers to prevent leaking. Among these four experimental groups, groups 1 and 2 were used as controls. Groups 3 and 4 enabled to study the upstream copper pipe effect on overall metal leaching, as well as the deposition of metals upon downstream plastic pipe [31, 32]. All testing was conducted with four replicates.

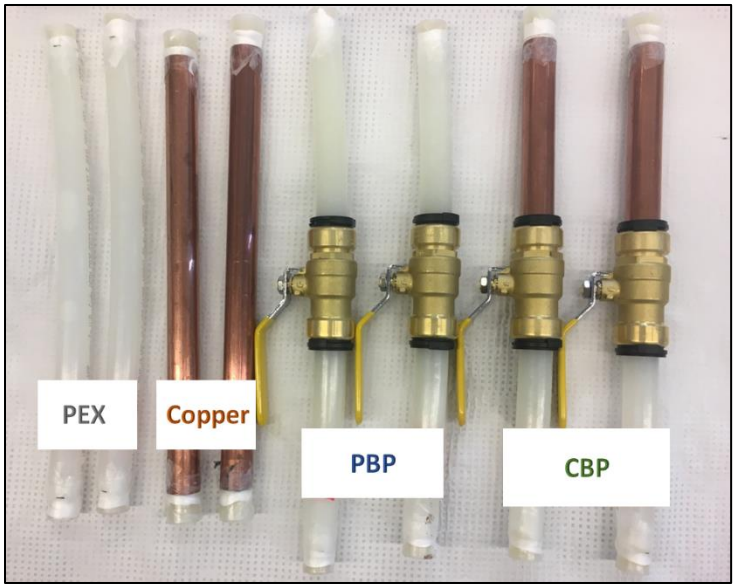

Figure 3.1 Illustration of pipe apparatus and experimental groups' layout.

3.2.2.2 Water conditions

To evaluate metal release under different scenarios, two water conditions and temperatures were selected based on the previous study [15] (Table 3.1). For all water solutions preparation, Millipore Mili-Q water (MQW) (18.2 MΩ cm) was used throughout the study. 4,000 mg/L as $CaCO_3$ hardness stock solution was prepared by dissolving 5.88 g calcium chloride dihydrate ($CaCl_2.2H_2O$) (Fisher Scientific, Catalog No. AC423525000) in 1L water [37]. Similarly, 4,000 mg/L as $CaCO_3$ alkalinity stock solution was made by adding 3.36 g sodium bicarbonate ($NaHCO_3$) (Fisher Scientific, Catalog No. S233-500) in 1L water. Then the desired hardness and alkalinity values could be achieved through series dilutions from the stock. The stock solutions were made every week. Solution hardness was fixed at 100 mg/L as $CaCO_3$. Both aggressive water (i.e., at pH 4 with no alkalinity) and moderate water (i.e., at pH 7.5 with 175 mg/L alkalinity as $CaCO_3$) were used. Cold (i.e., 23^{o}C) and hot (i.e., 55^{o}C) water conditions were also examined.

Table 3.1 A summary of tested water conditions

Water condition	pH	Alkalinity[a], mg/L as $CaCO_3$	Temp.[b], °C	Hardness[c], mg/L as $CaCO_3$
A	7.5	175	23	100
B	7.5	175	55	100
C	4	0	23	100
D	4	0	55	100

a. The desired alkalinity was achieved by adding sodium bicarbonate ($NaHCO_3$) buffer.
b. all experiments were conducted in the room (23°C) or constant high temperature room (55°C).
c. The desired hardness was achieved by adding calcium chloride dihydrate ($CaCl_2.2H_2O$).

3.2.2.3 Sample collection and analytical methods

Metal leaching from each plumbing configuration was examined under various water conditions (i.e., pH, alkalinity, hardness and temperature) by applying the dump-and-fill method [14, 15, 38]. Before starting the experiment, all pipe apparatus were disinfected with sodium hypochlorite solution (i.e., 100 mg/L as Cl_2) and stagnated for 24 hr at room temperature [5]. The sodium hypochlorite (10-15%, reagent grade) was purchased from Sigma-Aldrich, supply part No. 425044. Next, the pipes were rinsed three times with deionized water followed by thrice rinsing with Millipore Mili-Q water.

The leaching experiment was carried-out over a three-week period, and water quality parameters were monitored on day 3, 6, 9, 12, 15, 18, 21. Every three days, water was freshly prepared and filled into pipe apparatus (Figure 3.1). Water samples were collected in 125 ml HDPE bottles and water volume and end pH was measured. The three-day water change approach was implemented so that results between water changes could be directly compared against one another. At the end of each three day exposure period, 20 ml of sample underwent total organic carbon (TOC) measurement (TOC-LCPH analyzer, Shimadzu). A 10 ml aliquot was placed in a 15 ml metal-free centrifuge tube for total metals analysis. Dissolved metals were obtained by filtering 30 ml of water sample (i.e., through the 0.45 µm Nylon filter). Both total and dissolved water samples were acidified with 2% HNO_3 and examined by ICP-OES. The TOC method detection limit (MDL)

was determined as 0.168 mg/L from seven replicates [39]. Whereas, using the same method, target metal MDLs were Al (0.62 µg/L), Cd (0.11 µg/L), Co (1.34 µg/L), Cr (0.95 µg/L), Cu (0.28 µg/L), Fe (0.23 µg/L), Mn, (0.06 µg/L), Ni (0.41 µg/L), Pb (1.15 µg/L), Se (23.19 µg/L) and Zn (0.43 µg/L), respectively. Any measured values that fell below the corresponding MDL were not reported.

3.2.2.4 Characterization

Brass valve and copper pipe composition were determined by using a portable x-ray fluorescence (pXRF) (Tracer III-SD, Bruker). The calibration curve was developed to specifically detect brass alloy composition. In addition, at the end of each 21-day experimental period, metals that had deposited on the PEX were also characterized. One 7 cm segment of PEX-A pipe was cut from the end that connected to the brass valve and filled with 2% HNO_3 solution. After a minimum of 48 hr, the solution was collected and analyzed by ICP-OES. Also, a 1 cm ×1 cm plastic segment was cut from the PEX-A pipe and analyzed by Attenuated Total Reflectance (ATR) - Fourier Transform Infrared (FTIR) spectroscopy (TravellR HazMat FTIR spectrometer, coupled with a Diamond ATR sample interface). ATR-FTIR was applied to identify if any plastic degradation occurred, specifically the formation of oxygen containing functional groups (i.e., -OH, >C=O, and >C=O<). The spectra scan was ranged from 650 to 4000 cm^{-1}, with resolution of 2 cm^{-1}. The morphology of metal deposits on the PEX-A pipe surface was examined by scanning electron microscopy-energy dispersive X-ray spectroscopy (SEM-EDS) (Hitachi S-4800 Field Emission SEM). Because the plastic had very low conductivity, all samples (1 cm ×1 cm) were coated with a thin platinum film and fixed with the conductive tape. The measurement was operated at 20 keV and with a working distance of about 15 mm.

3.3. Results and discussion

3.3.1 Metal loadings on metallic and plastic materials from the field study

Solid materials were observed on the inner pipe walls for both upstream metallic (i.e., galvanized iron) and downstream plastic drinking water pipes (Figure 3.2). Characterization of the galvanized pipe inner wall scrapings indicated that iron (Fe) (25.6-56.0%) was the most abundant element, followed by calcium (Ca) (6.0-17.0%) and phosphorous (P) (2.4-15.4%) (Table 3.2). Fe levels in the municipal drinking was at the fairly low level (0.05 mg/L), so the concentrated Fe detected in the solids were likely originated from the galvanized iron pipe, pipe fittings, and the ductile iron water mains [8, 29]. The high Calcium abundance was likely due to the naturally hard water (i.e., 104 mg/L). Phosphorous was probably associated with the utility's phosphate-based corrosion inhibitor. For other trace metals, galvanized iron pipe solids' composition was in the order as Zn, Si > Mn, Ba > Cu, Pb > Ni, Cd (except M2). Zinc is a major component used in galvanized iron pipes and brass fitting, so the elevated zinc could be leached from these materials and accumulate on pipe surfaces [8, 25].

A brownish colored material was present on the inner wall of the PEX pipe that exhumed from the cold city water supply line (Figure 3.2). With the exception of two PEX pipe samples, the chemical composition of metals found on the PEX pipe inner walls was similar to the galvanized iron pipes (Table 3.2). For trace metals, heavy metal loadings on PEX pipes slightly differed from that of the galvanized iron pipe: Mn, Si > Zn, Cu > Ba, Pb > Ni, Cd (Table 3.2). Half of the PEX pipe samples (3 out of 6) had the Mn in range of 1.8-7.5 mg/m^2 which was similar to a study of the neighboring home's exhumed one year old PEX plumbing (0.5-6.0 mg/m^2) [29]. Both homes received drinking water from the same water distribution system. Mn has also been found on HDPE (2324 µg/g) and PVC (671 µg/g) plastic drinking water pipes outside of Indiana [25, 26]. The presence of concentrated manganese in plastic scales were likely resulted from the oxidation of Mn (II) and Mn (IV) by dissolved oxygen and chlorine content in the distribution

system. And the non-polar property of plastic drinking water pipes could accumulate manganese precipitate and form the superficial scale [23]. Mn loading was more than 100 times greater on PEX-1 and PEX-2 samples than other PEX samples from the same home. Blackish scales for these two samples were observed, which could be easily removed by finger wipe (Figure 3.3a and b). For the hot water PEX-3 and 6 supply pipe, a light yellowish color was observed on the inner pipe wall (Figure 3.3c and d). When metal loading on the same length of plastic pipe was characterized, Ca, Fe, Mn, P and Si loadings decreased with flow direction (Figure 3.4). SEM-EDS results indicated more metal deposits were present closer to the tee and decreased as water flowed down the pipe (Figure B.1). This dissimilar metal loading on the pipe may be due to hydraulic and/or physiochemical reasons but underscores the potential complexity of metal deposits within a single PEX pipe plumbing system. Additional work is suggested to characterize deposited metals within plumbing systems and focus on pipe location, flow, and temperature regimes.

Figure 3.2 Image of metal scales on exhumed galvanized and PEX drinking water pipes from the cold city water supply line.

Table 3.2 Composition of metal solids (M) (mg/g) from the galvanized iron pipe that connected to PEX piping and the corresponding PEX pipe metal loading (PEX) (mg/m^2).

Sample	Al	Ba	Ca	Cd	Cu	Fe	Mg	Mn	Ni	P	Pb	Si	Zn
Cold water line													
M-1	0.04	2.54	19.19	0.03	1.26	500.66	1.59	2.35	3.67	30.22	0.08	11.64	10.76
PEX-1	2.07	88.40	399.93	0.64	578.00	2048.50	35.87	1368.50	4.09	149.60	135.15	150.45	437.75
Cold water line													
M-2	0.47	16.59	38.83	0.01	3.41	353.17	3.57	122.73	0.10	27.32	0.37	11.73	5.60
PEX-2	2.55	44.63	245.65	0.38	493.00	807.50	20.61	888.25	2.03	76.50	135.15	103.70	335.75
Hot water line													
M-3	6.40	0.82	168.49	0.07	1.53	297.26	2.90	3.60	0.29	61.51	0.21	11.03	65.89
PEX-3	0.22	0.39	9.27	-	2.74	22.31	0.71	2.99	0.05	8.37	-	4.76	2.75
Cold water line													
M-4	0.69	2.94	29.85	0.02	1.37	479.19	2.23	1.82	0.11	37.77	0.29	12.37	17.81
PEX-4	0.58	2.53	30.09	-	4.97	163.63	8.63	7.48	0.35	27.84	0.91	18.87	7.06
Cold water line													
M-5	0.15	2.17	18.35	0.04	0.79	485.81	1.57	5.85	-	23.63	1.18	13.20	36.44
PEX-5	0.28	3.52	47.18	-	5.10	197.63	12.50	2.23	0.37	44.20	0.23	36.55	3.26
Thermal expansion tank line													
M-6	0.49	1.95	26.84	0.02	0.78	535.04	1.70	1.78	-	26.84	0.12	12.53	9.11
PEX-6	8.50	7.95	33.53	-	15.51	325.98	3.02	38.34	0.28	41.40	1.22	26.69	58.23

- Represents the metal was not detected or below the instrument detection limit.

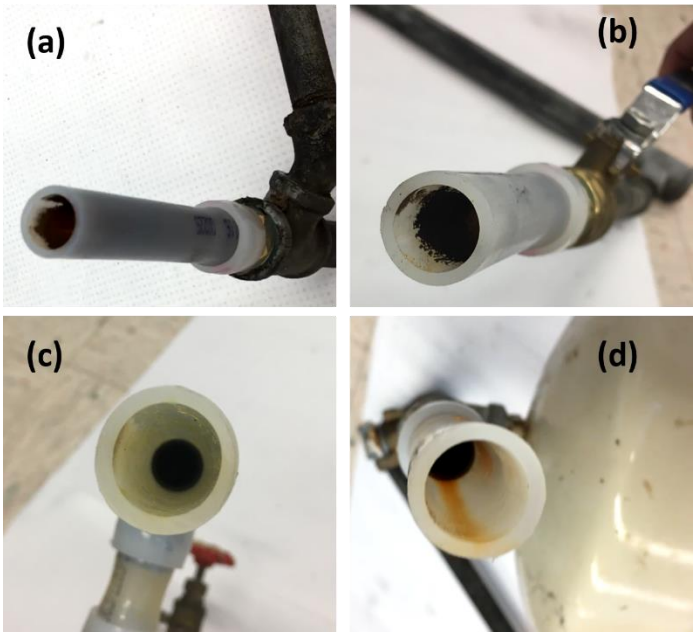

Figure 3.3 Image of inner wall metal scales on exhumed (a) PEX-1, (b) PEX-2, (c) PEX-3 and (d) PEX-6 pipes.

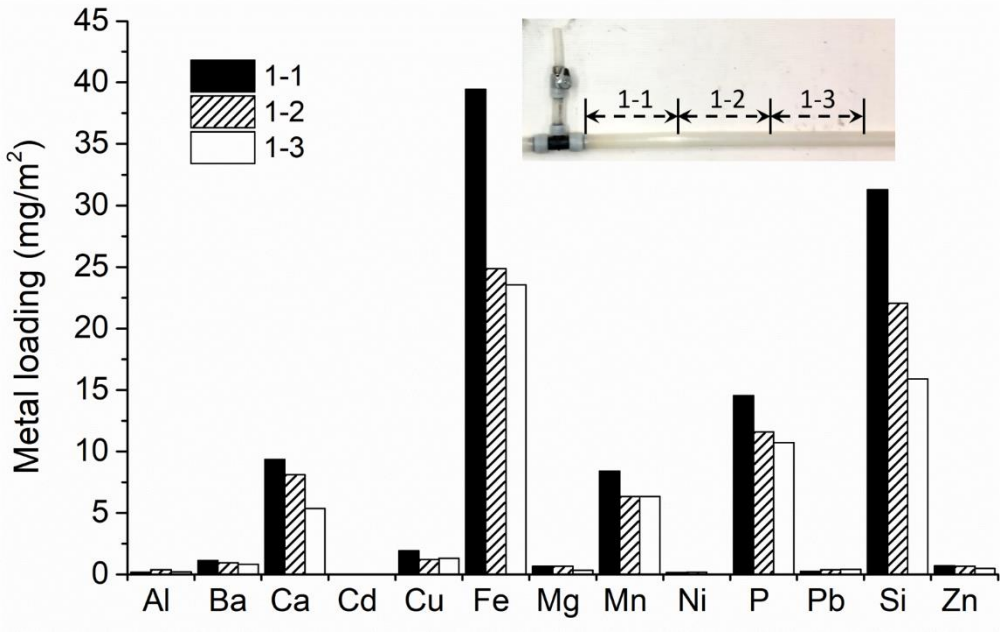

Figure 3.4 Metal distribution along the same length of an exhumed 3/4" diameter PEX pipe. Each pipe section was cut into 6 inch length.

3.3.2 Plumbing components and water conditions influenced water quality

Bench-scale experiments that included PEX pipes, brass valves, and copper pipes revealed that metal leaching was accelerated within the pH 4 water than the pH 7.5 water at room temperature (Figure 3.5), which is consistent with prior knowledge [15]. Among all detected metals in these experiments, Zn was detected in greatest level, followed by Cu, Ni, Pb, and Fe. On day 21, for the PEX Pipe-Brass Valve-PEX Pipe (PBP) apparatus, metal leaching under pH 4 vs pH 7.5 water conditions were Cu (315.6 vs 10.4 µg/L), Fe (0.7 vs not detected), Ni (26.2 vs 2.6 µg/L), Pb (6.3 vs 0.1 µg/L) and Zn (953.1 vs 45.9 µg/L), respectively. Lytle and Schock (1996) previously discovered, depended on the brass types and manufacturing processes, brass lead content was significantly varied [21]. XRF spectrometry revealed the brass valves[lead-free (<0.25 % Pb)] used in the current study were 64.29 ± 0.52% Cu, 34.88 ± 0.57% Zn, 0.42 ± 0.06% Fe, 0.16 ± 0.01% Ni, 0.1 ± 0.01% Mn, 0.09 ± 0.00% Co and 0.06 ± 0.00% As.

The role of copper pipe that many influence water quality in PEX plumbing was also investigated by connecting the PEX pipe-brass valve rig to a copper pipe (i.e., CBP groups). XRF spectrometry indicated that copper pipe was 99.77 ± 0.03% Cu, 0.13 ± 0.00% Zn, 0.07 ± 0.00% Ni, 0.02 ± 0.00% As, and 0.01 ± 0.00% Co. Under the same experimental conditions, Fe, Pb and Zn leaching was greater for the CBP than PBP apparatus (Figure 3.5b, d, and e). For example, although there was not significant difference prior day 9 on Pb leaching, CBP started leaching about 1.7 times more Pb than PBP at pH 4 (i.e., 12.3 vs 7.1 µg/L) on day 12 and remained consistent higher than the PBP rigs. This finding agreed well with Dudi (2004), who discovered 3 out of 6 galvanic connection cases (copper and brass) resulted 2 times more Pb leaching [19]. Surprisingly, under pH 4 water, a higher level of Cu was observed in PBP (i.e., without copper connection) than CBP **(**Figure 3.5a**)**. This may be associated with galvanic corrosion preventing copper from corroding ($Cu^{2+}+2e^{-}\rightarrow Cu$) [40] and the leached copper may have limited copper

dissolution from brass surfaces and copper pipe. For the pH 7.5 water condition, galvanic corrosion did not seem to affect copper leaching. Past investigators have also reported that copper leaching and the electrochemical potential of Cu did not markedly increase (within the detection limit) when copper was connected to a lead pipe under pH 8.5 water [19]. A Ni leaching spike (106.7 µg/L) was observed for the PBP rig under pH 4 water on Day 3 and then the concentration decreased to about the same level as CBP group (20 µg/L) after day 12 (Figure 3.5c). This phenomenon may have occurred due to accelerated brass corrosion under certain conditions (i.e., galvanic corrosion combined with aggressive pH 4 water).

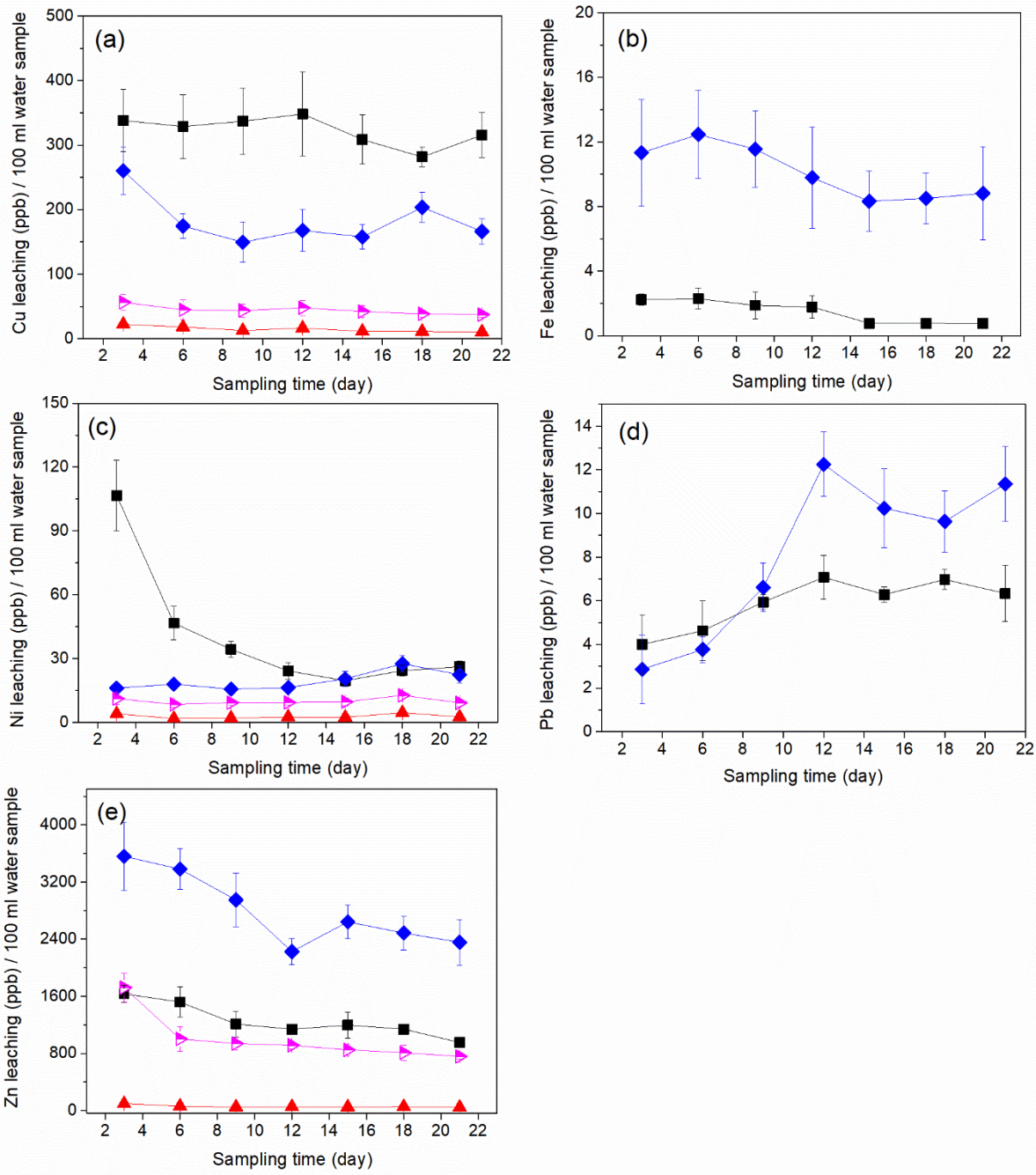

Figure 3.5 (a) Cu, (b) Fe, (c) Ni, (d) Pb and (e) Zn total metal leaching under pH4 and pH 7.5 water conditions. ■ PBP pH 4 water, ▲ PBP PH 7.5 water, ◆ CBP pH 4 water, ▷ CBP pH 7.5 water. Fe and Pb were not detected under pH 7.5 water condition. All experiments were conducted at room temperature (23^{o}C).

3.3.3 Effect of temperature on pipe apparatus leaching

Temperature affected total metal leaching, but the effect varied depended on the metal type (Figure 3.6). Compared with 23ºC, the 55ºC temperature resulted in higher concentrations of leached Ni, Pb and Zn, but hindered Cu and Fe leaching. This observation has been reported by Zlatanovic et al (2017) who found a higher maximum Cu level in both kitchen (1370 vs 1140 µg/L) and shower (1680 vs 1470 µg/L) tap water during winter stagnation (6-8 ºC) vs. summer stagnation (21.5-23 ºC) [41], and higher Zn levels were found during the summer (180 µg/L) vs. winter (200 µg/L). Sarver and Edwards (2011) also studied the temperature effect on metal leaching and brass corrosion [22]. They discovered hot water increased the meringue build-up and accelerated zinc and lead leaching, which agreed with the present work **(**Figure 3.6**)**. However, other studies found elevated temperature (60ºC) promoted total Cu leaching [20] or no clear effect had been found on lead release vs. temperature [11].

At the beginning water stagnation study, leached organic carbon levels were greater for 55 ºC than at 23ºC (Figure 3.6). On day 3, the leached TOC was as high as 16.4 mg/L and 9.7 mg/L for PBP and CBP at 55ºC, respectively, which slowly decreased over time. For the 23ºC temperature, the organic carbon levels were consistent with time (0.65-0.99 mg/L TOC). On Day 21, TOC values for both PBP and CBP experimental groups under both temperatures were almost at the same level (0.76 vs. 0.96 mg/L TOC). The source of organic carbon may be pipe additives and compounds formed during plastic pipe manufacture [42, 43]. The high temperature likely accelerated the extraction of organic carbon into the water. But it remains unclear about what role, if any, these organic compounds influenced heavy metals fate.

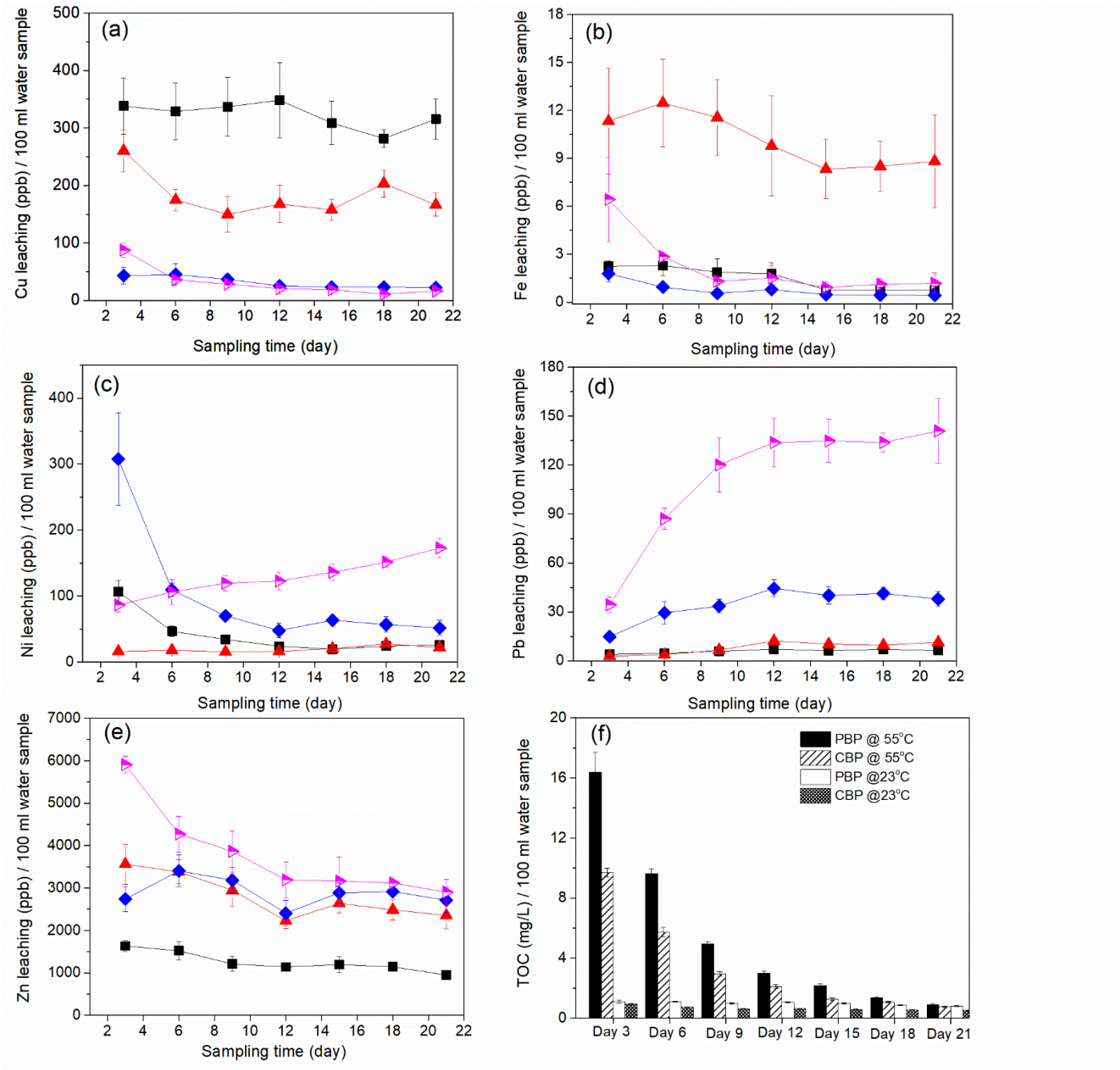

Figure 3.6 (a) Cu, (b) Fe, (c) Ni, (d) Pb and (e) Zn metal leaching under 23ºC and 55ºC temperature. ■ PBP @ 23ºC, ▲ CBP @ 23ºC, ◆ PBP @ 55ºC, ▷ CBP @ 55ºC. Water condition was pH 4 water.

3.3.4 Evidence of metal deposition onto plastic materials

At the end of the 21 day leaching experiment, the inner PEX pipe walls were exposed to an acid solution (i.e., 2% HNO_3) and ICP-OES confirmed that metals (i.e., Ca, Mg, Cu, Fe, Pb, and

Zn) were present on plastic surfaces (Figure 3.7). All presented data were subtracted from the PEX- only control group that count for originated metals from PEX pipes or water solutions. Significantly greater levels of metals were found at 55 ^{o}C compared to 23 ^{o}C temperature. For the pH 7.5 water condition, metals found at 23^{o}C vs 55 ^{o}C for the CBP experimental group were Ca (191 vs 1208 µg/m^2), Mg (67 vs 137 µg/m^2), Cu (33 vs 1732 µg/m^2), Fe (33 vs 88 µg/m^2), Pb (2 vs 101 µg/m^2), and Zn (24 vs 5447 µg/m^2), respectively. In the literature, Muryanto et al. (2014) found the growth of calcium carbonate scale on stainless steel pipes was about 1.3 time greater under 40^{o}C temperature than 25^{o}C [44]. These investigators hypothesized that, based on the classical Arrhenius equation, higher temperature would bring more energy to accelerate the calcium scale reaction rate and crystalline phases. A more recent study reported that a greater loading of Cu was found in hot water PEX-A plumbing pipes exhumed from a neighboring Indiana home compared to cold water pipes [29]. However, Ca, Fe, Pb, and Zn loadings from that neighboring home exhumed pipe were not similar to the present bench-scale study. For the current study, the high Zn loading on PEX pipe at 55^{o}C could be attributed to Zn leaching (up to 5908 µg/L) from the galvanic corrosion effect. The greater water solution pH value, and less dissolved metal content at 55^{o}C (Table B.1) may promote metal precipitation onto plastic surfaces under the stagnant conditions. SEM images support the author's hypothesis, where more metal was found at the PEX pipe bottom sections compared to the top from the same PEX pipes (Figure 3.8).

Other than temperature, in the current study, water conditions also played a substantial role of metal deposition onto plastic pipe surfaces. As shown in the figure, for most cases, pH 7.5 water resulted higher metal loading than pH 4 water **(**Figure 3.7**)**. An interesting finding was that for Ni, even though leaching levels were as high as 308 µg/L (i.e. at 55^{o}C, pH 4 water and CBP group), Ni was not detected on the plastic surfaces from all tested conditions. This was mainly due to the

high dissolution of Ni that resulted about 93.4-98.2 % dissolved Ni for all conditions, so Ni precipitation onto plastic surfaces was prevented. For other metals (i.e., Cu, Fe, Pb and Zn), higher pH values would result in the reduction of dissolved metals within water solutions. When pH 4 water was used, for the CBP at 55^{o}C, the percent of dissolved metals were 95.2 % Cu and 97.1 % Zn. Whereas, for pH 7.5 water conditions, values dropped to 67.0 % Cu and 71.4 % Zn, respectively. The pH effect was also observed when Robertson (1968) used polyethylene bottles to store sea water samples [45]. For pH 8 water samples, more than 90% of Fe was adsorbed onto the container wall. However, after adding hydrochloric acid brought pH down to 1.5, the adsorption was almost eliminated (i.e., less than 5%) till the end of storage period (i.e., 75 days). Turner et al. (2015) found the enhanced Pb and Zn adsorption onto plastic pellets, in fresh water, when pH increased from 4 to 8 [46]. The finding could be explained from different aspects, such as metal speciation, plastic surface characteristics and the affinity of metal-plastic surfaces. In this work, we adopted new plumbing materials (i.e., brass valve fitting, copper and PEX-A pipes) and the stagnation method (i.e., every 3 days) for a total of 21 days experimental period. Long term flow conditions monitoring and plumbing materials aging effects are recommended and worth study for the future work.

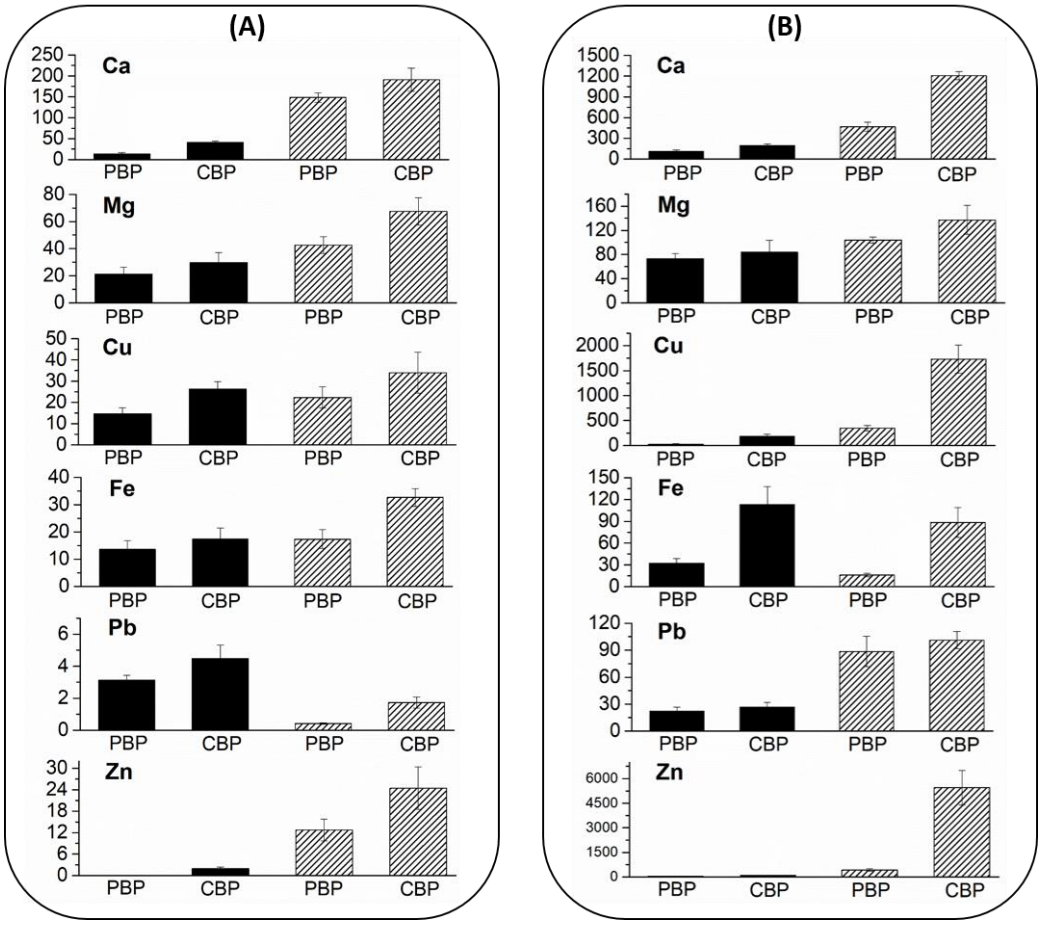

Figure 3.7 Metal loading (µg/m^2) on PEX pipe surfaces (■ pH 4 water condition and ▨ pH 7.5 water conditions) at (A) 23^{o}C and (B) 55^{o}C temperature. The presented data was subtracting from the metal loading on PEX-only control group under the same experimental condition.

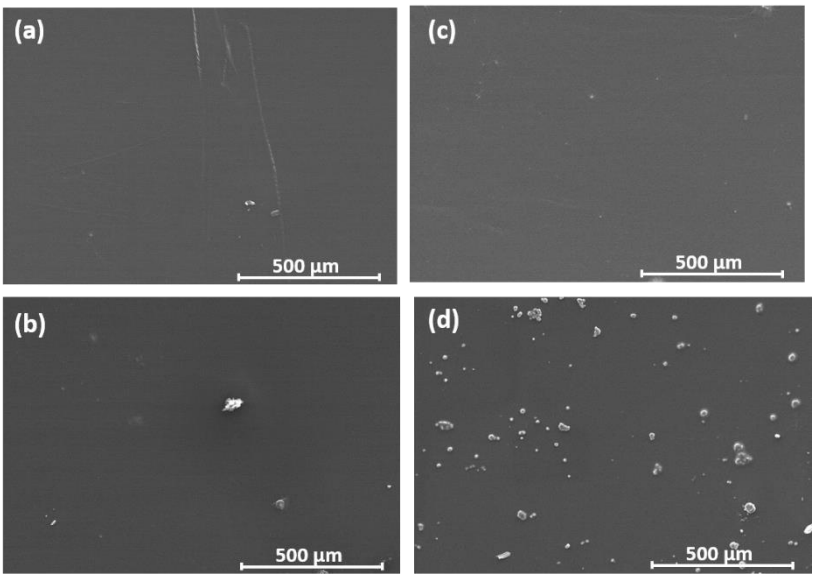

Figure 3.8 SEM images of metal deposition (top vs bottom) onto PEX surfaces from CBP experimental group at (a) 23ºC top section (b) 23ºC bottom section (c) 55ºC top section and (d) 55ºC bottom section. The pH 7.5 water conditions were used.

3.3.5 Indications of PEX pipe potential degradation

Inner wall and outer wall discoloration was observed for PEX pipes held at 55ºC, but this phenomenon was not seen at 23ºC (Figure 3.9). In addition, the PEX pipe that connected to both brass valve and copper pipe (i.e., CBP) seemed discolored the most. To further investigate this observation, PEX pipe surfaces were examined for oxygen containing functional groups that could be indicative of chemical oxidation. No bonds indicative of oxidation were found for the new PEX and PEX exposed to 55ºC water. For PEX pipe in the PBP apparatus, >C-O-O-C< (796.7 cm^{-1}), >C-O< (1020.5 and 1091.8 cm^{-1}) and >C-O-C< (1259.7 cm^{-1}) functional groups were detected (Figure 3.10) [29, 35, 47]. When PEX pipe was connected to brass followed by copper pipe (CBP), more intense peak signals were observed. The more aggressive water (i.e., pH 4 water) seemed to increase the intensity of oxygen containing functional groups.

Further studies are recommended to better understand the role of metal plumbing components on PEX pipe degradation. A prior investigator reported that the contact between polyethylene

(density: 0.92 g/cm^3) and polished copper plates can accelerate polyethylene degradation under high temperature [33]. Results showed after 1000 hrs of exposure time under 57^{o}C, the carbonyl function groups formed on the connecting to copper surface side had about 3 times more intensity than the outer surface. Graeme (2012) concluded that the failure of polypropylene pipe and Cu pipe hot water recirculation system was caused by high temperature and copper ions depleted the polypropylene pipe's stabilizers [32]. In the current study, high temperature (55^{o}C) retarded copper leaching. And for CBP groups, under 55^{o}C temperature, pH 4 water had less Cu deposition (40.4 µg/m^2) than pH 7.5 water onto PEX surfaces (282.1 µg/m^2). It seemed that neither the massive copper leaching nor the copper deposition was the reasons that resulted higher plastic degradation potential in our work. The reason for the detection of oxygen-containing function groups on PEX pipes in the present study deserves further scrutiny. In addition, others have proposed other metals (i.e., Fe) may also be responsible for plastic degradation [31, 48]. The difference in thermal properties of each component connected to the PEX pipe may also influence degradation.

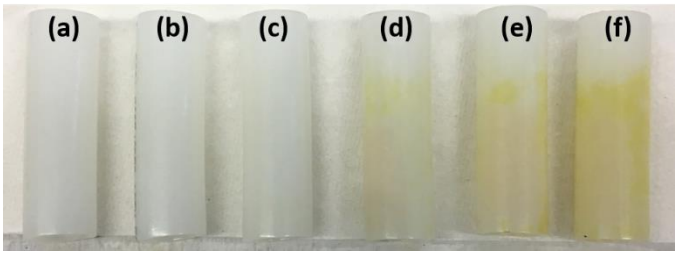

Figure 3.9 Images of (a) new PEX (b) PBP group @ pH 4 and 23^{o}C (c) CBP group @ pH 4 and 23^{o}C (d) PEX @ pH 4 and 55^{o}C (e) PBP group @ pH 4 and 55^{o}C and (f) CBP group @ pH 4 and 55^{o}C. PEX pipes were harvest at the end of 21 days exposure duration.

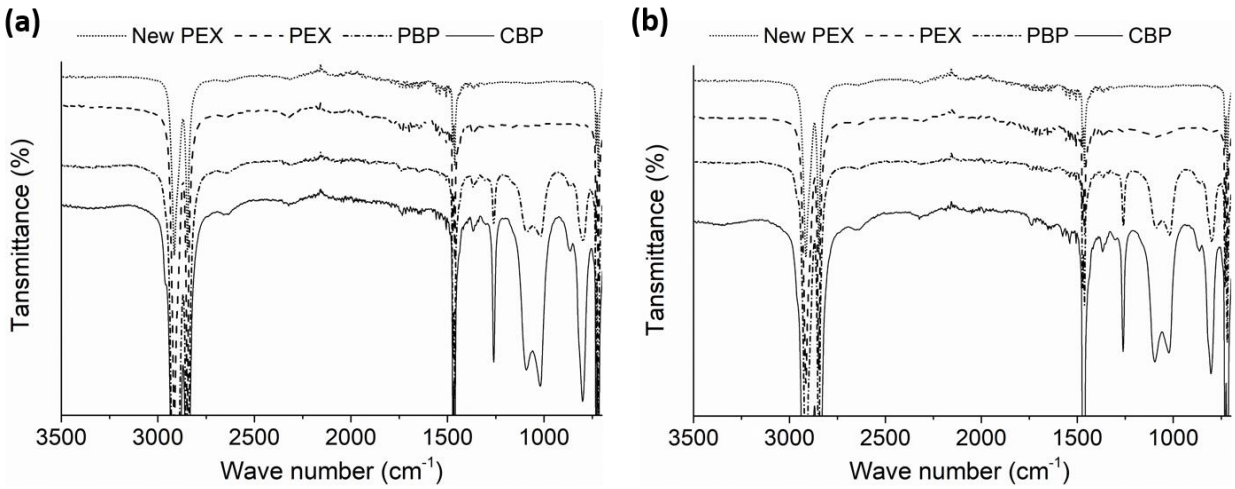

Figure 3.10 PEX pipes FTIR spectrum from different experimental groups of (a) pH 4 and (b) pH 7.5 water conditions @ 55ºC.

3.4. Conclusions

The removal and characterization of 12 galvanized iron and PEX plumbing pipes from a residential home's cold and hot water system revealed the complexity of metal accumulation on pipe surfaces process. For both exhumed galvanized iron and PEX pipes, Fe was the most abundant element, followed by Ca and P. These metals were likely originated from plumbing and water distribution materials (e.g., Fe) leaching, source water (i.e., Ca), and water treatment plant (i.e., P). In general, trace metals found in galvanized iron pipe solids were following the ranking as Zn, Si > Mn, Ba > Cu, Pb > Ni, Cd. For PEX pipes, metal loadings were Mn, Si > Zn, Cu > Ba, Pb > Ni, Cd. The high Mn abundance was likely from the water treatment plant (i.e., $KMnO_4$) and oxidation (i.e., related to dissolved oxygen and chlorine content) in the distribution system. Both SEM images and the ICP-OES data confirmed the metal distribution (Ca, Fe, Mn, P and Si) (i.e., metal loading decreased as the flow direction) along the same length of exhume PEX pipe.

For bench-scale experiments, new brass valves and copper pipes were characterized by XRF for metals composition. Brass valves were largely composed with Cu (64.29 ± 0.52%) , followed

by 34.88 ± 0.57% Zn, 0.42 ± 0.06% Fe and 0.16 ± 0.01% Ni. As expected, copper pipe was mainly containing Cu (99.77 ± 0.03%). Bench-scale experiments revealed that the most aggressive water condition (i.e., pH 4 water) induced more metal leaching (i.e., Cu, Fe, Ni, Pb, and Zn). Metals levels found in exposure waters were Zn > Cu > Ni > Pb > Fe. The pH 7.5 water condition resulted in a greater metal loadings on PEX pipe surfaces compared to the pH 4 water. This phenomena likely occurred because the higher water pH can promote metal precipitation. Hot water (i.e., 55^{o}C) promoted Ni, Pb and Zn leaching, as well as metal deposition onto plastic surfaces. In addition, the 55^{o}C temperature also resulted much greater organic carbon levels at the beginning of each experiment For example, on day 3, experimental groups (i.e., PBP and CBP) maximum measured TOC was 16.4 and 1.1 mg/L at 55^{o}C and 23^{o}C, respectively. When brass valve connected to both PEX and copper pipes, the galvanic corrosion took the place. Results indicated that galvanic connection promoted Fe, Pb and Zn leaching. On day 12, for the pH 4 water condition, the rig that contained copper pipe, brass, and PEX pipe (i.e., CBP) leached about 12.3 µg/L Pb, compared with 7.1 µg/L of Pb found when the rig did not contain copper pipe (i.e, PBP).

PEX pipes exposed to 55^{o}C became discolored after 21 days of exposure period. Rigs that contained PEX pipe, a brass valve, and copper pipe (i.e., CBP) had a greater degree of oxygen containing functional groups (i.e., >C-O-O-C<, >C-O< , and >C-O-C<) at 55^{o}C. This indicated that PEX pipe connected to brass vales and copper may be more subject to degradation. In the current study, water stagnation were applied. For the future work, it is recommended to study different plastic and metal materials configurations. In addition, other water condition and hydraulic factors, such as flow rate, free chlorine residual and corrosion inhibitor are worth further examination.

3.5. References

[1] A.J. Whelton, T. Nguyen, Contaminant migration from polymeric pipes used in buried potable water distribution systems: a review, Critical reviews in environmental science and technology, 43 (2013) 679-751.
[2] J. Lee, E. Kleczyk, D.J. Bosch, A.M. Dietrich, V.K. Lohani, G. Loganathan, Homeowners' decision-making in a premise plumbing failure–prone area, Journal-American Water Works Association, 105 (2013) E236-E241.
[3] Y. Zhu, H. Wang, X. Li, C. Hu, M. Yang, J. Qu, Characterization of biofilm and corrosion of cast iron pipes in drinking water distribution system with UV/Cl 2 disinfection, Water research, 60 (2014) 174-181.
[4] W.J. Rhoads, A. Pruden, M.A. Edwards, Survey of green building water systems reveals elevated water age and water quality concerns, Environmental Science: Water Research & Technology, 2 (2016) 164-173.
[5] M. Salehi, M. Abouali, M. Wang, Z. Zhou, A.P. Nejadhashemi, J. Mitchell, S. Caskey, A.J. Whelton, Case study: Fixture water use and drinking water quality in a new residential green building, Chemosphere, 195 (2018) 80-89.
[6] D.E. Kimbrough, Brass corrosion as a source of lead and copper in traditional and all-plastic distribution systems, Journal (American Water Works Association), 99 (2007) 70-76.
[7] G.R. Boyd, G.L. Pierson, G.J. Kirmeyer, M.D. Britton, R.J. English, Lead release from new end-use plumbing components in Seattle Public Schools, Journal (American Water Works Association), 100 (2008) 105-114.
[8] S. Gonzalez, R. Lopez-Roldan, J.-L. Cortina, Presence of metals in drinking water distribution networks due to pipe material leaching: a review, Toxicological & Environmental Chemistry, 95 (2013) 870-889.
[9] D.E. Kimbrough, Brass corrosion and the LCR monitoring program, Journal-American Water Works Association, 93 (2001) 81-91.
[10] C. Elfland, P. Scardina, M. Edwards, Lead-contaminated water from brass plumbing devices in new buildings, American Water Works Association. Journal, 102 (2010) 66.
[11] Y. Tam, P. Elefsiniotis, Corrosion control in water supply systems: Effect of pH, alkalinity, and orthophosphate on lead and copper leaching from brass plumbing, Journal of Environmental Science and Health Part A, 44 (2009) 1251-1260.
[12] Y. Zhang, Dezincification and brass lead leaching in premise plumbing systems: effects of alloy, physical conditions and water chemistry, in, Virginia Tech, 2009.
[13] B.P. Zietz, K. Richter, J. Laß, R. Suchenwirth, R. Huppmann, Release of metals from different sections of domestic drinking water installations, Water Quality, Exposure and Health, 7 (2015) 193-204.
[14] S. Triantafyllidou, M. Raetz, J. Parks, M. Edwards, Understanding how brass ball valves passing certification testing can cause elevated lead in water when installed, Water research, 46 (2012) 3240-3250.
[15] K.J. Pieper, L.-A. Krometis, M. Edwards, Quantifying Lead-Leaching Potential From Plumbing Exposed to Aggressive Waters, Journal: American Water Works Association, 108 (2016).
[16] K.J. Pieper, M. Tang, M.A. Edwards, Flint water crisis caused by interrupted corrosion control: Investigating “ground zero” home, Environmental science & technology, 51 (2017) 2007-2014.

[17] M. Edwards, L. Hidmi, D. Gladwell, Phosphate inhibition of soluble copper corrosion by-product release, Corrosion science, 44 (2002) 1057-1071.
[18] M. Edwards, A. Dudi, Role of chlorine and chloramine in corrosion of lead-bearing plumbing materials, Journal (American Water Works Association), 96 (2004) 69-81.
[19] A. Dudi, Reconsidering lead corrosion in drinking water: product testing, direct chloramine attack and galvanic corrosion, in, Virginia Tech, 2004.
[20] N. Boulay, M. Edwards, Role of temperature, chlorine, and organic matter in copper corrosion by-product release in soft water, Water research, 35 (2001) 683-690.
[21] D.A. Lytle, M.R. Schock, Stagnation time, composition, ph, and orthophosphate effects on metal leaching from brass, National Risk Management Research Laboratory, Office of Research and Development, US Environmental Protection Agency, 1996.
[22] E. Sarver, M. Edwards, Effects of flow, brass location, tube materials and temperature on corrosion of brass plumbing devices, Corrosion Science, 53 (2011) 1813-1824.
[23] J.M. Cerrato, L.P. Reyes, C.N. Alvarado, A.M. Dietrich, Effect of PVC and iron materials on Mn (II) deposition in drinking water distribution systems, Water Research, 40 (2006) 2720-2726.
[24] D.A. Lytle, T.J. Sorg, C. Frietch, Accumulation of arsenic in drinking water distribution systems, Environmental science & technology, 38 (2004) 5365-5372.
[25] J. Liu, H. Chen, Q. Huang, L. Lou, B. Hu, S.-D. Endalkachew, N. Mallikarjuna, Y. Shan, X. Zhou, Characteristics of pipe-scale in the pipes of an urban drinking water distribution system in eastern China, Water Science and Technology: Water Supply, 16 (2016) 715-726.
[26] M. Friedman, A. Hill, S. Reiber, R. Valentine, G. Larsen, A. Young, G. Korshin, C. Peng, Assessment of inorganics accumulation in drinking water system scales and sediments, Water Research Foundation, Denver, (2010).
[27] T.A. Ranney, L.V. Parker, Comparison of Fiberglass and Other Polymeric Well Casings, Part III. Sorption and Leaching of Trace-Level Metals, Groundwater Monitoring & Remediation, 18 (1998) 127-133.
[28] A.D. Hewitt, Potential of common well casing materials to influence aqueous metal concentrations, Groundwater Monitoring & Remediation, 12 (1992) 131-136.
[29] M. Salehi, X. Li, A.J. Whelton, Metal Accumulation in Representative Plastic Drinking Water Plumbing Systems, Journal: American Water Works Association, 109 (2017).
[30] X. Huang, S. Zhao, M. Abu-Omar, A.J. Whelton, In-situ cleaning of heavy metal contaminated plastic water pipes using a biomass derived ligand, Journal of Environmental Chemical Engineering, 5 (2017) 3622-3631.
[31] D. Tanemura, Investigation of degradation mechanism by copper catalytic activity and mechanical property of polythylene pipes for hot water supply, (2014).
[32] G. Graeme, Expert opinion: performance of polyolefin (PP-R, PEX and PB) piping and fittings in recirculating hot water systems under Australian operating conditions, in, Queensland University of Technology, Brisbane, 2012.
[33] M. Chan, D. Allara, Infrared reflection studies of the mechanism of oxidation at a copper—polyethylene interface, Journal of colloid and interface science, 47 (1974) 697-704.
[34] M. Salehi, C.T. Jafvert, J.A. Howarter, A.J. Whelton, Investigation of the Factors that Influence Lead Accumulation onto Polyethylene: Implication for Potable Water Plumbing Pipes, Journal of Hazardous Materials, (2017).

[35] J.C. Montes, D. Cadoux, J. Creus, S. Touzain, E. Gaudichet-Maurin, O. Correc, Ageing of polyethylene at raised temperature in contact with chlorinated sanitary hot water. Part I– Chemical aspects, Polymer degradation and stability, 97 (2012) 149-157.
[36] A.J. Whelton, A.M. Dietrich, D.L. Gallagher, Impact of chlorinated water exposure on contaminant transport and surface and bulk properties of high-density polyethylene and cross-linked polyethylene potable water pipes, Journal of Environmental Engineering, 137 (2011) 559-568.
[37] NSF International, NSF/ANSI 61-2016 Drinking Water System Components-Health Effects, in, 2016.
[38] M. Lasheen, C. Sharaby, N. El-Kholy, I. Elsherif, S. El-Wakeel, Factors influencing lead and iron release from some Egyptian drinking water pipes, Journal of hazardous materials, 160 (2008) 675-680.
[39] C.J.O. Childress, W.T. Foreman, B.F. Connor, T.J. Maloney, New reporting procedures based on long-term method detection levels and some considerations for interpretations of water-quality data provided by the US Geological Survey National Water Quality Laboratory.
[40] Y. Wang, H. Jing, V. Mehta, G.J. Welter, D.E. Giammar, Impact of galvanic corrosion on lead release from aged lead service lines, Water research, 46 (2012) 5049-5060.
[41] L. Zlatanović, J. Van Der Hoek, J. Vreeburg, An experimental study on the influence of water stagnation and temperature change on water quality in a full-scale domestic drinking water system, Water research, 123 (2017) 761-772.
[42] K.M. Kelley, A.C. Stenson, R. Dey, A.J. Whelton, Release of drinking water contaminants and odor impacts caused by green building cross-linked polyethylene (PEX) plumbing systems, Water research, 67 (2014) 19-32.
[43] V. Lund, M. Anderson-Glenna, I. Skjevrak, I.-L. Steffensen, Long-term study of migration of volatile organic compounds from cross-linked polyethylene (PEX) pipes and effects on drinking water quality, Journal of water and health, 9 (2011) 483-497.
[44] S. Muryanto, A. Bayuseno, H. Ma'mun, M. Usamah, Calcium carbonate scale formation in pipes: effect of flow rates, temperature, and malic acid as additives on the mass and morphology of the scale, Procedia Chemistry, 9 (2014) 69-76.
[45] D.E. Robertson, The adsorption of trace elements in sea water on various container surfaces, Analytica Chimica Acta, 42 (1968) 533-536.
[46] A. Turner, L.A. Holmes, Adsorption of trace metals by microplastic pellets in fresh water, Environmental Chemistry, 12 (2015) 600-610.
[47] J. Coates, Interpretation of infrared spectra, a practical approach, Encyclopedia of analytical chemistry, (2000).
[48] K. Martel, K. Klewicki, State of the Science: Plastic Pipe, Water Research Foundation, (2016).

CHAPTER 4. IN-SITU CLEANING OF HEAVY METAL CONTAMINATED PLASTIC WATER PIPES USING A BIOMASS DERIVED LIGAND

4.1 Introduction

Much of the aging U.S. drinking water infrastructure consists of metal components. Cast iron, copper, ductile iron, lead, galvanized iron and steel pipes, along with valves and appurtenances are some of the metal conveyance materials in use. A challenge with metal pipes is that they corrode and release heavy metals into drinking water such as Al, As, Cd, Cr, Cu, Fe, Mn, Pb and Zn. This is a concern because these compounds have health and aesthetic based drinking water standards. Also problematic is that metal scales can form on the inner pipe walls due to precipitation. Scales can decrease disinfectant residual meant to limit microbial growth, can provide surface area for biofilm growth, and scale constituents can adsorb other metals present (i.e., U, Ra-226 and As) [1-3]. Water chemistry and hydraulic changes can cause scale release and prompt an exceedance of primary or secondary drinking water standards. Because metal scales can affect drinking water quality, scale formation on metal water infrastructure materials has been studied.

As metal drinking water pipes near the end of their service-life, many are being replaced with plastic pipes. Plastic pipes are also being installed for new construction because they are inexpensive, do not corrode, and have estimated 20 year service-lives. An emerging body of evidence however indicates that plastic drinking water pipe surfaces can accumulate heavy metal scales [4-8]. A few studies have indicated that copper deposited on the plastic pipe surface can prompt polymer degradation and lead to premature failure [8-10]. Metals found on plastic water pipe surfaces have originated from upstream metal piping components, water treatment processes (i.e., $Al(OH)_3$, $FeCl_3$, $KMnO_4$) and drinking water sources. Several researchers have reported that

heavy metals deposited onto polyvinylchloride (PVC) and high density polyethylene (HDPE) water distribution plastic pipes (Table 4.1). To better control drinking water heavy metal concentrations, a better understanding of scale formation on plastic pipe is needed.

Table 4.1 Mass of metal deposits (μg/g solid scale) found on plastic water distribution pipes

Metal	Type of Plastic Water Pipe[Reference]							DWS?
	PVC[11]	PVC[11]	PVC[11]	PVC[11]	PVC[4]	HDPE[12]	PVC[5]	
Al	1,906	1,025	2,329	574	19.72 w%	641	106	*SMCL*
As	13,650	1,416	7,842	2,008	nr	49.9	nr	*MCL*
Ca	22,939	28,859	4,455	3,541	1.29 w%	2,856	nr	-
Cd	<4.8	36	375	19	nr	34.1	35	*MCL*
Cr	nr	nr	nr	nr	nr	nr	35	*MCL*
Cu	nr	nr	nr	nr	nr	nr	35	*AL*
Fe	442,528	77,030	237,293	46,137	1.42 w%	5.5 w%	5,159	*SMCL*
Mg	1,492	1,736	442	371	0.1 w%	2,435	nr	-
Mn	5,142	290	1,267	1,143	6.12 w%	2,324	671	*SMCL*
Ni	6	110	137	30	nr	330	nr	-
Pb	210	4,667	9,681	2,009	0.96 w%	25.1	141	*AL*
Si	1,0452	8,719	4,074	5,420	19.26 w%	nr	nr	-
Zn	8,915	535,783	541,564	84,002	0.35 w%	1,846	1,873	*SMCL*

nr: stands for the value was not reposted in the cited paper; "–"represents no drinking water standard (DWS) for the corresponding metal; SMCL is the secondary maximum contaminant level; MCL is the maximum contaminant level; AL is the action level; Lytle et al. (2004) examined pipe scales from four PVC samples at different locations [11].

Heavy metal accumulation on large diameter water distribution pipes ($\geq$ 5.08 cm diameter) can be managed by *in-situ* mechanical, hydraulic, and chemical methods [13-15]. Although, methods for cleaning small diameter service line and building water pipes (< 5.08 cm diameter) have received little scrutiny. Mechanical and hydraulic cleaning approaches are extensively used

for water distribution pipes, but can damage pipe surfaces and scales are not always removed [16, 17]. While water distribution pipes are commonly cleaned by flushing and mechanical scraping, small diameter water pipes pose unique challenges. Flowrates for small diameter pipes can be limited due to headloss, the presence of low-flow fixtures, and physical access can be difficult. Studies that report scale removal by chemical methods are limited. For one cement-lined ductile iron pipe, a $KMnO_4$ solution coupled with flushing removed 72% to 96% of Hg [14]. Other researchers discovered that a greater amount of As was released from water distribution system solids, when water pH was increased from 7 to 9 [15, 18]. In addition, low pH water (< 3) showed effective desorption of Co from Fe particulates [19]. In one instance, citric acid has been recommended for cleaning copper pipes [20]. The cleaning process involved a pipe flush for 1.5 h with a warm 10% citric acid tap water solution, followed by a tap water rinse, and then pipe flush with a 10% $NaHCO_3$ tap water solution for another 1 h. Another chelating agent, ethylenediaminetetraacetic acid (EDTA), has also been proposed for removing radionuclides from water infrastructure [15], but no water pipe cleaning data were found in the literature. EDTA has been used for removing metals from contaminated soils, groundwater, urban and industrial sludge, wastewater, and hard surfaces (e.g., glass, ceramic, and metallic materials) [21], but it is reported as environmentally persistent [22].

Biomass derived agents show promise as water pipe cleaning agents because some of them have been used to remove and recover metals from wastewater and contaminated soils [23, 24]. These compounds are created from raw materials such as sawdust, algae, chitin, chitosan and lignin etc. [25, 26]. Especially, as an abundant and low-cost biomass waste, lignin can be depolymerized into various phenol derivatives (e.g., 2-methoxy-4-propylphenol, DHE). [27] Through reasonable chemical modifications, lignin derivatives could be converted to water soluble reagents that may

be used for water pipe cleaning. For example, reaction of DHE with iminodiacetic acid via the Mannich reaction has the potential to enhance the synthesized ligand's water solubility and metal chelating capacity [28].

The study goal was to synthesize a lignin derived ligand and explore its effectiveness for removing heavy metals from plastic drinking water pipes. Plastic drinking water pipes were from a one year old residential plumbing system. The specific research objectives were to 1) determine the Fe^{3+}-DHEL complex association constant and reaction stoichiometry, 2) quantify total heavy metal loading on the exhumed plastic pipe surfaces, 3) explore the DHEL heavy metal removal kinetics and performances, and 4) propose heavy metal-DHEL reaction mechanisms.

4.2. Materials and methods

4.2.1 Materials and Conditions

A 10 mM Fe^{3+} stock solution was prepared using $FeCl_3.6H_2O$ (> 99% for analysis; Sigma Aldrich, St. Louis, MO). Dihydroeugenol (DHE) (≥ 99%; Sigma Aldrich, St Louis, MO), iminodiacetic acid (≥ 98%; Sigma Aldrich, St Louis, MO), ethanol (200 proof; Decon Labs, Inc., King of Prussia, PA), and formaldehyde solution (37%; Macron Fine Chemicals, Center Valley, PA) were used without further purification. 0.1N HCl and 0.1N NaOH solutions were adopted to adjust the solution's pH. HNO_3 (TraceMetal^{TM} Grade) was used for ICP-MS analysis and digestions. In addition, solutions were prepared by using deionized water (DI) and were adjusted to pH 7. All experiments were conducted at room temperature.

4.2.2 Equipment

An Accumet AB 150 pH/mV benchtop meter (Fisher Scientific, Pittsburgh, PA) was used to measure pH values. The Fe^{3+}-DHEL complex concentration was measured by a UV-vis spectrophotometer (Shimadzu UV-2700) by using the scanning mode. Metal concentrations were

measured by inductively coupled plasma-mass spectrometry (ICP-MS) (Perkin Elmer II). The structure of DHEL was determined by nuclear magnetic resonance spectroscopy (NMR, Bruker Avance ARX−400 spectrometer), in which deuterated water was used as the solvent. Metal deposits of exhumed plastic pipe surfaces before and after decontamination process were examined by the field emission scanning electron microscopy-energy dispersive X-ray spectroscopy (FESEM-EDS) (Hitachi S-4800 SEM, Japan). Pipe samples were coated with a thin layer of carbon under vacuum to increase the electrical conductivity [29].

4.2.3 Synthesis of lignin derived DHEL

A solution mixture of DHE (3.32 g, 20 mmol), iminodiacetic acid (2.92 g, 22 mmol), 37% aqueous formaldehyde (1.63 g, 20 mmol) and NaOH (1.6 g, 40 mmol) in H_2O/ethanol (1:2 v/v, 40 mL) was stirred and refluxed overnight. The reaction scheme is shown below (Scheme 4.1). The resulting white precipitate was collected via filtration. The substance was dried in an oven at 60 ^oC for 24 h and yielded DHEL as a white solid (5.3 g, 86% yield).

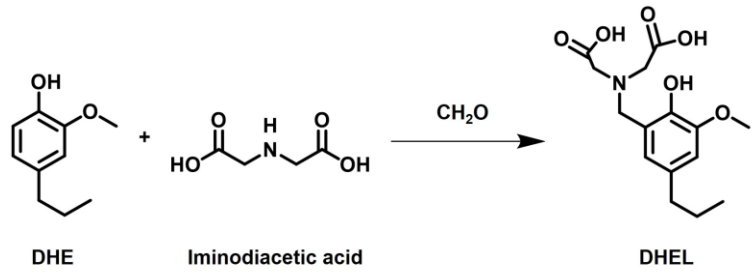

Scheme 4.1 Synthesis of DHEL

4.2.4 Bench scale metal-DHEL complexation experiment

Iron was selected for this study because it is one of the most abundant metals found on plastic drinking water pipe scales [5, 11]. In this experiment, Fe^{3+} was selected as the representative metal and it was hypothesized to chelate with the synthesized DHEL. The Fe^{3+}-DHEL complex stability constant was determined through the Benesi-Hildebrand method [30]. A DHEL solution (50 mL

of 1 mM) was prepared in a 100 mL beaker, another 50 mL of 1 mM $FeCl_3$ solution was filled in a 50 mL burette for titration. Various volumes of the metal solution were titrated into the DHEL solution. After solutions were mixed, the pH was adjusted at the pre-determined values (i.e., pH 4 or 7). In addition, the volume of titrated metal solution was recorded and the Fe^{3+}-DHEL complex absorbance was measured using a UV spectrophotometer.

With the assumption of 1:1 stoichiometry (Fe: DHEL), the adopted Benesi-Hildebrand equation used was [31, 32]:

$$\frac{1}{A - A_0} = \frac{1}{K_f(A_{max} - A_0)[Fe^{3+}]} + \frac{1}{A_{max} - A_0}$$

where A represents the absorbance of Fe^{3+}-DHEL complex during continuous titration of Fe^{3+} solution, A_0 is the absorbance of the original DHEL solution without Fe^{3+} solution added, A_{max} is the maximum absorbance during the continuous titration experiment, K_f is the association constant (M^{-1}) and $[Fe^{3+}]$ represents the added Fe^{3+} concentration. Then the graph could be generated as $1/ (A-A_0)$ vs $1/ [Fe^{3+}]$. Through linear fit, the association constant (K_f) would be determined from the slope ($K_f = \frac{1}{slope \times (A_{max} - A_o)}$).

The method of continuous variation was performed to generate a Job's plot to determine the stoichiometry of Fe: DHEL binding. The same concentration of DHEL (1 mM) and $FeCl_3$ (1 mM) was prepared for these experiments and the total volume of the mixture was set to be 10 mL. The volume ratio between DHEL and Fe solutions was varied from 0.1 to 0.9 and the complex absorbance value was recorded for each condition. After placing the certain parts of Fe^{3+} and DHEL solutions in the 50 ml centrifuge tube, the tube was vigorously mixed by shaking. After mixing, the solution pH was adjusted to 4 and 7.

4.2.5 Performance of DHEL to remove heavy metals from exhumed pipes

DHEL metal removal performance was examined using a one year old, 1.91 cm diameter, and 1.22 m long PEX pipe. This pipe represented the buried water service line removed from the single-family residential property located in Indiana, USA. While other indoor plumbing PEX pipes were also removed as part of a parallel study, preliminary experiments indicated that the service line contained the greatest loading of metals [33]. Cu, Fe, Pb, Zn and a variety of other metals found on the pipe surface were also present in the drinking water. In the present study, the service line PEX pipe was used for all kinetic and other metal removal experiments. Before use, the pipe was triple rinsed with deionized water (DI) to remove loose debris.

Experiments were conducted to determine DHEL metal removal kinetics and to determine if DHEL concentration influenced metal removal efficiency. Pipe segments were cut into 3 cm length and all solutions were adjusted to pH 7. After filling pipe segments with the dilute DHEL-DI water solution or control water (DI only), each pipe was plugged with Teflon® wrapped silicon stoppers. Metal removal kinetics were examined for 0.1 mM, 1 mM, and 5 mM DHEL concentration, during a 7 day period. For each DHEL level, eight pipe segments were prepared. Periodically, the pipe segment was sacrificed and the water sample's volume and pH was characterized. Water samples were acidified using HNO_3 and removed metal concentrations were analyzed by ICP-MS. The remaining metals on each pipe segment was determined by filling pipes with 2.5 % of HNO_3 and allowing stagnation for a minimum of 48 h. The experimental data was used to fit kinetic models stated as following:

First order kinetic model [34, 35]:

$$\frac{m_t}{m_0} = e^{-k_{R1}t}$$

$$1 - \frac{m_R}{m_0} = e^{-k_{R1}t}$$

$$Metal\ removal\ \% = 1 - e^{-k_{R1}t}$$

Where m_t is the remaining metals on the plastic segment at time t, m_0 is the total amount of metals detected on exhumed plastic pipe's inner wall at time zero, k_{R1} is the first order metal removal rate constant (h^{-1}), m_R is the amount of removed metals from plastic pipe surfaces and Metal removal % = $\frac{m_R}{m_0} \times 100\%$.

Second order kinetic model [36, 37]:

$$\frac{m_t}{m_0} = \frac{1}{\beta_2 + k_{R2}t}$$

$$1 - \frac{m_R}{m_0} = \frac{1}{\beta_2 + k_{R2}t}$$

$$Metal\ removal\ \% = 1 - \frac{1}{\beta_2 + k_{R2}t}$$

Where β_2 and k_{R2} are the second order kinetic metal removal constant and rate (h^{-1}), respectively. By plotting Metal removal % vs time and fitting kinetic models, k_{R1} and k_{R2} should be obtained.

The DHEL performance was evaluated over a range of concentrations (i.e., 0.01-10 mM) during a 7 day period at pH 7. Under each condition, triplicate pipe segments were used. Water and pipe samples were acidified and analyzed as stated in the kinetic experiment. ICP-MS calibration curves were developed for a total of 19 metals. For the more abundant elements (Ca, Fe, Mg, Na and P), the concentration range was set from 25 to 1000 ppb, whereas, other metals (Al, As, Be, Cd, Co, Cr, Cu, Hg, Mn, Ni, Pb, Se, V and Zn) the concentration range was 5 to 200 ppb. The recovery percentage for all metals was $\geq$ 85%. All calibration curves had regression coefficient R^2 values of > 0.98.

4.2.6 Statistical analysis

NCSS statistical software was applied to conduct the single factor one way analysis of variance (ANOVA) and multivariate analysis of variance (MANOVA) in order to examine interaction effects. The significant level of all data set was set as 0.05. For each experimental condition, arithmetic mean and standard deviation values were reported.

4.3. Results and discussion

4.3.1 Characterization of DHEL structure

^{1}H and ^{13}CNMR spectra revealed DHEL's chemical structure (Figure 4.1). The proton peak at 3.9 ppm corresponded to the methylene linkage (f), which indicated successful DHE coupling with iminodiacetic acid (Figure 4.1 (A)). Aromatic protons were found at 6.5 and 6.7 ppm. The methylene groups (d) connecting to carboxylic acid were observed at 3.3 ppm, while DHE's methyl and propyl groups were found at 3.7, 2.3, 1.4 and 0.8 ppm, respectively. The appearance of characteristic methylene linkage (f) was also confirmed by ^{13}C NMR. This linkage was detected at 55.5 ppm (Figure 4.1 (B)). Carboxylic acid, methylene (d) and methoxy were also observed at 176.1, 57.3 and 56.5 ppm, respectively.

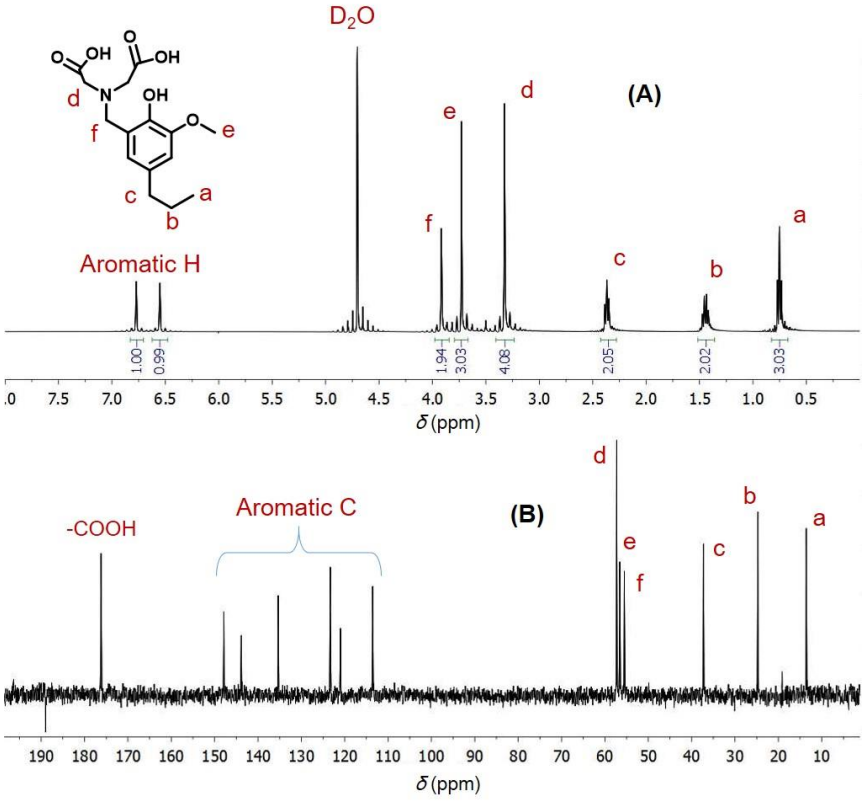

Figure 4.1 Proton and carbon NMR spectra of DHE based DHEL.

4.3.2 Fe3+-DHEL complex stability constant and binding ratio

Results showed that Fe^{3+} (ranged from 1.96×10^{-5} M to 5.83×10^{-4} M) bound with DHEL and pH conditions did not significantly affect the complex's stability (Figure 4.2 (b) and (d)). According to the Benesi-Hildebrand equation, the K_f values obtained for pH 4 and pH 7 were (2.25 ± 0.07) $\times 10^3$ M^{-1} and (2.14 ± 0.10) $\times 10^3$ M^{-1}, respectively. UV spectra indicated that upon continuous titration of Fe^{3+}, the peak absorbance gradually increased until the molar ratio of Fe^{3+} and DHEL was close to 1:1 (Figure 4.2 (a) and (c)). This observation inferred the potential reaction stoichiometry, and no shift in maximum wavelength was detected.

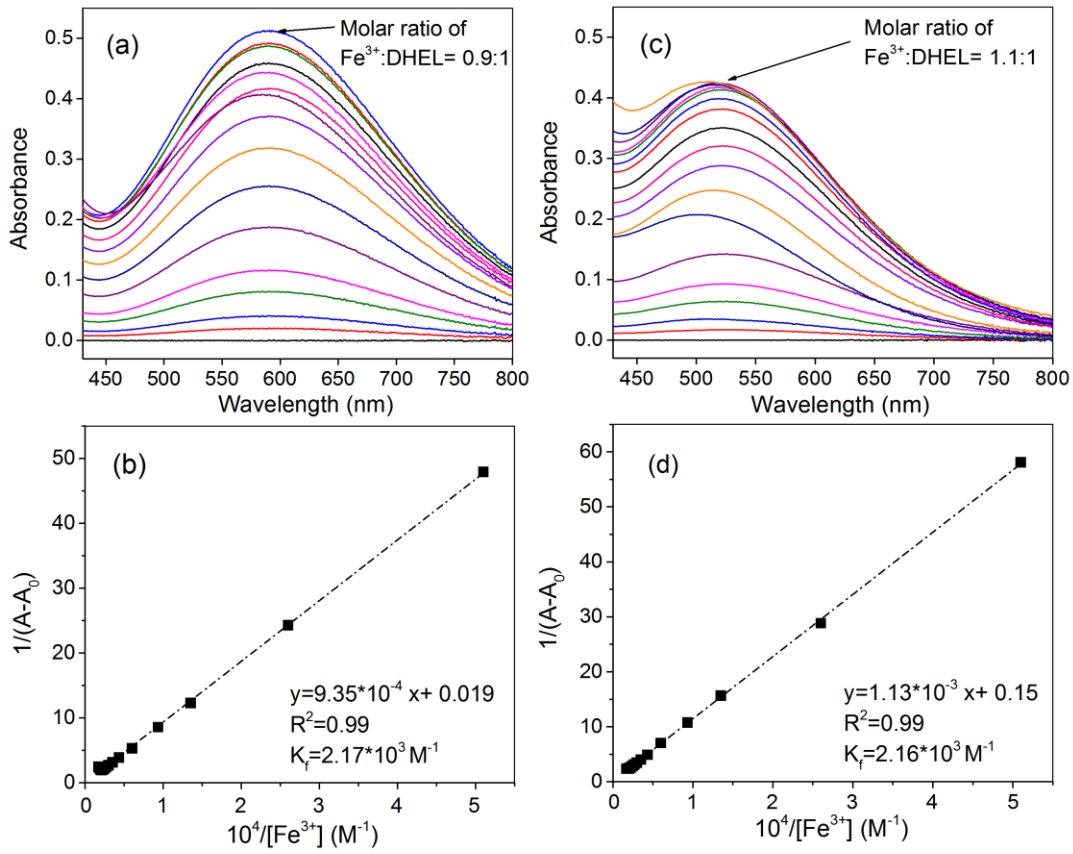

Figure 4.2 UV-spectra of Fe^{3+}-DHEL complex upon increasing of [Fe^{3+}] at pH 4 (a) and pH 7 (c); Benesi-Hildebrand plot of DHEL with Fe^{3+} at pH 4 (b) pH 7 (d).

Job's plot experiments confirmed the 1:1 reaction ratio between Fe and DHEL at pH 4 and pH 7. As shown in Figure 4.3, the maximum absorbance at 588 nm and 523 nm wavelength for pH 4 and pH 7 was plotted against the DHEL mole fraction. The peak absorbance value was observed when the molar fraction value was 0.5 which indicated a 1:1 reaction ratio. A 1:1 stoichiometry of Fe: ligand complex has been found in other studies in the aqueous phase [38, 39]. However, the magnitude of association constants in the literature varied (10^3 vs. 10^{20}) likely because of ligand property and experimental condition differences (i.e., solvent solution, temperature and pH). In the present work, absorbance values shifted upward (i.e., when ligand mole fraction < 0.5) for the pH 7 condition compared to the pH 4 condition. This shift likely

occurred due to the formation of iron hydroxides or oxides in solution at greater pH (i.e., $FeOH^{2+}$, $Fe(OH)_{2(s)}$, $Fe(OH)_3$). Because the ionic radii for iron hydroxides and oxides were greater than ferric ion's radius, this may have retarded the Fe and DHEL reaction [40].

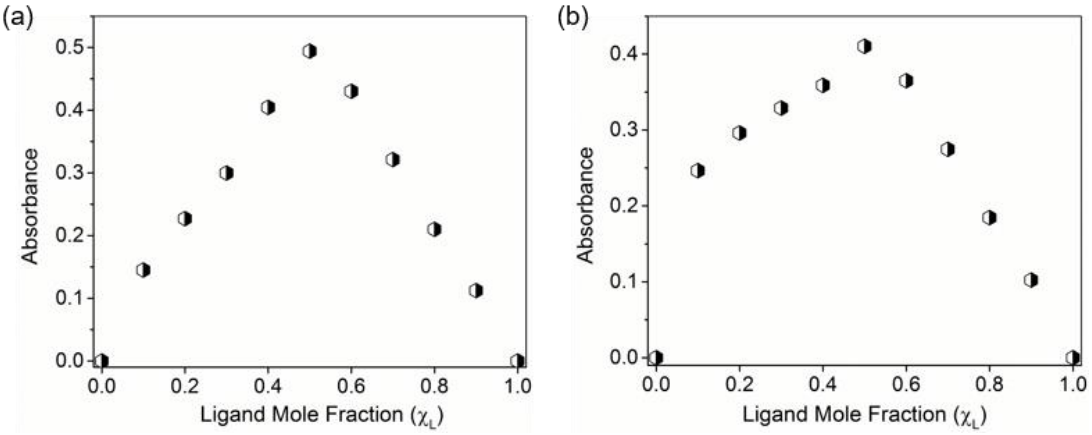

Figure 4.3 Job's plot of a 1:1 Fe-DHEL complex at a) pH 4 and b) pH 7, where the absorbance was measured at 588 nm and 523 nm, respectively.

4.3.3 Variation of metal loading on the service line plastic pipe material

Total metal loadings differed across pipe segment samples, which indicated metal loadings differed down the length of the service line pipe (probability value, $p < 0.01$) (Figure 4.4). The metal's abundance found in the plastic pipe scale was: Fe > Mn > Ca > Zn > Mg, Cu > Pb > Al. While P is not a metal, a notable amount of P (19.13 ± 3.25 µg/dm^2) was also detected in the scale and is likely due to the orthophosphate/polyphosphate blend corrosion inhibitor added by the local water utility to treated drinking water. The metals detected in the current work were similar to those found by others. Liu et al. (2016) found the most abundant heavy metals on a PVC water distribution system pipe scale were Fe > Zn > Mn > Pb > Al > Cu [5]. Cerrato et al. (2006) also found Fe and Mn were present on PVC water distribution pipe scale, but Mn was in greater abundance [4]. For the present study, the water distributed by the water utility contained low levels of Fe (0.05 mg/L) and Mn (0.02 mg/L) exiting the water treatment plant [41]. In addition, drinking

water that entered the building was very hard (248 to 416 mg/L as $CaCO_3$). As a result, Ca, Fe, Mg and Mn from the plastic pipe scales likely originated from the source water. Other metals (Al, Pb and Zn) detected on plastic pipe surfaces, as well as additional amount of Fe and Mn, were likely released from water conveyance components (i.e., pipes, fixtures and fittings). The reasons for unequal metal deposits on the plastic service line remain unclear and no studies were found that explained this phenomenon in much detail. Unequal metal deposits on the service line could be due to hydraulic condition changes (i.e., hydraulic force and residence time), pipe surface morphology (i.e., scratches and oxidative condition), and biofilm activity. Additional work should be considered to examine scale formation on plastic pipe surfaces.

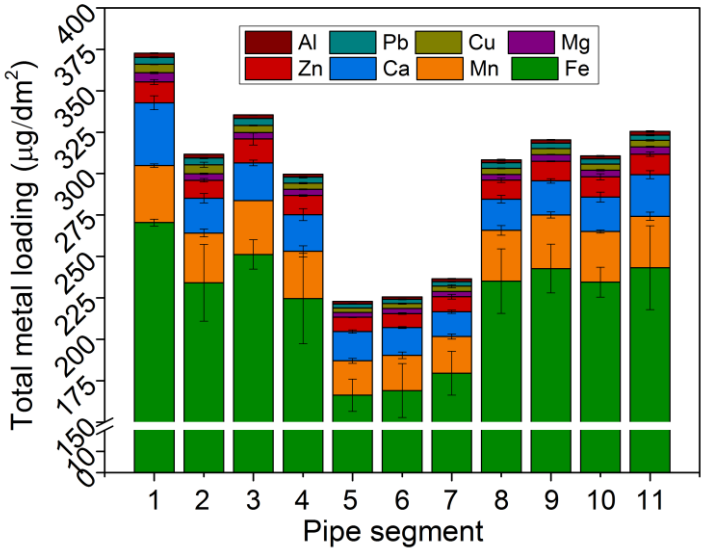

Figure 4.4 Total metal loading along the same length of exhumed PEX-A pipes: initial pH was 7; error bars are representing standard deviations from triplicate 3 cm length pipe segments.

4.3.4 Preliminary test and SEM-EDS analysis of DHEL interaction with exhumed plastic pipe

A screening experiment was conducted to determine DHEL's heavy metal removal effectiveness. Triplicate pipe segments were exposed to solutions and the DHEL concentration was varied from 0 to 5 mM. The exposure duration was up to 48 h. After the exposure procedure, the exhumed pipe segments were visually observed to be scale-free for experimental groups, but

deposits were still visible for the control group (Figure 4.5). SEM images and accompanying EDS spectra of the original exhumed plastic pipe surfaces and after decontamination process were compared in Figure 4.6. The SEM image indicated that DHEL removed most metal deposits (Figure 4.6 (a) and (b)). The original metal deposits were mainly shown as aggregates, whereas, the size of remaining metals on plastic pipe surface was much smaller after decontamination procedure. Further confirmation of DHEL's effectiveness was found by EDS analysis (Figure 4.6. (c) and (d)). Results showed that, the most abundant element was C, followed by O, which was mainly due to the polymer properties and the metal forms on the plastic surface (i.e. oxides), respectively. After decontamination, the peak intensity for metals (i.e., Fe) was much less than thoese before DHEL exposure. Ca and Zn were not detected after DHEL treatment. Based on these observations, additional tests were conducted to explore reaction kinetics and evaluate DHEL removal effectiveness.

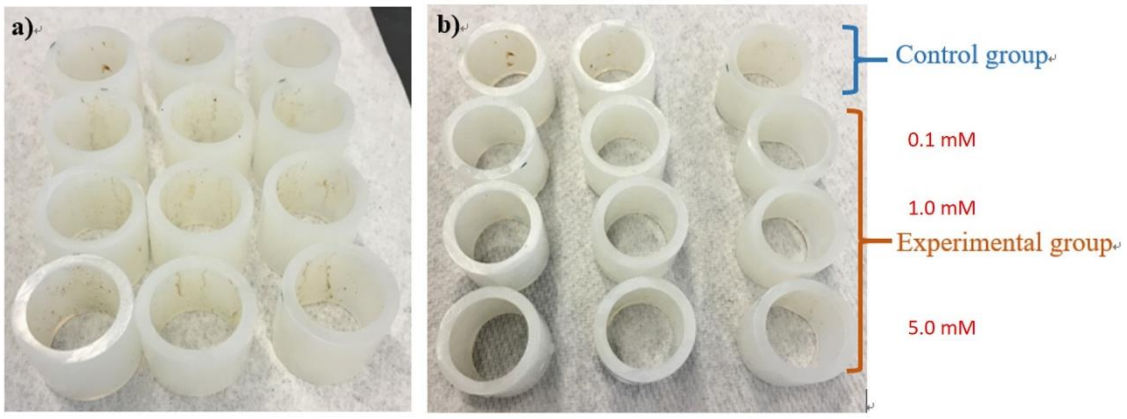

Figure 4.5 Cross-section images of one year old PEX-A potable water pipe segments removed from residential plumbing: a) original, b) after treated with biomass derived DHEL.

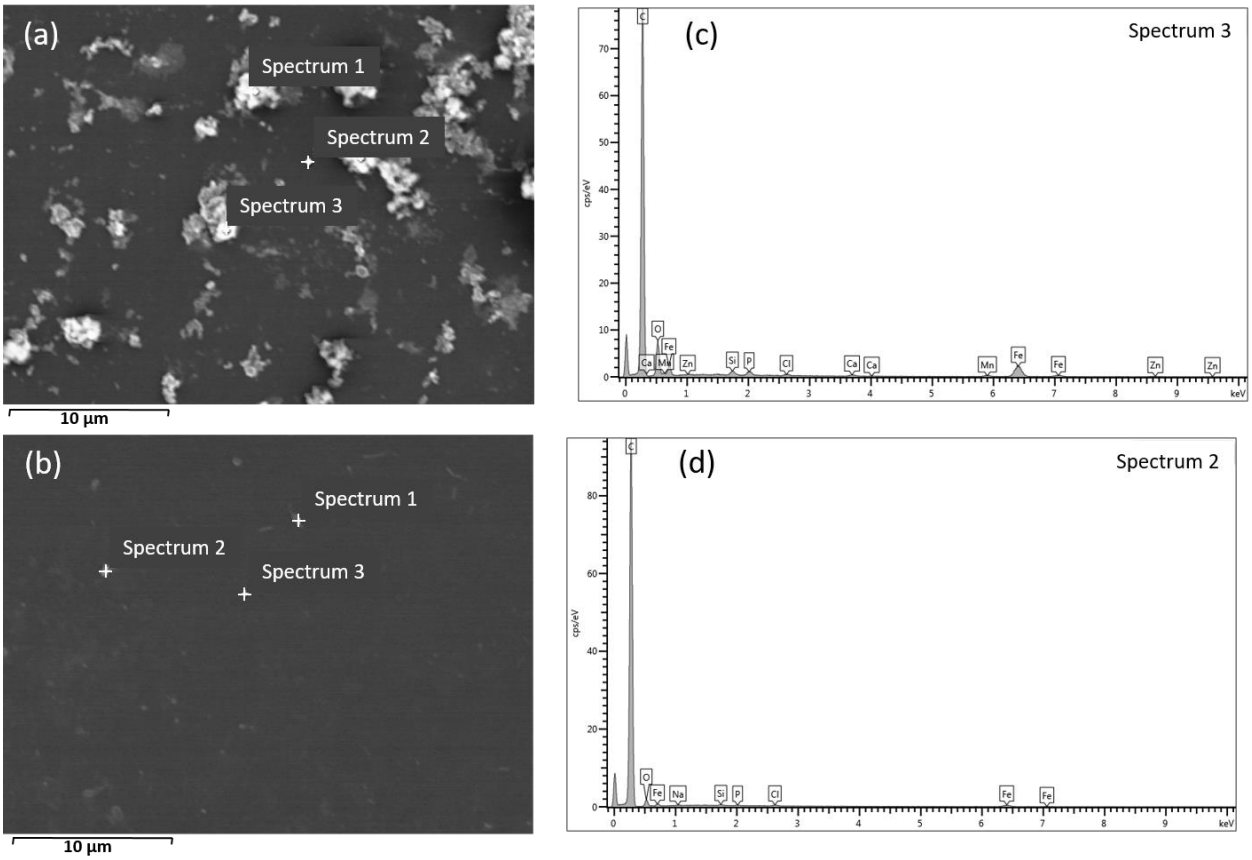

Figure 4.6 SEM and EDS analysis of metals on exhumed plastic pipe surfaces: (a) and (b) SEM images, (c) and (d) EDS analysis before and after decontamination process (i.e., 5 mM DHEL for *48 h).*

4.3.5 Kinetic study of DHEL interaction with exhumed plastic pipe

Kinetic study results showed that the DHEL solution exposure time and DHEL concentration significantly influenced metal removal from pipe segments (Figure 4.7). DHEL's performance was examined for five target metals: Cu, Fe, Mn, Pb, and Zn. These metals were chosen based on their abundance on the pipe segments and they had U.S. drinking water standards. Considering the unequal distribution of heavy metals along the pipe (refer to section 3.3), the metal removal % ($\frac{mass_{removed}}{mass_{original}} \times 100\%$) was adopted instead of the metal loading (µg/dm^2). As shown in Figure 4.7, for the first 80 h, the DHEL metal removal rate was the greatest for all metals and then it's decreased with time. By day 7, the 5 mM DHEL concentration removed ≥ 95% of Cu Fe, Mn, Pb

and Zn from the pipe surface. Among five target metals, Fe, Mn, and Pb exhibited similar removal behavior (p = 0.64) vs Zn and Cu (p = 0.43) (Figure 4.7). The DHEL was more favorable for Cu and Zn rather than Fe, Mn, and Pb, even though Cu and Zn were not the most abundant metals present on the pipe surface (Figure 4.4). Under the control condition (DI only, no DHEL), except for Zn (about 30% released into the water), less than 5% of the total metals were released.

Both first and second kinetic models were fitted and compared with the experimental data (Figure 4.7). In general, both kinetic models had a good agreement with Fe, Mn and Pb metal removal data (R^2 was as high as 0.99). However, Cu and Zn data fitted poorly with kinetic models and may be due to the rapid release of metals into the water. The first and second order kinetic parameters and the corresponding R^2 are presented in Table 4.2. More specifically, when DHEL concentration was high (i.e., 5.0 mM), the first order kinetic model showed the better fit than and second order kinetic model. Whereas, the second order kinetic model could represent the data better within the lower range of DHEL concentrations (i.e. 0.1mM and 1.0 mM).

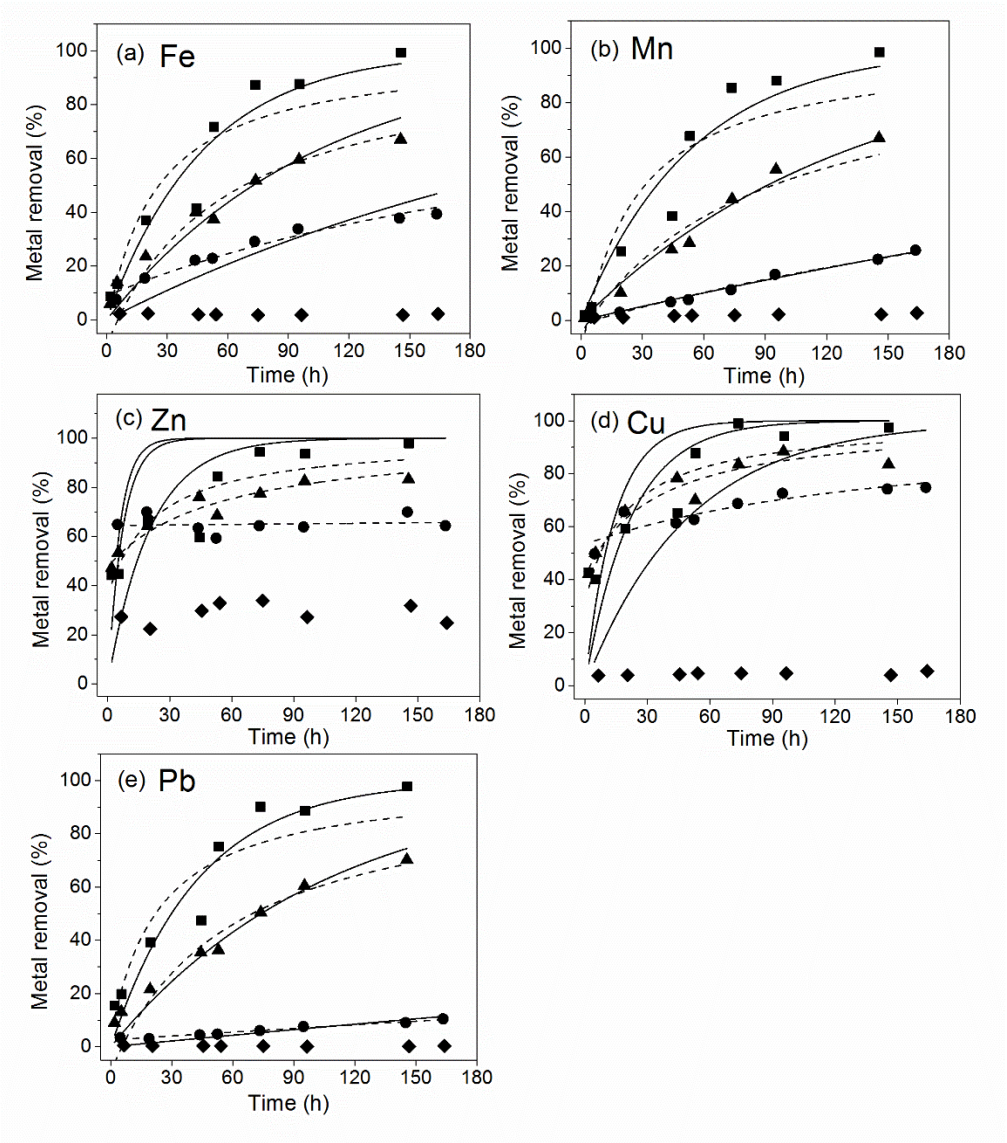

Figure 4.7 Percentage of metal removed kinetic test (7 days) a) Fe, b) Mn, c) Zn, d) Cu, e) Pb: room temperature at 22 ± 1 ^{o}C ; initial pH was 7; (◆) blank, (●) 0.1 mM, (▲), 1 mM, (■)-5mM. ( ) first kinetic model fit, (---) second kinetic model fit.

Table 4.2 Kinetic parameters and regression coefficients for DHEL metal removal from exhumed plastic pipe

Target metals and conditions		First order kinetic fit		Second order kinetic fit	
Metals	*DHEL Conc. (mM)*	k_{R1} (h^{-1})	R^2	k_{R2} (h^{-1})	R^2
Fe	0.1	0.23	0.67	0.23	0.96
	1.0	0.57	0.92	0.96	0.98
	5.0	1.25	0.94	2.40	0.87
Mn	0.1	0.11	0.99	0.13	0.99
	1.0	0.45	0.99	0.66	0.95
	5.0	1.11	0.95	2.11	0.87
Pb	0.1	0.04	0.63	0.03	0.97
	1.0	0.56	0.95	0.94	0.98
	5.0	1.40	0.92	2.62	0.87

4.3.6 DHEL metal removal performance with exhumed plastic pipes

DHEL's metal removal performance agreed well with kinetic experiment observations where two different behavior groups were identified: Fe, Mn and Pb (p = 0.77) and Cu and Zn (p = 0.33) (Figure 4.8). DHEL was more favorable to removing Cu and Zn than Fe, Mn and Pb. For the low range DHEL concentrations (i.e., <5 mM), metal removal efficiency increased as the amount of DHEL increased. However, when DHEL concentrations exceeded 5 mM, metal removal efficiency ($\geq$ 95%) did not increase further. This phenomenon is likely due to the fact that when DHEL concentration reached 5 mM, a maximum amount of metals had been removed; above 5 mM, DHEL became the excess reagent. In addition, during the pipe exposure experiment, the final pH ranged from 6.3 to 7.3 (Figure 4.8) depending on DHEL concentration. The lower final pH value (pH <7) likely resulted from Fe^{3+} hydrolysis of the scale that released protons into the solution (i.e. Fe^{3+}) [42]:

$$Fe^{3+} + H_2O \rightarrow Fe(OH)^{2+} + H^+$$

$$Fe^{3+} + 2H_2O \rightarrow Fe(OH)_2^+ + 2H^+$$

$$Fe^{3+} + 3H_2O \rightarrow Fe(OH)_3^0 + 3H^+$$

$$Fe^{3+} + 4H_2O \rightarrow Fe(OH)_4^- + 4H^+$$

Or the reaction of ions with hydroxide [43]:

$$2Fe^{3+} + Fe^{2+} + 8OH^- \xrightarrow{water} Fe_3O_4 + 4H_2O$$

However, pH >7 could be explained by the ligand promoted mineral dissolution process where H^+ was acting as the reactant (i.e., FeOOH), where L stands for the ligand [44]:

$$FeOOH + nL^- + 3H^+ \rightarrow [FeL_n]^{3-n} + 2H_2O$$

The favorability of DHEL for Cu and Zn may have been influenced by the metal's ionic radius, absolute electronegativity, and complex stability. For metal cations, according to the charge-to-radius ratio (Z/r), the favorability sequence was expected to be Fe^{3+} (4.69) > Fe^{2+} (3.28) > Cu^{2+} (2.74) ≈ Zn^{2+} (2.70) > Mn^{2+} (2.50) > Pb^{2+} (1.55) [45, 46]. Except for Fe, the observed metal favorability was proportional to the Z/r ratio. Metal ions with higher absolute electronegativity would have a stronger attraction to the lone pair electrons in the functional groups (i.e., -COOH and -OH). This might have led to the observed higher favorability. Pearson (1988) calculated the absolute electronegativity of metal cations as Fe^{3+} (42.73 eV) > Zn^{2+} (28.84 eV) ≈ Cu^{2+} (28.56 eV) > Pb^{2+} (26.18 eV) > Mn^{2+} (24.66 eV) > Fe^{2+} (23.42 eV) [47]. Except for Fe^{3+}, the work of Pearson (1988) also agrees with the observed DHEL metal favorability in the present study.

The metal complex stability constant is another factor that could impact ligand favorability. Irving and Williams (1953) examined complex stability constants for a number of natural or synthetic ligands and concluded the general order as Mn < Fe < Co < Ni < Cu, > Zn [48]. However, as one of the most common used metal chelators, metal-EDTA complex stability was found to be Fe^{3+} (25.00) > Cu^{2+} (18.70) > Pb^{2+} (17.88) > Zn^{2+} (16.44) > Mn^{2+} (13.56) [49]. Metal ligand complex formation is a complicated process, which cannot be predicted from only considering Z/r,

electronegativity, or complex stability. Other factors that could influence metal removal from the plastic pipe are ionic radii, the replacement of water by more polarized ligand molecules, metal coordination states and orbital theory [48]. Furthermore, the form of metal and hydrolyzed metal species on the plastic pipe surface or in the aqueous solution could also have influenced the result. For instance, under the certain circumstances (i.e., pH 5.5 and initial metal concentration as 100 mM), Bhattacharyya (1998) found Pb was about 50% Pb^{2+} and 40% $[Pb_4(OH)_4]^{4+}$, whereas, Cu was about 80% Cu^{2+} and 20% $[Cu_2(OH)_2]^{2+}$ [50]. The presence of different metal species in solution could potentially affect metal-ligand complex formation, reaction molar ratio and bonding capacities. Additional work should be considered to isolate which factors are most significant on influencing metal removal from plastic pipe surfaces.

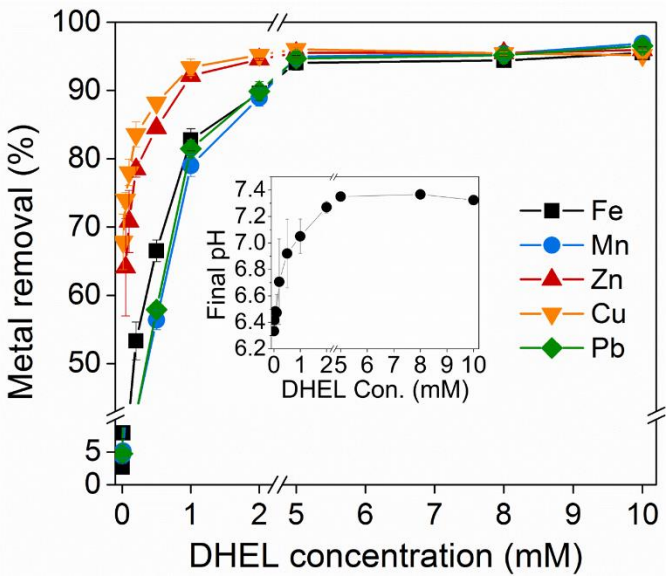

Figure 4.8 DHEL performance test as showing the percentage of metal removed from the pipe inner surface, 7 day exposure period: 22 ± 1 ºC; initial pH 7; error bars represent standard deviation for triplicates

4.3.7 Relationship between total metal loading and total metal removed on pipe segments

The total metal removed by DHEL from each pipe segment was directly correlated to the initial metal loading on pipe segments, but this was not the case for the control group (no DHEL added) (Figure 4.9). Linear regression analysis showed correlation coefficients of 0.93 or greater when DHEL was present (Figure 4.9 (b)). In the absence of DHEL, the amount of metal leached into the water was not correlated to the total metal loading (Figure 4.9 (a)). Only a noticeable amount of Zn (R^2=0.95) leached into control water from the exhumed plastic pipe surface.

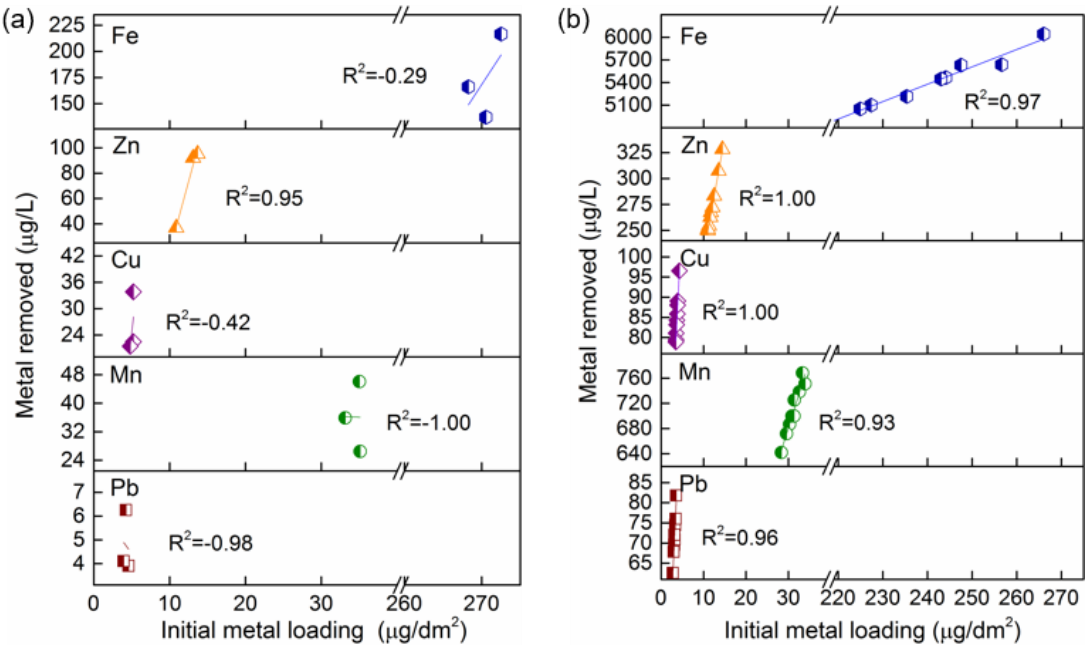

Figure 4.9 The correlation between metal desorption with amount of metal loadings (7 days): (a) blank group, (b) DHEL dosages varied from 5 mM to 10 mM: 22 ± 1 ^{o}C; initial pH 7.

4.3.8 Proposed reaction mechanism

Results from the present study indicate that plastic service lines can accumulate heavy metals on their surface, and the deposited metals were successfully removed by short-term exposure to a DHEL solution. While metal speciation and forms were not examined in this work, metal deposits found on metal drinking water pipes have been reported to contain Cu_2O, α-FeOOH, Fe_3O_4, MnO_2,

$PbCO_3$ and ZnO [51, 52]. Soluble metal forms coupled with minerals are also expected to be found on or releasing from the exhumed plastic pipes. Like past metal pipe scale characterization studies, additional work is needed to understand forms of metal deposits that are most common for plastic pipes.

The factors that control metal adsorption and release from plastic pipe surfaces have receive limited scrutiny, but DHEL effectively removed metal deposits from the pipe surface. Past studies have reported that aged plastics adsorbed higher amount of metals than new plastics [6, 33]. These phenomena have been hypothesized to occur due to increased surface porosity and presence of oxygen functional groups, as well as negatively charged plastic surface having induced metal ion adsorption and coprecipitation. Additional work is needed to further understand the mechanism of metal accumulation onto plastic drinking water pipes and effects of various water and hydraulic conditions (i.e., natural organic matter, hardness, flow velocity and pressure).

Several researchers have proposed that metal oxide dissolution can occur by proton-promoted, ligand-promoted, reductive, and synergistic pathways [53, 54]. Compared with proton-promoted dissolution, the rate of ligand-promoted dissolution process has been reported to be faster. Water pH, ionic strength, and the presence of organic ligands are some key factors which could significantly influence metal oxide solubility in the solution. Because experiments in the present study were conducted at pH 7, both the proton-promoted and reductive dissolution could be neglected [55]. Considering only a single type of ligand (i.e., DHEL) was examined, the synergistic pathway where multiple ligands act could be ignored. As stated above, the ligand-promoted minerals dissolution pathway should be the dominant mechanism that controls DHEL to remove metal deposits from exhumed plastic pipes. In addition, considering soluble metals that released from pipe scales, we also proposed the ligand-metal complex formation pathway. The complex

formation process can through consuming metal ions in the solution to drive the minerals' dissolution process further (Figure 4.10).

Based on the literature, the following steps during the ligand-promoted mineral dissolution process were likely occurring [54]: (1) formation of surface complex, (2) detachment of the complex from mineral surface, and (3) re-adsorption of ligand on the oxide surface through ligand exchange mechanism. While ligand-mineral binding phenomena in solution phase has been examined by others, the interactions between minerals, ligands, and plastic pipe has not been addressed.

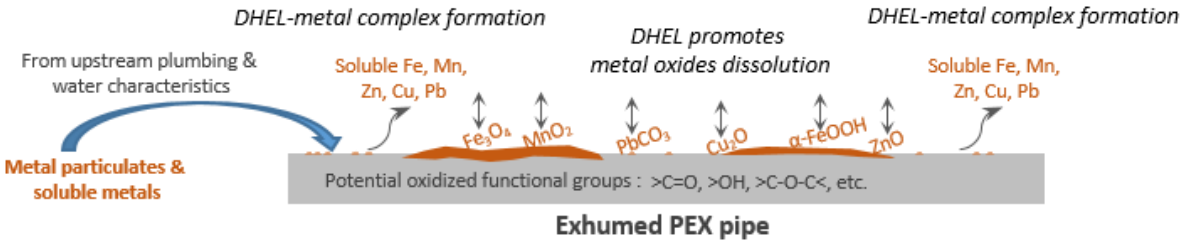

Figure 4.10 Proposed DHEL metal removal mechanism from exhumed plastic pipe.

4.4 Conclusion

In the current study, a biomass derived ligand (DHEL) was synthesized and used to remove heavy metals from exhumed plastic materials. First, the interaction of DHEL and Fe^{3+} was studied. The DHEL-Fe^{3+} complex constant was estimated to be (2.25 ± 0.07) $\times 10^3$ M^{-1} and (2.14 ± 0.10) $\times 10^3$ M^{-1} at pH 4 and 7 and a 1: 1 stoichiometry between DHEL and Fe was discovered. Characterization of plastic pipe surface revealed unequal metal distributions along the same length of exhumed plastic pipe. Fe was present in the greatest abundance, followed by Mn, Ca, Zn, Mg, Cu, Pb and Al. SEM-EDS analysis confirmed DHEL removed heavy metal deposits from the surface of exhumed plastic pipes. Further experiments (i.e., DHEL metal removal kinetic and performance evaluation) confirmed that when DHEL was ≥ 5 mM, more than 95% of target metals

(i.e., Cu, Fe, Mn, Pb and Zn) could be removed. More specifically, the first order kinetic model fitted better for the higher DHEL concentration (i.e., 5 mM). In addition, DHEL showed higher favorability for Cu and Zn than Fe, Mn and Pb. A good correlation ($R^2 \geq 0.93$) between metal removal and total metal loadings supports the hypothesis that DHEL efficiently removed metals from exhumed plastic pipes. Two metal removal mechanisms were also hypothesized and include: (1) ligand-promoted mineral dissolution, and (2) formation of ligand-metal complexes. Work is needed to identify the factors that control heavy metal accumulation onto plastic pipes. In addition, the types, amount, and speciation of metals on plastic water pipe surfaces should be considered for characterization in the future work. While the ligand-mineral binding phenomena in solution phase has been examined by others, the interactions between minerals, ligands, and plastic pipe has not been addressed. Understanding the application of biomass derived ligands as a cleaning agent for water infrastructure deserves further study.

4.5 References

[1] L.S. MCNEIILL, M. Edwards, Iron pipe corrosion in distribution systems, Journal of the American Water Works Association 93 (2001) 88-100.

[2] Y. Zhu, H. Wang, X. Li, C. Hu, M. Yang, J. Qu, Characterization of biofilm and corrosion of cast iron pipes in drinking water distribution system with UV/Cl 2 disinfection, Water Research 60 (2014) 174-181.

[3] Z. Zhang, J.E. Stout, L.Y. Victor, R. Vidic, Effect of pipe corrosion scales on chlorine dioxide consumption in drinking water distribution systems, Water Research 42 (2008) 129-136.

[4] J.M. Cerrato, L.P. Reyes, C.N. Alvarado, A.M. Dietrich, Effect of PVC and iron materials on Mn (II) deposition in drinking water distribution systems, Water Research 40 (2006) 2720-2726.

[5] J. Liu, H. Chen, Q. Huang, L. Lou, B. Hu, S.D. Endalkachew, N. Mallikarjuna, Y. Shan, X. Zhou, Characteristics of pipe-scale in the pipes of an urban drinking water distribution system in eastern China, Water Science and Technology: Water Supply 16 (2016) 715-726.

[6] L.A. Holmes, A. Turner, R.C. Thompson, Adsorption of trace metals to plastic resin pellets in the marine environment, Environmental Pollution 160 (2012) 42-48.

[7] C.Y. Peng, G.V. Korshin, Speciation of trace inorganic contaminants in corrosion scales and deposits formed in drinking water distribution systems, Water Research 45 (2011) 5553-5563.

[8] G. Graeme, Expert opinion: performance of polyolefin (PP-R, PEX and PB) piping and fittings in recirculating hot water systems under Australian operating conditions, Queensland University of Technology, Brisbane, 2012.

[9] D. Wagner, H. Siedlarek, M. Kropp, W.R. Fischer, Plastic Pipes IX, IOM, (1995) 497.

[10] D. Wright, Failure of plastics and rubber products: causes, effects and case studies involving degradation, iSmithers Rapra Publishing, 2001.

[11] D.A. Lytle, T.J. Sorg, C. Frietch, Accumulation of arsenic in drinking water distribution systems, Environmental Science & Technology 38 (2004) 5365-5372.

[12] M.J. Friedman, A.S. Hill, S.H. Reiber, R.L. Valentine, G. Larsen, A. Young, G.V. Korshin, C.Y. Peng, Assessment of inorganics accumulation in drinking water system scales and sediments, Water Research Foundation, Denver, 2010.

[13] American Water Works Association (AWWA), M28 Rehabilitation of Water Mains, Third Edition, American Water Works Association (AWWA), Denver, 2014.

[14] U.S. Envirionmental Protection Agency (EPA), Pilot-scale tests and systems evaluation for the containment, treatment, and decontamination of selected materials from T&E building pipe loop equipment. https://cfpub.epa.gov/si/si_public_record_report.cfm?address=nhsrc/&dirEntryId=188411, 2008 (accessed 16. 10. 01). Washington, D.C.

[15] U.S. Environmental Protection Agency (EPA), Decontamination of drinking water infrastructure: A literature review and summary. https://cfpub.epa.gov/si/si_public_file_download.cfm?p_download_id=519689, 2014 (accessed 16. 09. 05). Cincinnati, OH.

[16] D.O. Siringi, P.G. Home, E. Koehn, Cleaning Methods for Pipeline Renewals, International Journal of Engineering and Technical Research 2 (2014) 44-47.

[17] K.S. Casteloes, R.H. Brazeau, A.J. Whelton, Decontaminating chemically contaminated residential premise plumbing systems by flushing, Environmental Science: Water Research & Technology 1 (2015) 787-799.

[18] R.C. Copeland, D.A. Lytle, D.D. Dionysious, Desorption of arsenic from drinking water distribution system solids, Environmental Monitoring and Assessment 127 (2007) 523-535.
[19] A.D. Ebner, J.A. Ritter, J.D. Navratil, Adsorption of cesium, strontium, and cobalt ions on magnetite and a magnetite− silica composite, Industrial & Engineering Chemistry Research 40 (2001) 1615-1623.
[20] G. P. Fritzke, A letter regarding copper pipe treatment, Copper Development Association (CDA) Inc., 1991.
[21] D. Leštan, C.L. Luo, X.D. Li, The use of chelating agents in the remediation of metal-contaminated soils: a review, Environmental Pollution 153 (2008) 3-13.
[22] C. Oviedo, J. Rodríguez, EDTA: the chelating agent under environmental scrutiny, Quimica Nova 26 (2003) 901-905.
[23] S.S. Ahluwalia, D. Goyal, Microbial and plant derived biomass for removal of heavy metals from wastewater, Bioresource Technology 98 (2007) 2243-2257.
[24] M.E. Argun, S. Dursun, C. Ozdemir, M. Karatas, Heavy metal adsorption by modified oak sawdust: Thermodynamics and kinetics, Journal of Hazardous Materials 141 (2007) 77-85.
[25] S.E. Bailey, T.J. Olin, R.M. Bricka, D.D. Adrian, A review of potentially low-cost sorbents for heavy metals, Water Research 33 (1999) 2469-2479.
[26] S.O. Lesmana, N. Febriana, F.E. Soetaredjo, J. Sunarso, S. Ismadji, Studies on potential applications of biomass for the separation of heavy metals from water and wastewater, Biochemical Engineering Journal 44 (2009) 19-41.
[27] T.H. Parsell, B.C. Owen, I. Klein, T.M. Jarrell, C.L. Marcum, L.J. Haupert, L.M. Amundson, H.I. Kenttämaa, F. Ribeiro, J.T. Miller, M.M. Abu-Omar, Cleavage and hydrodeoxygenation (HDO) of C–O bonds relevant to lignin conversion using Pd/Zn synergistic catalysis, Chemical Science 4 (2013) 806-813.
[28] M.M. Abu-Omar, B. Saha, I. Klein, Compounds and compositions for delivery of nutrients and micronutrients to plants, WO 2017004052, 2017.
[29] K. Ashton, L. Holmes, A. Turner, Association of metals with plastic production pellets in the marine environment, Marine Pollution Bulletin 60 (2010) 2050-2055.
[30] H.A. Benesi, J. Hildebrand, A spectrophotometric investigation of the interaction of iodine with aromatic hydrocarbons, Journal of the American Chemical Society 71 (1949) 2703-2707.
[31] S. Goswami, D. Sen, N.K. Das, H.K. Fun, C.K. Quah, A new rhodamine based colorimetric ‘off–on’fluorescence sensor selective for Pd 2+ along with the first bound X-ray crystal structure, Chemical Communications 47 (2011) 9101-9103.
[32] X. Yu, T. Qin, P. Zhang, Q. Hu, J. Li, Novel Rhodamine-Coumarin Conjugate as an Effective Colorimetric Probe for Copper Ions in Aqueous Solution and Test Kits, Sensor Letters 12 (2014) 142-146.
[33] M. Salehi, Exploring Contaminant Fate within Plastic Water Infrastructure: The Nexus of Environmental Engineering and Material Science Frontiers, Civil Engineering, Purdue University, West Lafayette, IN, 2017.
[34] B. Özkaya, Adsorption and desorption of phenol on activated carbon and a comparison of isotherm models, Journal of Hazardous Materials 129 (2006) 158-163.
[35] Z. Li, Sorption kinetics of hexadecyltrimethylammonium on natural clinoptilolite, Langmuir 15 (1999) 6438-6445.
[36] Y.S. Ho, J.C.Y Ng, G. McKay, Kinetics of pollutant sorption by biosorbents: review, Separation and Purification Methods 29 (2000) 189-232.

[37] N.K. Lazaridis, T.A. Pandi, K.A. Matis, Chromium (VI) Removal from Aqueous Solutions by Mg− Al− CO3 Hydrotalcite: Sorption− Desorption Kinetic and Equilibrium Studies, Industrial & Engineering Chemistry Research 43 (2004) 2209-2215.
[38] S. Andrianirinaharivelo, G. Mailhot, M. Bolte, Photodegradation of organic pollutants induced by complexation with transition metals (Fe3+ and Cu2+) present in natural waters, Solar Energy Materials and Solar Cells 38 (1995) 459-474.
[39] C.A. Blanco, I. Caballero, A. Rojas, M. Gomez, J. Alvarez, Chelation of aqueous iron (III) by 2-acetyl-1, 3-cyclohexanedione and beer ageing, Food Chemistry 81 (2003) 561-568.
[40] G.A. Parks, The isoelectric points of solid oxides, solid hydroxides, and aqueous hydroxo complex systems, Chemical Reviews 65 (1965) 177-198.
[41] M. Salehi, X. Li, A.J. Whelton, Metal Accumulation in Representative Plastic Drinking Water Plumbing Systems, Journal of the American Water Works Association, accepted on May 30, 2017, in press.
[42] A. Stefánsson, Iron (III) hydrolysis and solubility at 25 C, Environmental Science & Technology 41 (2007) 6117-6123.
[43] Y. Yang, J.S. Jiang, Gradual phase and morphology transformation of Fe 3 O 4 nanoparticles to α-FeOOH nanorods in alcohol/water media in the presence of surfactant F127, Journal of Materials Science 43 (2008) 4340-4343.
[44] U. Schwertmann, Solubility and dissolution of iron oxides, in: Iron nutrition and interactions in plants, Springer Netherlands (1991) 3-27.
[45] R. Lacomba-Perales, J. Ruiz-Fuertes, D. Errandonea, D. Martínez-García, A. Segura, Optical absorption of divalent metal tungstates: Correlation between the band-gap energy and the cation ionic radius, Europhysics Letters 83 (2008) 37002.
[46] G. Bacquet, J. Dugas, C. Escribe, J. Gaite, J. Michoulier, Comparative electron paramagnetic resonance study of Fe3+ and Gd3+ ions in monoclinic zirconia, Journal of Physics C: Solid State Physics 7 (1974) 1551.
[47] R.G. Pearson, Absolute electronegativity and hardness: application to inorganic chemistry, Inorganic Chemistry 27 (1988) 734-740.
[48] H. Irving, R. Williams, 637. The stability of transition-metal complexes, Journal of the Chemical Society (Resumed) (1953) 3192-3210.
[49] A.E. Martell, R.D. Hancock, Metal complexes in aqueous solutions, Springer Science & Business Media 2013.
[50] D. Bhattacharyya, J.A. Hestekin, P. Brushaber, L. Cullen, L.G. Bachas, S.K. Sikdar, Novel poly-glutamic acid functionalized microfiltration membranes for sorption of heavy metals at high capacity, Journal of Membrane Science 141 (1998) 121-135.
[51] Z. Tang, S. Hong, W. Xiao, J. Taylor, Characteristics of iron corrosion scales established under blending of ground, surface, and saline waters and their impacts on iron release in the pipe distribution system, Corrosion Science 48 (2006) 322-342.
[52] E.J. Kim, J.E. Herrera, Characteristics of lead corrosion scales formed during drinking water distribution and their potential influence on the release of lead and other contaminants, Environmental Science & Technology 44 (2010) 6054-6061.
[53] O.W. Duckworth, S.T. Martin, Surface complexation and dissolution of hematite by C 1-C 6 dicarboxylic acids at pH= 5.0, Geochimica et Cosmochimica Acta 65 (2001) 4289-4301.
[54] B.A. Holmén, W.H. Casey, Hydroxamate ligands, surface chemistry, and the mechanism of ligand-promoted dissolution of goethite [α-FeOOH (s)], Geochimica et Cosmochimica Acta 60 (1996) 4403-4416.

[55] S.F. Cheah, S.M. Kraemer, J. Cervini-Silva, G. Sposito, Steady-state dissolution kinetics of goethite in the presence of desferrioxamine B and oxalate ligands: implications for the microbial acquisition of iron, Chemical Geology 198 (2003) 63-75.

APPENDIX A

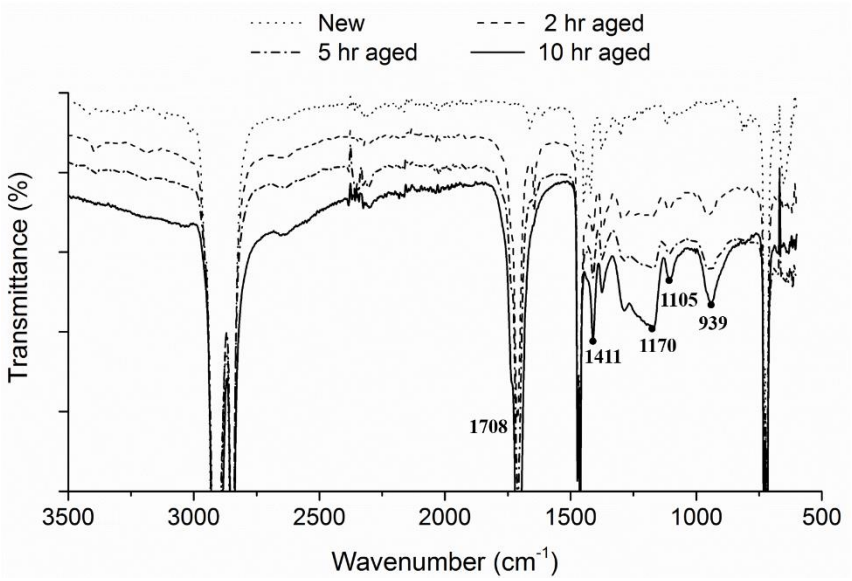

Figure A.1 FTIR spectra of new and aged LDPE pellets.

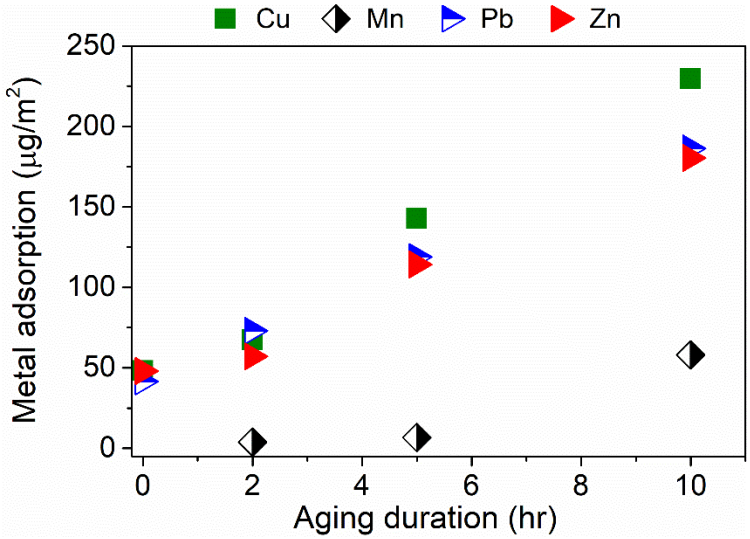

Figure A.2 Metal adsorption onto new and aged (i.e., 2, 5 and 10 hr aged) LDPE pellets. The exhibiting data was the adsorbed metal at the end of 24 hr (i.e., equilibrium point). Initial metal concentration was 30 ppb for each metal, at pH 7.5.

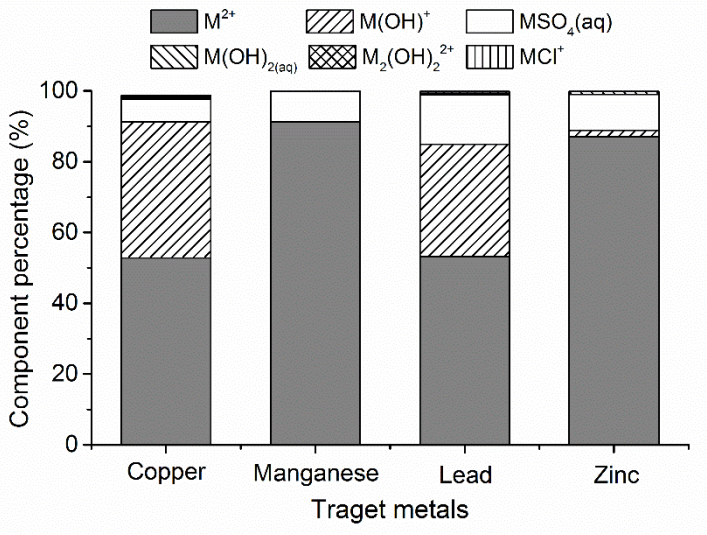

Figure A.3 Metal speciations in the metal mixed solution (i.e., Cu, Mn, Pb and Zn) by using Visial Minteq ver. 3.1. Initial metal concentration was 30 ppb for each metal, at pH 7.5.

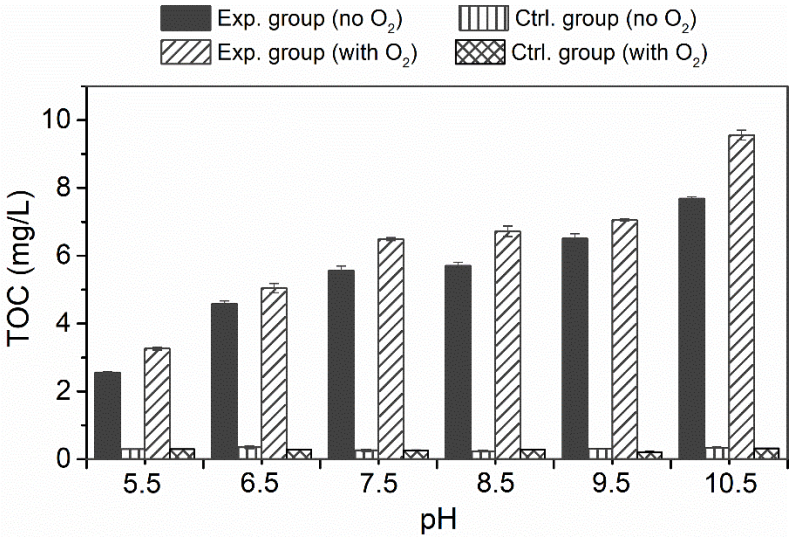

Figure A.4 Organics leaching from 10 hr aged LDPE pellets by changing water pH. The exhibiting data was averaged from triplicate experimental values (with error bars showing standarized deviation). Initial metal concentration was 30 ppb for each metal.

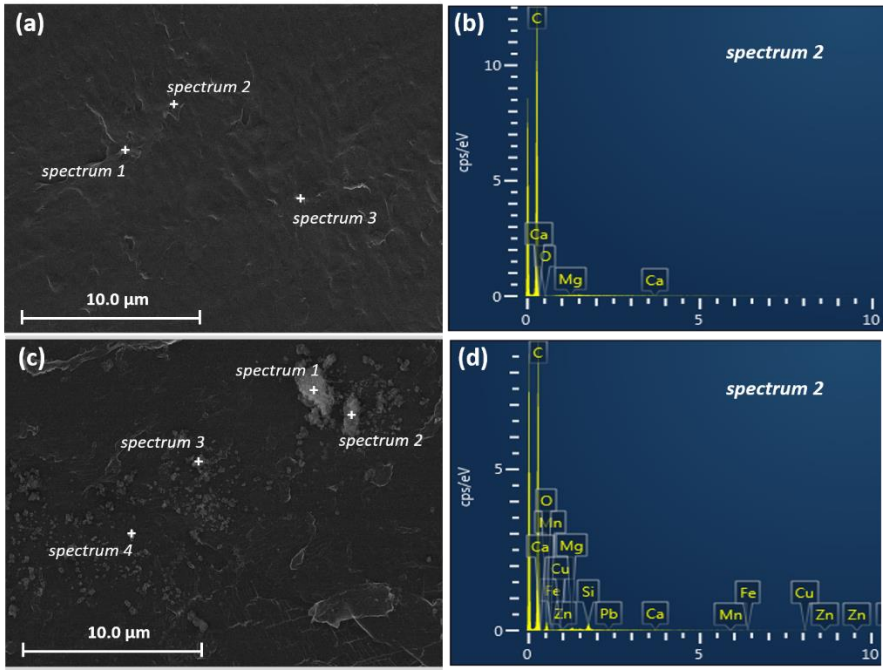

Figure A.5 (a) The SEM image and (b) the selected EDS spectrum of new LDPE segment from the blank solution (water only). (c) The SEM image and (b) the selected EDS spectrum of new LDPE segment from the metal solution (with 3 ppm of Cu, Fe, Mn, Pb, and Zn, respectively).

APPENDIX B

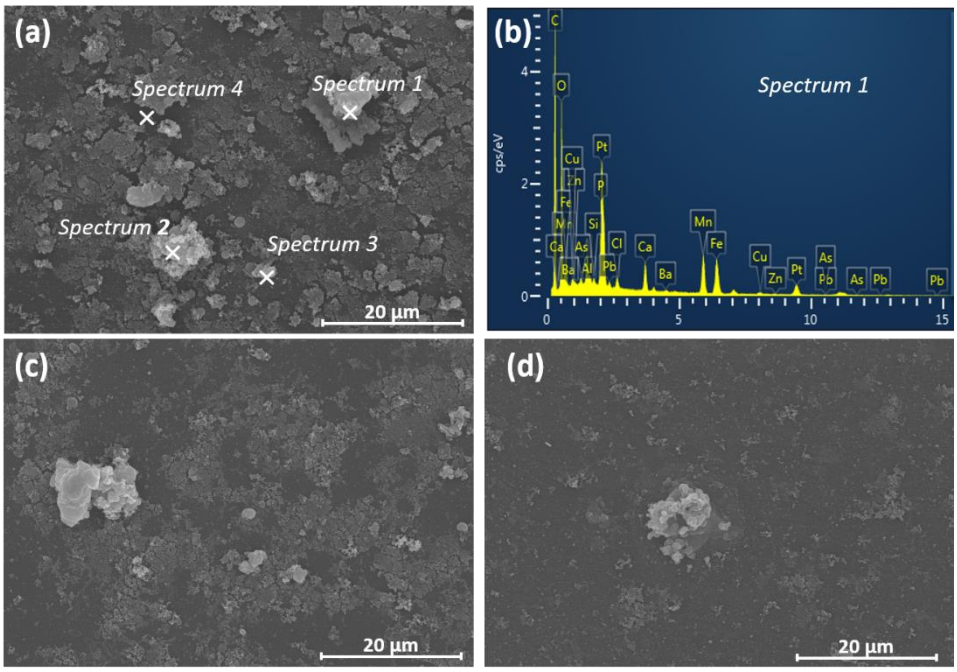

Figure B.1 SEM images and EDS spectrum of exhumed PEX piping surfaces at (a) (b) section 1-1 (c) 1-2 and (d) 1-3.

Table B.1 End pHs and % of dissolved metals during the 21 days metal leaching test**.**

Water cond.	Exp. group	End pH	Cu %	Fe %	Ni %	Pb %	Zn %
					23°C		
pH 4	PBP	4.97 *± 0.19*	95.63 *± 0.76*	ND	98.06 *± 0.34*	ND	97.90 *± 0.42*
pH 7.5	PBP	7.84 *± 0.05*	87.21 *± 3.71*	-	94.87 *± 0.49*	-	85.06 *± 1.95*
pH 4	CBP	6.65 *± 0.14*	96.02 *± 0.93*	ND	98.17 *± 0.99*	ND	97.26 *± 0.77*
pH 7.5	CBP	7.90 *± 0.09*	77.65 *± 3.27*	-	94.79 *± 1.31*	-	78.27 *± 1.76*
					55°C		
pH 4	PBP	6.99 *± 0.08*	96.24 *± 0.62*	ND	96.59 *± 1.63*	35.51 *± 3.48*	97.15 *± 1.79*
pH 7.5	PBP	8.34 *± 0.1*	78.93 *± 1.19*	-	93.48 *± 1.77*	-	77.66 *± 2.25*
pH 4	CBP	7.41 *± 0.06*	95.22 *± 1.72*	ND	95.79 *± 0.53*	21.06 *± 1.89*	97.10 *± 1.32*
pH 7.5	CBP	8.36 *± 0.09*	67.02 *± 2.25*	-	93.42 *± 1.18*	-	71.35 *± 1.84*

- represents no metal data (including total and dissolved metals) was detected under the certain experimental condition.
ND standards for the dissolved metal data was not detected.